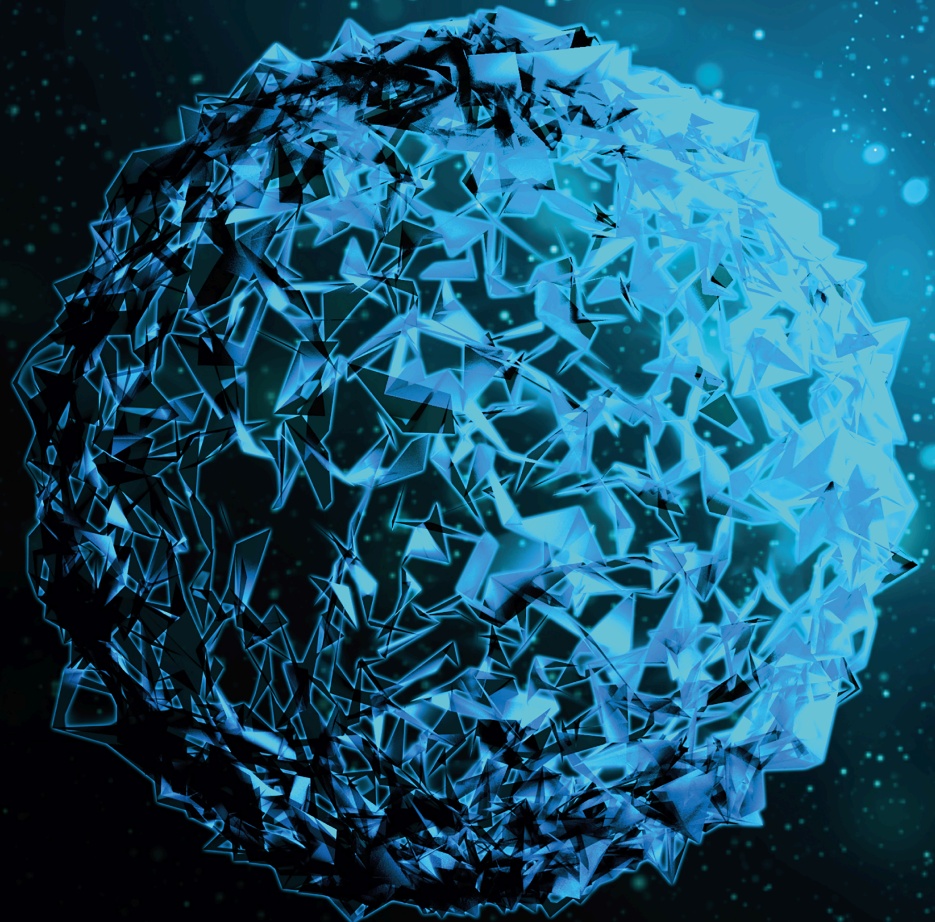


# Diagnosis of Coronary Artery Disease after the ESC Guidelines 2019

Lead Guest Editor: Andrea I. Guaricci

Guest Editors: Marco Guglielmo, Andrea Baggiano, Giuseppe Muscogiuri, and Mark Rabbat



---



# **Diagnosis of Coronary Artery Disease after the ESC Guidelines 2019**

BioMed Research International

---

## **Diagnosis of Coronary Artery Disease after the ESC Guidelines 2019**

Lead Guest Editor: Andrea I. Guaricci

Guest Editors: Marco Guglielmo, Andrea Baggiano,  
Giuseppe Muscogiuri, and Mark Rabbat



---

Copyright © 2021 Hindawi Limited. All rights reserved.

This is a special issue published in "BioMed Research International." All articles are open access articles distributed under the Creative Commons Attribution License, which permits unrestricted use, distribution, and reproduction in any medium, provided the original work is properly cited.



## Section Editors

Penny A. Asbell, USA  
David Bernardo , Spain  
Gerald Brandacher, USA  
Kim Bridle , Australia  
Laura Chronopoulou , Italy  
Gerald A. Colvin , USA  
Aaron S. Dumont, USA  
Pierfrancesco Franco , Italy  
Raj P. Kandpal , USA  
Fabrizio Montecucco , Italy  
Mangesh S. Pednekar , India  
Letterio S. Politi , USA  
Jinsong Ren , China  
William B. Rodgers, USA  
Harry W. Schroeder , USA  
Andrea Scribante , Italy  
Germán Vicente-Rodriguez , Spain  
Momiao Xiong , USA  
Hui Zhang , China

## Academic Editors




### Cardiology

Ramazan Akdemir , Turkey  
Pablo Avanzas , Spain  
Dirk Bandorski , Germany  
Raffaella Bloise, Italy  
Nazario Carrabba , Italy  
Cheng-I Cheng , Taiwan  
Dragos Cretoiu , Romania  
Claudio De Lucia , USA  
Chengming Fan , China  
Nicola Gaibazzi , Italy  
Nicola Galea , Italy  
Natig Gassanov , Germany  
Michael Gotzmann , Germany  
Ernesto Greco , Italy  
Marco Guglielmo, Italy  
Miklos Illyes, Hungary  
Christof Kolb , Germany

Mitja Lainscak, Slovenia  
Ping-Yen Liu , Taiwan  
Claudia Loardi , Italy  
Shinro Matsuo , Japan  
Rocco Antonio Montone, United Kingdom  
Francesco Nappi , France  
David Platts , Australia  
Kimimasa Tobita , USA  
Jörn Tongers, Germany  
Kazunori Uemura , Japan  
Thamizhiniyan Venkatesan, USA  
Xinhua Yu, USA



## Contents

### **Cardiac Phase Space Analysis: Assessing Coronary Artery Disease Utilizing Artificial Intelligence**

Mark G. Rabbat , Shyam Ramchandani , and William E. Sanders Jr. 

Review Article (5 pages), Article ID 6637039, Volume 2021 (2021)

### **Relationship of Stress Test Findings to Anatomic or Functional Extent of Coronary Artery Disease Assessed by Coronary Computed Tomography Angiography-Derived Fractional Flow Reserve**

Demetrios Doukas , Sorcha Allen, Amy Wozniak, Siri Kunchakarra, Rina Verma, Jessica Marot, John J. Lopez, Koen Nieman, Gianluca Pontone, Jonathon Leipsic, Jeroen Bax, and Mark G. Rabbat 











Research Article (9 pages), Article ID 6674144, Volume 2021 (2021)

### **Speckle Tracking Echocardiography: Early Predictor of Diagnosis and Prognosis in Coronary Artery Disease**

Maria Concetta Pastore , Giulia Elena Mandoli , Francesco Contorni, Luna Cavigli, Marta Focardi, Flavio D'Ascenzi, Giuseppe Patti, Sergio Mondillo, and Matteo Cameli 


Review Article (11 pages), Article ID 6685378, Volume 2021 (2021)

### **Stress CMR in Known or Suspected CAD: Diagnostic and Prognostic Role**

Francesca Baessato , Marco Guglielmo , Giuseppe Muscogiuri , Andrea Baggiano , Laura Fusini , Stefano Scafuri , Mario Babbaro , Rocco Mollace , Ada Collevocchio, Andrea I. Guaricci , and Gianluca Pontone 

Review Article (12 pages), Article ID 6678029, Volume 2021 (2021)

### **Artificial Intelligence in Coronary Computed Tomography Angiography: From Anatomy to Prognosis**

Giuseppe Muscogiuri, Marly Van Assen, Christian Tesche, Carlo N. De Cecco, Mattia Chiesa, Stefano Scafuri, Marco Guglielmo, Andrea Baggiano, Laura Fusini, Andrea I. Guaricci, Mark G. Rabbat, and Gianluca Pontone 

Review Article (10 pages), Article ID 6649410, Volume 2020 (2020)

## Review Article

# Cardiac Phase Space Analysis: Assessing Coronary Artery Disease Utilizing Artificial Intelligence

Mark G. Rabbat <sup>1</sup>, Shyam Ramchandani <sup>2</sup>, and William E. Sanders Jr. <sup>3,4</sup>

<sup>1</sup>Loyola University Medical Center, USA

<sup>2</sup>CorVista Health, Toronto, Ontario, Canada

<sup>3</sup>University of North Carolina at Chapel Hill, Chapel Hill, North Carolina, USA

<sup>4</sup>CorVista Health, Cary, North Carolina, USA

Correspondence should be addressed to Mark G. Rabbat; rabbatma@hotmail.com

Received 30 October 2020; Revised 4 December 2020; Accepted 26 March 2021; Published 10 April 2021

Academic Editor: Ernesto Greco

Copyright © 2021 Mark G. Rabbat et al. This is an open access article distributed under the Creative Commons Attribution License, which permits unrestricted use, distribution, and reproduction in any medium, provided the original work is properly cited.

The bridge of artificial intelligence to cardiovascular medicine has opened up new avenues for novel diagnostics that may significantly enhance the cardiology care pathway. Cardiac phase space analysis is a noninvasive diagnostic platform that combines advanced disciplines of mathematics and physics with machine learning. Thoracic orthogonal voltage gradient (OVG) signals from an individual are evaluated by cardiac phase space analysis to quantify physiological and mathematical features associated with coronary stenosis. The analysis is performed at the point of care without the need for a change in physiologic status or radiation. This review will highlight some of the scientific principles behind the technology, provide a description of the system and device, and discuss the study procedure, clinical data, and potential future applications.

## 1. Background

Cardiovascular disease is the leading cause of death worldwide. Thus, accurate diagnosis in patients with suspected coronary artery disease (CAD) is critical in clinical medicine. For the majority of patients, standard of care assessment for CAD begins with a functional stress test. In the United States alone, millions of stress tests are performed on an annual basis to evaluate patients with suspected CAD. However, this pathway has been reported to have low diagnostic yield at the time of invasive coronary angiography (ICA) [1]. Obstructive CAD was noted in less than half of patients undergoing exercise treadmill testing, stress echocardiography, single-photon emission computed tomography (SPECT) imaging, and stress cardiac magnetic resonance imaging at the time of their ICA in a contemporary analysis from the National Cardiovascular Data Registry (NCDR) of more than 385,000 patients from >1,100 United States hospitals [2]. Noninvasive testing has demonstrated similar prediction of obstructive CAD com-

pared to clinical factors [2]. Moreover, a recent study of over 15,000 patients found that among patients referred for ICA, those with a positive stress test were less likely to have obstructive CAD and receive revascularization compared to those either with a negative stress test or no testing at all [3].

The bridge of artificial intelligence to cardiovascular medicine has opened up new avenues for novel cardiovascular diagnostics that may significantly enhance the care of patients [4–6]. Unlike traditional imaging modalities to assess for CAD, cardiac phase space analysis (cPSA) is a dynamic assessment that captures data related to electrical signals over consecutive cardiac cycles which is unique to a given individual [7]. The resultant thoracic phase signals are analyzed by cPSA to quantify physiological and mathematical features associated with coronary stenosis without the need for a change in physiologic status such as stress-induced vasodilation.

cPSA is an easy-to-use, portable device utilized at the point-of-care without radiation, contrast, or patient preparation. This review will highlight some of the scientific



FIGURE 1: Data acquisition setup: (a) signal acquisition device and (b) patient and electrodes/lead placement and PPG configurations.

principles behind the technology, provide a description of the system and device, and discuss the study procedure, clinical data, and potential future applications.

## 2. Cardiac Phase Space Analysis

**2.1. Signal Acquisition.** Two sources of time series data are simultaneously acquired from each subject: (i) orthogonal voltage gradient (OVG) signals and (ii) photoplethysmography (PPG) signals. These signals are collected with a sampling rate of 8 kHz using a specialized instrument (both hardware and firmware), shown in Figure 1. Signals are acquired for 3.5 minutes, resulting in a short overall procedure time, conducive to an outpatient-based single visit clinical assessment. Signal quality scores quantified nonbiological interference that could affect the performance of subsequent analyses. The OVG signal is assessed for powerline interference (60 Hz based on the main frequency in North America) and excessive frequency content greater than 170 Hz (high-frequency noise). Additionally, the quality of the PPG signal is assessed through quantifying the segments of the signal affected by jumps and dropouts (abrupt jump noise) and epochs that do not have dynamic variations reflecting the change in the blood flow volume changes (railing noise). Signals exceeding the threshold for any of the described scores are excluded, and signals passing the quality assessment are preconditioned by removing baseline wander and filtering the high-frequency noise and powerline interference.

**2.2. Photoplethysmography (PPG).** PPG is used to optically measure the variations of the volume of blood perfusing the tissue. In this measurement modality, a specific wavelength of light is emitted from an LED illuminating the tissue (e.g., skin, subcutaneous tissue, and fat); the intensity of this light after passing through the tissue (in this case, fingertip) is then registered by photodetectors. The amount of light absorbed by the interrogated tissue depends on the volume of the blood. This variation is observed in the PPG signals and can provide valuable information with regard to, among other things, to cardiac activity.

The PPG signals can be used for various purposes such as monitoring the blood oxygen saturation level when two light sources are used as well as for measuring and analyzing heart

rate variability. The PPG signals are recorded using a sensor with red and near-infrared light sources. These PPG waveforms are then employed for analysis and feature extraction.

**2.3. Orthogonal Voltage Gradient (OVG).** The three-dimensional OVG measures the electrical activity, the product of the action potential generation, of the heart. There are various configurations of the leads that can be used to obtain such signals. With the signal acquisition device configuration shown in Figure 1, seven leads are used which result in three orthogonal channels, denoted  $X$ ,  $Y$ , and  $Z$ . These signals are measured in the patient's coronal, sagittal, and transverse planes, respectively.

**2.4. Machine Learning.** Measurements of the signals are made using Phase Space mathematics and other mathematical approaches such as dynamical system analysis to create a set of measurements or features. These features are then paired with the corresponding "ground truth labels" (actual catheterization results) to form the input to the machine learning (ML) models. Many types of ML models can be applied to these data (Random Forests, Neural Networks, Genetic Algorithms, and Support Vector Machines), but the choice(s) of ML method can drive specific settings of the data set and parameters to be evaluated. A standard example of a ML campaign: the data are split into training-validation and test sets (usually 80% training 20% validation but this can be adjusted from campaign to campaign). The training-validation set is used to train and fine-tune several machine learning models using 5-fold cross-validation. To find an optimal set of hyperparameters for each model, a grid search is performed over a range of hyperparameters. Then, using the average AUC of 100 runs as the performance metric, the set of hyperparameters that results in the highest validation AUC is selected for each model. The models are ranked by performance on the validation dataset. In the final step, the selected models are trained on the entire train-validation set, and their AUC performance on the held-out naïve test set is assessed.

**2.5. System and Device Description (Figure 1).** The cPSA System is a medical device system that uses novel features and machine-learned algorithms to analyze phase signals and assess the presence of significant epicardial CAD. The first

TABLE 1: Demographics of population.

Characteristics	Development ( $n = 512$ )	Verification ( $n = 94$ )	$p$ value
Mean age, years (range)	61.5 ± 10.7	59.0 ± 9.8	0.04
Male (%)	60.2%	69.1%	0.11
Female (%)	39.8%	30.9%	0.11
Mean BMI (range)	31.3 ± 7.0	32.5 ± 7.6	0.14
Diabetes mellitus (%)	31.4%	35.1%	0.47
Hypertension (%)	72.9%	75.5%	0.70
Hypercholesterolemia/hyperlipidemia (%)	71.3%	70.2%	0.90
Angiographic results = CAD negative (%)	69.1%	73.4%	0.46
Angiographic results = CAD positive (%)	30.9%	26.6%	0.46

Reproduced with permission (Stuckey TD, et al. PLOS ONE. 2018).

TABLE 2: Detecting flow-limiting CAD. Machine-learned predictor (cPSTA) compared to exercise SPECT [8] and exercise ECG [8, 9].

Test	Sensitivity range	Specificity range
Rest cPSTA ( $N = 94$ )*	92% (95% CI = 74% to 100%)	62% (95% CI = 51% to 74%)
Exercise SPECT	82-88%	70-88%
Exercise ECG	54-75%	64-75%

Reproduced with permission (Stuckey TD, et al. PLOS ONE. 2018).

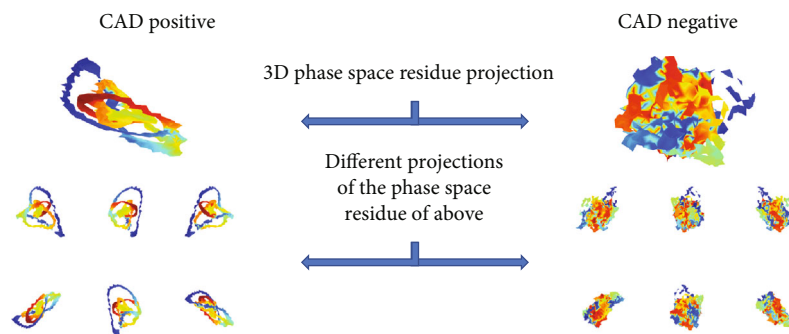


FIGURE 2: Phase Space (PS) Residues from a CAD positive subject and CAD negative subject. The PS Residues are 3D computation objects generated from the difference of the actual signal from the modelled signal in three dimensions. These objects can be evaluated geometrically to produce features (such as surface area or volume). The coloring can represent another measurable dimension. Here, the images are colored by where in the depolarization/repolarization cycle the point difference comes from. The top image is a single projection of the 3D PS Residue image. The 6 smaller projections are different views of the larger object.

element is the Phase Signal Acquisition (PSAQ) System. The PSAQ includes the phase signal recorder (PSR) and the phase signal data repository (PSDR). The PSR is a hand-held instrument that acquires and transmits resting phase signals along with additional patient-specific information such as gender and age. The cloud-based PSDR accepts, stores, and allows retrieval of the signals as well as patient-specific information. The second element is a CAD analytical engine (CAD AE). Utilizing machine-learned algorithms, the CAD AE processes and evaluates the phase signals from approximately 10 million data points to assess the presence and significance of CAD. The final element is the health care provider (HCP) Web Portal that the clinician utilizes to interpret images, review results, and generate a report. The results are subsequently displayed as a phase space analysis model, and the report can be saved as a record for inclusion in the patient’s electronic medical record.

2.6. *Study Procedure.* Signals are acquired utilizing the hand-held PSR device via seven sensors positioned on the chest and back and a PPG sensor clipped to a finger. Phase signal data are collected for approximately 3 minutes, and the data is then transmitted wirelessly to the cloud based PSDR. An analytic engine, consisting of software based on the machine-learned algorithms, analyzes the acquired data and generates predictions of physiological status. The results are made available through a secure web portal.

2.7. *Clinical Data.* The primary objective of the Coronary Artery Disease Learning and Algorithm Development (CADLAD) trial was designed to collect resting phase signals from eligible subjects using the PSR prior to ICA to machine learn and test an algorithm for detecting the presence of significant CAD in symptomatic patients [7]. In addition, machine-learned algorithms were developed and tested to



identify the location of significant CAD. Demographics and patient characteristics for the studied population are shown in Table 1. With the aim of a generalized machine-learned algorithm in mind, a broad cross section of clinical practices at twelve enrolling centers throughout the United States, representing a diverse array of facilities providing care to patients with heart disease, were utilized as investigational sites. First, OVG signals were paired with clinical outcomes data to develop machine-learned algorithms for the assessment of significant CAD. Subsequently, a blinded paired comparison of the machine-learned algorithm was performed against the “gold standard” (ICA) for assessment of CAD. Significant CAD was defined as a diameter reduction  $\geq 70\%$  or at least one lesion with reduced fractional flow reserve (FFR) of  $\leq 0.80$  at the time of ICA. Initial results from the CADLAD trial included 606 participants. The machine-learned algorithm cohort consisted of phase signals from 512 patients with 94 patients serving as the verification cohort. Blindly testing the cPSA System in the naïve verification cohort demonstrated a sensitivity of 92% (95% CI: 74%-100%) and specificity of 62% (95% CI: 51%-74%) for the assessment of significant CAD, which is comparable to commonly performed standard of care functional testing (Table 2) [7–9]. The negative predictive value (NPV) was 96% (95% CI: 85%-100%), and the PPV was 46% (95% CI: 33%-62%) [7]. In order not to miss significant CAD in clinical practice, the system was optimized (threshold chosen using the AUC-ROC curve) to maximize safety and therefore sensitivity. The specificity of 62% remains comparable to other functional tests [7]. Figure 2 presents cases of patients with and without CAD.

Conventional diagnostic pathways for detecting CAD are less accurate in women than men. Preliminary data from the CADLAD trial revealed that the diagnostic performance of cPSA for women compared to men was equivalent if not superior demonstrating an overall area under the receiver-operator characteristic curve (AUC) (0.82 (0.60-0.96) vs. 0.76 (0.62-0.86)), sensitivity (100% (100%-100%) vs. 83% (56%-95%)), specificity (73% (42%-92%) vs. 64% (49%-76%)), and NPV (100% (100%-100%) vs. 91% (76%-97%)), respectively ( $p = ns$  for all).

When stratified by age, initial data from the CADLAD trial demonstrates comparable diagnostic performance of cPSA for those  $< 65$  years of age and  $\geq 65$  years of age with an overall AUC (0.79 (0.66-0.88) vs. 0.72 (0.50-0.88)), sensitivity (100% (100%-100%) vs. 86% (56%-100%)), specificity (63% (49%-75%) vs. 67% (40%-88%)), and NPV (100% (100%-100%) vs. 83% (50%-100%)), respectively ( $p = ns$  for all).

In addition, those with obesity (body mass index  $\geq 30$  kg/m<sup>2</sup>) had similar diagnostic performance with cPSA compared to subjects without obesity (body mass index  $< 30$  kg/m<sup>2</sup>) demonstrating an overall AUC (0.78 (0.64-0.88) vs. 0.80 (0.62-0.92)), sensitivity (83% (46%-100%) vs. 92% (50%-100%)), specificity (67% (51%-79%) vs. 67% (44%-84%)), and NPV (94% (79%-100%) vs. 94% (68%-100%)), respectively ( $p = ns$  for all).

SPECT is the most ubiquitous functional stress test performed in the United States. In the CADLAD trial, SPECT was performed in a subgroup of 607 subjects prior to their ICA. Positive SPECT results were compared to the

machine-learned cPSA algorithm using ICA as the reference standard. Overall sensitivity (86% (81%-91%) vs. 92% (86%-96%)), specificity (23% (19%-27%) vs. 33% (27%-39%)), PPV (36% (32%-41%) vs. 42% (36%-48%)), and NPV (77% (68%-84%) vs. 89% (81%-95%)) were comparable between SPECT and cPSA, respectively ( $p = ns$  for all).

**2.8. Future Directions.** The bridge of AI utilizing cPSA and cardiovascular medicine has a very bright future. The same principles and methods developed for assessment of CAD can be utilized for other cardiovascular conditions. Ongoing clinical research with cPSA in pulmonary hypertension and left ventricular end diastolic pressure are underway. As a society, we need to assure these algorithms and others developed are used wisely. Thus, larger and more heterogeneous data sets are required in order to limit bias and increase the generalizability in patient populations such as women and minority groups [10–12].

### 3. Conclusion

Features extracted from thoracic phase signals can be employed in machine learning to develop final mathematical predictors that assess the presence of significant CAD. Performance of the cPSA appears comparable to the most commonly employed functional stress tests without the need for ionizing radiation, contrast media, or stress (exercise or pharmacological) and requires minimal patient time.

### Conflicts of Interest

Dr. Rabbat is a consultant for CorVista Health. Drs. Sanders and Ramchandani are CorVista Health employees.



### References

- [1] M. R. Patel, E. D. Peterson, D. Dai et al., “Low diagnostic yield of elective coronary angiography,” *The New England Journal of Medicine*, vol. 362, no. 10, pp. 886–895, 2010.
- [2] M. R. Patel, D. Dai, A. F. Hernandez et al., “Prevalence and predictors of nonobstructive coronary artery disease identified with coronary angiography in contemporary clinical practice,” *American heart journal*, vol. 167, no. 6, pp. 846–852.e2, 2014.
- [3] J. P. Vavalle, L. Shen, S. Broderick, L. K. Shaw, and P. S. Douglas, “Effect of the presence and type of angina on cardiovascular events in patients without known coronary artery disease referred for elective coronary angiography,” *JAMA Cardiology*, vol. 1, no. 2, pp. 232–234, 2016.
- [4] M. Rabbat, J. Leipsic, J. Bax et al., “Fractional flow reserve derived from coronary computed tomography angiography safely defers invasive coronary angiography in patients with stable coronary artery disease,” *Journal of clinical medicine*, vol. 9, no. 2, p. 604, 2020.
- [5] F. Lopez-Jimenez, Z. Attia, A. M. Arruda-Olson et al., “Artificial intelligence in cardiology: present and future,” *Mayo Clinic Proceedings*, vol. 95, no. 5, pp. 1015–1039, 2020.
- [6] G. Muscogiuri, M. Chiesa, M. Trotta et al., “Performance of a deep learning algorithm for the evaluation of CAD-RADS classification with CCTA,” *Atherosclerosis*, vol. 294, pp. 25–32, 2020.

- [7] T. D. Stuckey, R. S. Gammon, R. Goswami et al., “Cardiac phase space tomography: a novel method of assessing coronary artery disease utilizing machine learning,” *PLoS One*, vol. 13, no. 8, article e0198603, 2018.
- [8] S. D. Fihn, J. M. Gardin, J. Abrams et al., “2012 ACCF/AHA/ACP/AATS/PCNA/SCAI/STS guideline for the diagnosis and management of patients with stable ischemic heart disease: a report of the American College of Cardiology Foundation/American Heart Association Task Force on Practice Guidelines, and the American College of Physicians, American Association for Thoracic Surgery, Preventive Cardiovascular Nurses Association, Society for Cardiovascular Angiography and Interventions, and Society of Thoracic Surgeons,” *Journal of the American College of Cardiology*, vol. 60, no. 24, pp. e44–e164, 2012.
- [9] Y. Kwok, C. Kim, D. Grady, M. Segal, and R. Redberg, “Meta-analysis of exercise testing to detect coronary artery disease in women,” *The American Journal of Cardiology*, vol. 83, no. 5, pp. 660–666, 1999.
- [10] Z. Obermeyer, B. Powers, C. Vogeli, and S. Mullainathan, “Dissecting racial bias in an algorithm used to manage the health of populations,” *Science*, vol. 366, no. 6464, pp. 447–453, 2019.
- [11] L. Nordling, “A fairer way forward for AI in health care,” *Nature*, vol. 573, no. 7775, pp. S103–S105, 2019.
- [12] E. Tat, D. L. Bhatt, and M. G. L. U. Rabbat, “Addressing bias: artificial intelligence in cardiovascular medicine,” *The Lancet Digital Health*, vol. 2, no. 12, pp. e635–e636, 2020.

## Research Article

# Relationship of Stress Test Findings to Anatomic or Functional Extent of Coronary Artery Disease Assessed by Coronary Computed Tomography Angiography-Derived Fractional Flow Reserve

Demetrios Doukas <sup>1</sup>, Sorcha Allen,<sup>1</sup> Amy Wozniak,<sup>2</sup> Siri Kunchakarra,<sup>3</sup> Rina Verma,<sup>4</sup> Jessica Marot,<sup>2</sup> John J. Lopez,<sup>1</sup> Koen Nieman,<sup>5</sup> Gianluca Pontone,<sup>6</sup> Jonathon Leipsic,<sup>7</sup> Jeroen Bax,<sup>8</sup> and Mark G. Rabbat <sup>1</sup>

<sup>1</sup>Division of Cardiology, Loyola University Medical Center, Maywood, IL 60153, USA

<sup>2</sup>Department of Medicine, Loyola University Medical Center, Maywood, IL 60153, USA

<sup>3</sup>Division of Cardiology, UCSF Fresno Medical Education Program, Fresno, CA 93701, USA

<sup>4</sup>Division of Cardiology, Alexian Brothers Medical Center, Elk Grove Village, IL 60997, USA

<sup>5</sup>Department of Cardiovascular Medicine and Radiology, Stanford University, Stanford, CA, USA

<sup>6</sup>Department of Cardiovascular Imaging, Cardiologico Monzino, Via Carlo Parea, 4, 20138 Milan, Italy

<sup>7</sup>Department of Radiology, St. Paul's Hospital and the University of British Columbia, Vancouver, BC, Canada V6T 1Z4

<sup>8</sup>Department of Cardiology, Leiden University Medical Center, Albinusdreef 2, 2333 ZA Leiden, Netherlands

Correspondence should be addressed to Mark G. Rabbat; [mrabbat@lumc.edu](mailto:mrabbat@lumc.edu)

Received 7 December 2020; Revised 8 January 2021; Accepted 4 February 2021; Published 24 February 2021

Academic Editor: Luca Liberale

Copyright © 2021 Demetrios Doukas et al. This is an open access article distributed under the Creative Commons Attribution License, which permits unrestricted use, distribution, and reproduction in any medium, provided the original work is properly cited.

**Background.** In the United States, functional stress testing is the primary imaging modality for patients with stable symptoms suspected to represent coronary artery disease (CAD). Coronary computed tomography angiography (CTA) is excellent at identifying anatomic coronary artery disease (CAD). The application of computational fluid dynamics to coronary CTA allows fractional flow reserve (FFR) to be calculated noninvasively (FFR<sub>CT</sub>). The relationship of noninvasive stress testing to coronary CTA and FFR<sub>CT</sub> in real-world clinical practice has not been studied. **Methods.** We evaluated 206 consecutive patients at Loyola University Chicago with suspected CAD who underwent noninvasive stress testing followed by coronary CTA and FFR<sub>CT</sub> when indicated. Patients were categorized by stress test results (positive, negative, indeterminate, and equivocal). Duke treadmill score (DTS), METS, exercise duration, and chest pain with exercise were analyzed. Lesions  $\geq 50\%$  stenosis were considered positive by coronary CTA. FFR<sub>CT</sub>  $< 0.80$  was considered diagnostic of ischemia. **Results.** Two hundred and six patients had paired noninvasive stress test and coronary CTA/FFR<sub>CT</sub> results. The median time from stress test to coronary CTA was 49 days. Average patient age was 60.3 years, and 42% were male. Of the 206 stress tests, 75% were exercise (70% echocardiographic, 26% nuclear, and 4% EKG). There were no associations of stress test results with CAD  $> 50\%$  or FFR<sub>CT</sub>  $< 0.80$  ( $p = 0.927$  and  $p = 0.910$ , respectively). Of those with a positive stress test, only 30% (3/10) had CAD  $> 50\%$  and only 50% (5/10) had FFR<sub>CT</sub>  $< 0.80$ . Chest pain with exercise did not correlate with CAD  $> 50\%$  or FFR<sub>CT</sub>  $< 0.80$  ( $p = 0.66$  and  $p = 0.12$ , respectively). There were no significant correlations between METS, DTS, or exercise duration and FFR<sub>CT</sub> ( $r = 0.093$ ,  $p = 0.274$ ;  $r = 0.012$ ,  $p = 0.883$ ; and  $r = 0.034$ ,  $p = 0.680$ ; respectively). **Conclusion.** Noninvasive stress testing, functional capacity, chest pain with exercise, and DTS are not associated with anatomic or functional CAD using a diagnostic strategy of coronary CTA and FFR<sub>CT</sub>.



## 1. Introduction

In the United States, functional stress testing is the primary imaging modality for patients with stable symptoms suspected to represent coronary artery disease (CAD). Metrics of functional capacity derived from stress tests such as exercise duration, metabolic equivalents (METs), and Duke treadmill score (DTS), an index that provides information calculated using data from exercise treadmill EKG, are commonly reported and incorporated in clinical decision-making to determine the presence of CAD [1]. However, functional stress testing has been shown to have low diagnostic yield at the time of ICA and, consequently, is no longer recommended as the first line diagnostic testing in the National Institute for Health and Care Excellence (NICE) guidelines for the assessment of recent onset chest pain [2]. The necessity of improved methods for the noninvasive evaluation of CAD was highlighted in a retrospective study of the National Cardiovascular Data Registry, which demonstrated that only 37.6% of the 398,978 patients without known CAD who underwent ICA had obstructive CAD, and having a positive noninvasive stress test only increased the rate of obstructive disease from 35% to 41% [3].

Coronary computed tomographic angiography (CTA) has emerged as an excellent noninvasive test for detecting CAD. However, the identification of CAD alone is insufficient as the relationship between coronary stenosis and ischemia is complex and frequently discordant. Over the past few years, there has been strong interest in computing fractional flow reserve (FFR) noninvasively using coronary CTA [4]. The application of computational fluid dynamics (CFD) to resting coronary CTA datasets allows FFR to be calculated noninvasively ( $FFR_{CT}$ ). The emergence of  $FFR_{CT}$  provides a noninvasive test that yields both anatomic and functional data and has been validated through a number of accuracy studies [5, 6]. Furthermore, several studies now suggest that  $FFR_{CT}$  leads to the reduction of unnecessary ICA in patients with CAD [7–9].

We sought to determine the relationship between noninvasive stress testing, metrics of functional capacity, DTS, and chest pain with exercise and anatomic or functional CAD using a diagnostic strategy of coronary CTA and  $FFR_{CT}$ .

## 2. Methods

**2.1. Study Population.** We retrospectively evaluated 597 consecutive patients at Loyola University Chicago with suspected CAD who underwent coronary CTA at the treating physician's discretion. Patients with known CAD were excluded from the analysis, and no patients underwent revascularization between stress testing and coronary CTA. Of those patients, 206 had paired noninvasive stress testing and coronary CTA/ $FFR_{CT}$  and were included in the analysis. The median time between coronary CTA and stress testing was 49 days.

Due to the retrospective nature of this study, the ordering physicians were not blinded to the results of either the coronary CTA or noninvasive stress test. The coronary CTA studies were read by cardiology attendings with board certifi-

cation in cardiovascular CT imaging, with support from diagnostic radiology for extracardiac pathology. Exercise treadmill EKGs and stress echocardiograms (exercise and pharmacological) were read by cardiology attendings with board certification in echocardiography. Nuclear stress tests were interpreted by nuclear medicine attendings with board certification in nuclear cardiology.

Coronary artery lesions with  $\geq 50\%$  stenosis were considered positive by coronary CTA whereas  $FFR_{CT} \leq 0.80$  at the distal vessel tip was considered diagnostic of ischemia. Modalities of noninvasive stress testing included exercise treadmill EKG, stress echocardiogram (exercise and pharmacological), and single-photon emission computed tomography myocardial perfusion imaging (SPECT-MPI [exercise and pharmacological]). Patients were categorized by stress test results (positive, negative, indeterminate, and equivocal). The definition of a positive stress test depended on the stress modality and is described in detail for each below. Patients with discordant stress EKG compared with stress imaging were considered to have equivocal stress tests (i.e., abnormal stress EKG but normal stress echocardiographic images). Indeterminate stress tests were defined as patients who failed to achieve target heart rate or had uninterpretable exercise stress imaging.

**2.2. Exercise Treadmill EKG.** A symptom-limited standard exercise treadmill test (ETT) was conducted, using the Bruce or modified-Bruce protocol. Patients with the following resting EKG changes were excluded: preexcitation (Wolff-Parkinson-White) syndrome, electronically paced ventricular rhythm, greater than 1 mm of resting ST depression, or complete left bundle branch block. The test was preceded by 48-hour discontinuation of  $\beta$ -blockers, calcium antagonists, and long-lasting nitrates. The patients were monitored continuously during the test with 12-lead EKG. Exercise duration, METs, chest pain during exercise, arrhythmia, and hypertensive response with stress and ST segment changes were recorded. A positive exercise treadmill EKG was defined as greater than or equal to 1 mm of horizontal or downsloping ST-segment depression or elevation for at least 60 to 80 milliseconds after the end of the QRS complex in 2 or more contiguous leads [10]. Arrhythmia that occurred during exercise included premature ventricular contractions, ventricular tachycardia/fibrillation, or supraventricular tachycardia. A systolic blood pressure  $> 220$  mmHg for men or  $> 210$  mmHg for women was considered a hypertensive response. Duke treadmill score was calculated using the following equation:  $DTS = \text{exercise time} - (5 \times \text{ST deviation}) - (4 \times \text{exercise angina})$ , with 0 = none, 1 = non-limiting, and 2 = exercise limiting angina. Patients were further categorized into low risk (score  $> 5$ ), intermediate risk (score between 4 and -11), and high risk (score  $< -11$ ) DTS [11].

**2.3. Stress Echocardiogram.** Stress echocardiograms were performed following the guidelines of the American Society of Echocardiography [11]. For stress echocardiography with treadmill testing, the Bruce protocol was utilized and images were obtained at rest, immediately after peak exercise, and at recovery. The patient exercised at 3-minute stages of

progressively increasing difficulty until exercise-limiting symptoms, or significant abnormalities in blood pressure, heart rhythm, or ST segments were noted. Postexercise images were obtained as soon as possible and ideally within 1 minute. An ischemic response to exercise was defined by the development of a new wall motion abnormality in a segment with normal function at rest, worsening of function with stress in a segment with a resting wall motion abnormality, increase in the ventricular cavity size with exercise, or a decrease in the ejection fraction compared with rest [11].

**2.4. Single-Photon Emission Computed Tomography Myocardial Perfusion Imaging.** SPECT-MPI was acquired following the guidelines of the American Society of Nuclear Cardiology [12]. Similar to stress echocardiography, patients who underwent exercise SPECT-MPI followed the Bruce protocol and were continuously monitored during the exercise test and for at least 5 minutes into the recovery phase. A 12-lead EKG was obtained at every stage of exercise, at peak exercise, and at the termination or recovery phase. The heart rate and blood pressure were recorded at least every 3 minutes during exercise, at peak exercise, and for at least 5 minutes into the recovery phase. The radiopharmaceutical was injected as close to peak exercise as possible. An abnormal response to stress was a perfusion defect within one or more of the 17-segment heart model territories compared to rest. In addition, an increase in the ventricular cavity with stress was considered an abnormal ischemic response.

**2.5. Coronary CTA Acquisition and Analysis.** Coronary CTA was performed with electrocardiographic gated prospective or retrospective gating on  $\geq 64$  detector row scanners (Siemens Sensation Cardiac 64, Siemens Medical Solutions, Malvern, Pennsylvania; Discovery HD 750, GE Healthcare, Milwaukee, USA; Revolution CT 256-row, GE Healthcare, Milwaukee, USA) in accordance with the Society of Cardiovascular Computed Tomography (SCCT) guidelines [13]. Oral, and when needed, intravenous beta-blocker was administered to achieve a target heart rate (HR) of 60 beats per minute (bpm). Sublingual nitroglycerin 0.4-0.8 mg was given approximately 5 minutes prior to contrast administration. CTA datasets were interpreted using a commercially available dedicated workstation (Aquarius 3D Workstation, TeraRecon, San Mateo, CA, USA). A coronary lesion with  $\geq 50\%$  diameter of stenosis by the interpreting physician was considered obstructive on coronary CTA [14–16]. Coronary vessel branches for the left anterior descending, left circumflex, and right coronary arteries were categorized according to the SCCT guidelines.

**2.6. Computation of  $FFR_{CT}$ .**  $FFR_{CT}$  analysis was performed by HeartFlow Inc. (Redwood City, California) as previously described [17]. After semiautomated segmentation of the epicardial coronary arteries and determination of left ventricular mass, calculations of  $FFR_{CT}$  were performed by CFD modeling. Three-dimensional (3D) blood flow modeling of the coronary arteries was performed, with blood modeled as a Newtonian fluid using incompressible Navier–Stokes equations and solved subject to appropriate initial and boundary conditions using a finite element method on a parallel super-

computer. Coronary blood flow was simulated under conditions modeling intravenous adenosine-mediated coronary hyperemia. A positive  $FFR_{CT}$  was defined as the distal tip value  $< 0.80$  in a vessel of diameter  $> 1.8$  mm.

**2.7. Statistical Analysis.** Baseline characteristics of the selected subjects were calculated and presented as frequencies and percentages for categorical variables and mean  $\pm$  SD for continuous variable. General descriptive statistics (means, standard deviations, and frequencies) were used to summarize patient characteristics and stress-test results for the entire cohort and separately for each group. Student's *t*-test were used to compare associations of continuous variables, and chi-sq test or Fisher's exact test was used to compare associations of categorical variables. Pearson's correlation coefficients estimated correlation between continuous predictors and continuous  $FFR_{CT}$ . All analyses were performed using SAS Proprietary software (version 9.2, SAS Institute, Cary, North Carolina).

### 3. Results

206 patients had a noninvasive stress test and coronary CTA/ $FFR_{CT}$  result. Using the Diamond–Forrester score, 86.1% of patients were at an intermediate clinic risk. Associations between clinical characteristics, functional capacity, stress test findings, and  $FFR_{CT}$  results with CAD  $> 50\%$  are outlined in Table 1. The average patient age was 60.3 years, and 42% of the cohort were male. The average patient BMI was 29.5 kg/m<sup>2</sup>. Older age, hypertension, hyperlipidemia, and  $FFR_{CT} < 0.80$  were all significantly associated with CAD  $> 50\%$ . Arrhythmia and hypertensive response with stress, DTS, METS, and exercise duration were not associated with CAD  $> 50\%$  ( $p = 0.66$ ,  $p = 0.70$ ,  $p = 0.59$ ,  $p = 0.07$ , and  $p = 0.25$ , respectively). Furthermore, the development of chest pain during exercise did not correlate with CAD  $> 50\%$  ( $p = 0.66$ ).

Table 2 outlines clinical characteristics, functional capacity, stress test findings, and the association with  $FFR_{CT}$ . Hyperlipidemia was associated with positive  $FFR_{CT}$  ( $p = 0.007$ , Table 2). Arrhythmia and hypertensive response with stress, DTS, METS, and exercise duration were not associated with positive  $FFR_{CT}$  ( $p = 0.56$ ,  $p = 0.53$ ,  $p = 0.30$ ,  $p = 0.90$ , and  $p = 0.54$ , respectively). Development of chest pain during the stress test was not associated with positive  $FFR_{CT}$  ( $p = 0.121$ , Table 2).

Of the 206 stress tests performed, 75% were exercise (70% echocardiographic, 26% nuclear, and 4% EKG alone). Thirty-four percent of patients had an abnormal ETT with  $\geq 1$  mm ST depression, but this was not associated with anatomic or functional CAD on CTA and  $FFR_{CT}$  ( $p = 0.12$  and  $p = 0.20$ , respectively). There was no association between stress test results (positive, negative, equivocal, or indeterminate) and positive CAD  $> 50\%$  ( $p = 0.91$ ) or  $FFR_{CT} < 0.80$  ( $p = 0.927$ ) (Table 3, Figure 1). Of those with a positive stress test, only 30% (3/10) had CAD  $> 50\%$  and only 50% (5/10) had  $FFR_{CT} < 0.80$  ( $p = 0.910$  and  $p = 0.927$ , respectively). Of those with a negative stress test, 40% (31/77) had CAD  $> 50\%$  and 48% (37/77) had  $FFR_{CT} < 0.80$  ( $p = 0.910$  and  $p = 0.927$ , respectively). There was no significant correlation between METS, DTS, or exercise duration and  $FFR_{CT}$  ( $r = 0.093$ ,  $p = 0.274$ ;  $r = 0.012$ ,  $p = 0.883$ ;  $r = 0.034$ ,  $p = 0.680$ , respectively)

TABLE 1: Patient characteristics and associations with CAD &gt; 50%.

Patient characteristics	Total, N = 206, n (%)	CAD > 50%, N = 79, n (%)	CAD < 50%, N = 127, n (%)	p value*
Age, mean (SD)	60.3 (11.5)	62.9 (11.5)	58.7 (11.2)	0.011
BMI, mean (SD)	29.5 (5.6)	30 (5.4)	29.2 (5.7)	0.316
Male	87 (42)	36 (46)	51 (40)	0.444
Diabetes	38 (18)	19 (24)	19 (15)	0.102
HPL	145 (70)	63 (80)	82 (65)	0.020
HTN	135 (66)	63 (80)	72 (57)	0.001
Chest pain during study	14 (7)	6 (8)	8 (6)	0.660
Arrhythmia**	60 (30)	24 (32)	36 (29)	0.658
Hypertensive response	15 (8)	5 (7)	10 (8)	0.699
ST depression $\geq$ 1 mm	71 (34)	22 (28)	49 (39)	0.115
DTS: intermediate risk	74 (50)	25 (51)	49 (50)	0.907
DTS: low risk	73 (50)	24 (49)	49 (50)	
Duke treadmill score, mean (SD)	4.8 (4.8)	4.5 (4.7)	5 (4.9)	0.590
METS score, mean (SD)	10.3 (3.4)	9.6 (3.4)	10.7 (3.4)	0.065
Exercise duration	8.6 (3.3)	8.2 (3.3)	8.9 (3.3)	0.249
<i>FFR-CT:</i>				
FFR-CT < 0.80	94 (46)	54 (68)	40 (31)	<0.001

\*p value calculated with *t*-test, chi-sq test, or Fisher's exact test, where appropriate. \*\*58 PVCs and 2 NSVT/VT.

TABLE 2: Patient characteristics and associations with FFR-CT &lt; 0.80.

Patient characteristics	Total, N = 206, n (%)	FFR-CT < 0.80, N = 94, n (%)	FFR-CT > 0.80, N = 112, n (%)	p value*
Age, mean (SD)	60.3 (11.5)	61 (12.3)	59.7 (10.7)	0.421
BMI, mean (SD)	29.5 (5.6)	29.4 (4.9)	29.6 (6.1)	0.782
Male	87 (42)	43 (46)	44 (39)	0.350
Diabetes	38 (18)	20 (21)	18 (16)	0.337
Hyperlipidemia	145 (70)	75 (80)	70 (63)	0.007
HTN	135 (66)	65 (69)	70 (63)	0.317
Chest pain during study	14 (7)	9 (10)	5 (5)	0.121
Arrhythmia**	60 (30)	29 (32)	31 (28)	0.563
Hypertensive response	15 (8)	8 (9)	7 (6)	0.526
ST depression $\geq$ 1 mm	71 (34)	28 (30)	43 (38)	0.196
DTS: intermediate risk	74 (50)	29 (45)	45 (54)	0.284
DTS: low risk	73 (50)	35 (55)	38 (46)	
Duke treadmill score, mean (SD)	4.8 (4.8)	5.3 (5)	4.5 (4.7)	0.297
METS score, mean (SD)	10.3 (3.4)	10.4 (3.6)	10.3 (3.3)	0.902
Exercise duration	8.6 (3.3)	8.8 (3.3)	8.5 (3.2)	0.536

\*p value calculated with *t*-test, chi-sq test, or Fisher's exact test, where appropriate. \*\*58 PVCs and 2 NSVT/VT.

TABLE 3: Percentage of CAD > 50% and FFR<sub>CT</sub> < 0.80 by stress test result.

CAD	Negative N = 77	Equivocal N = 97	Positive N = 10	Indeterminate N = 22	p value
<50%	46 (59.7%)	61 (62.9%)	7 (70%)	13 (59.1%)	0.910
>50%	31 (40.3%)	36 (37.1%)	3 (30%)	9 (40.9%)	
<i>FFR<sub>CT</sub></i>					
>0.80	40 (51.9%)	55 (56.7%)	5 (50%)	12 (54.5%)	0.927
<0.80	37 (48.1%)	42 (43.3%)	5 (50%)	10 (45.5%)	

(Figures 2–4). Tables 1 and 2 in the supplementary section outline patient characteristics and stress test findings stratified by CAD severity ranges.

## 4. Discussion

We identified a number of important findings:

- (1) In this real-world clinical cohort, positive stress testing in patients without known CAD was not

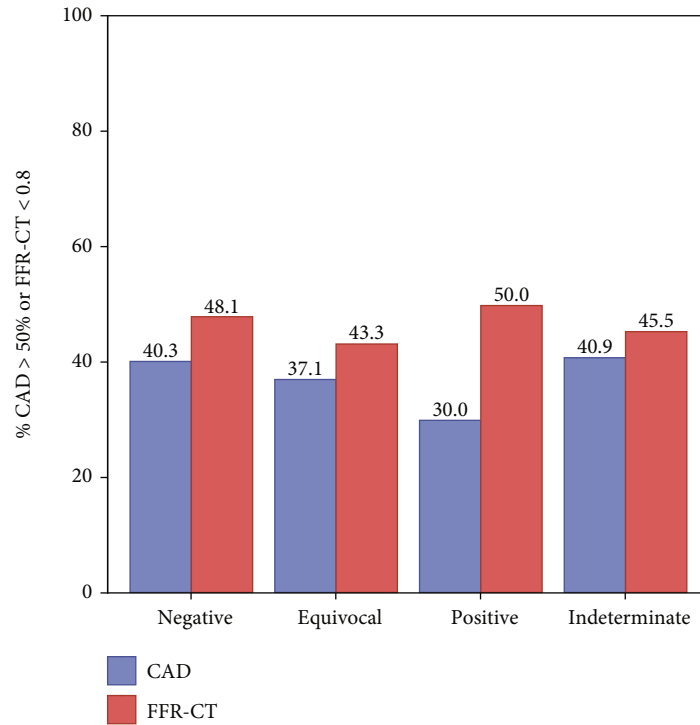


FIGURE 1: Percentage of CAD > 50% or FFR-CT < 0.80 by stress test result.

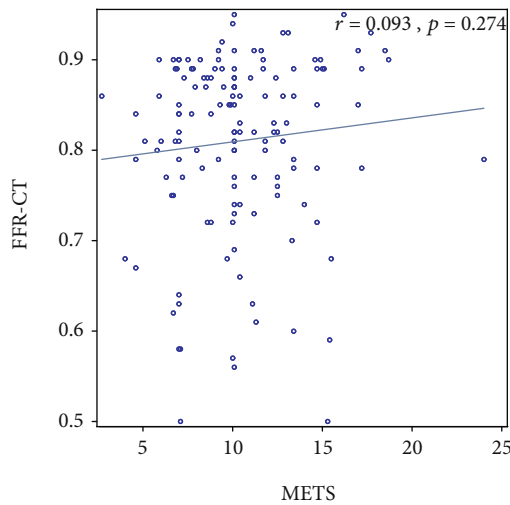


FIGURE 2: Scatter plot showing correlation between metabolic equivalents achieved and  $FFR_{CT}$ .

associated with anatomic or functional CAD using a diagnostic strategy of coronary CTA and  $FFR_{CT}$

- (2) Exercise duration, exercise capacity/achieved workload, and DTS were not correlated with anatomic or functional CAD
- (3) There was no association between chest pain with exercise and anatomic and functional CAD
- (4) Coronary CTA and  $FFR_{CT}$  identified CAD in at-risk patients with equivocal stress tests

For over four decades, functional stress testing has served as the standard cardiovascular diagnostic pathway for those with stable symptoms suggestive of CAD, although it has been reported to have low diagnostic yield at the time of ICA with approximately two-thirds of patients with a positive stress test having no obstructive CAD and 28% of patients with a negative stress test having CAD [3]. An analysis from more than 385,000 patients from >1100 United States hospitals noted that less than half of patients undergoing exercise-treadmill testing, stress echocardiography, and SPECT imaging, prior to their ICA, were found to have obstructive CAD [18]. Noninvasive testing made a similar prediction of obstructive CAD compared to clinical factors. In addition, a Duke University study of over 15,000 patients found that among patients referred for ICA, those with a positive stress test were less likely to have obstructive CAD compared to those with either a negative stress test or no testing at all [19]. Recently, the NIH-funded international ISCHEMIA trial demonstrated that in patients with moderate-severe ischemia on functional stress testing, over 14% demonstrated no obstructive CAD on coronary CTA [20]. Coronary CTA has become an established diagnostic modality for the assessment of CAD [14–16, 21]. It is a sensitive study, reliably confirms the absence of CAD, and aids in the identification of nonobstructive CAD for which providers can institute optimal medical therapy to reduce cardiac events [22]. In the multicenter randomized controlled trial SCOT-HEART, the use of coronary CTA in addition to standard care in patients with stable chest pain resulted in a significantly lower rate of death from heart disease or nonfatal myocardial infarction (MI) than standard care alone [23]. Similar to prior studies, in our



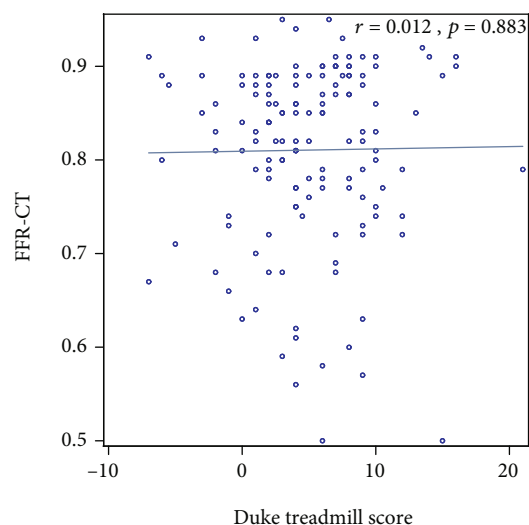


FIGURE 3: Scatter plot showing correlation between Duke treadmill score and  $FFR_{CT}$ .

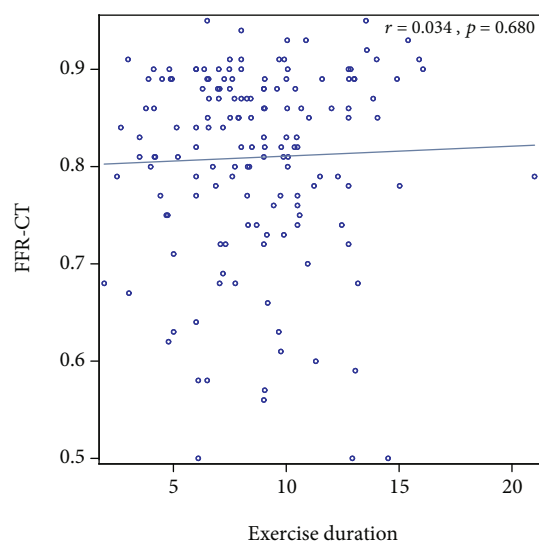


FIGURE 4: Scatter plot showing correlation between exercise duration and  $FFR_{CT}$ .

analysis, stress testing positivity did not accurately identify obstructive CAD. Only 30% of patients with a positive stress test had obstructive CAD. In addition, of those with a negative stress test, 40% had obstructive CAD.

Similar to ICA, coronary CTA alone does not allow for the interpretation of functional importance of intermediate stenoses. It is well known that there is poor correlation between the angiographic severity of a coronary stenosis and its functional significance and numerous studies have shown that FFR is better at identifying lesions responsible for ischemia and improves outcomes when guiding revascularization [24]. The addition of  $FFR_{CT}$  has improved the performance of coronary CTA for the diagnosis of clinically important CAD [5, 25] and decreases the need for ICA [26, 27]. In our analysis, approximately 50% of patients with a negative stress

test had a positive  $FFR_{CT}$  in at least one epicardial coronary artery. Importantly, only 50% of patients with a positive stress test had a positive  $FFR_{CT}$ .

Despite its rather low sensitivity for the prediction of obstructive CAD, functional capacity, as assessed by ETT, is often regarded as one of the most important prognostic variables [28, 29]. In a seminal work by McNeer et al., patients with poor functional capacity were more likely to have anatomic CAD and worse survival [30]. Whether patients with a high exercise capacity are at a low risk for functional CAD as assessed by  $FFR_{CT}$  is unknown. In this analysis, patients had excellent functional capacity, achieving on average 10 METS with a mean exercise duration > 8 minutes. Patients with CAD > 50% had similar functional capacity to those with CAD < 50% disease. Likewise, patients with positive  $FFR_{CT}$  had similar achieved workload and exercise duration to those with negative  $FFR_{CT}$ . In addition, there were no significant correlations between METS, or exercise duration and  $FFR_{CT}$ .

Although the DTS has been shown to predict adverse outcome and mortality, this analysis did not find an association of DTS with anatomic or functional CAD as assessed by coronary CTA and  $FFR_{CT}$ . On average, study patients had a low risk DTS. The mean DTS for our cohort was 4.8, with 55% of patients being low annual risk and 45% intermediate risk of death [31]. Although we did not assess mortality, patients with a low DTS may be mistakenly inferred to have nonsignificant CAD translating to a missed opportunity for medical optimization and improved outcomes. Both low and intermediate DTS patients had similar rates of CAD > 50% and/or  $FFR_{CT}$  < 0.80, highlighting that the low and intermediate DTS may not be associated with anatomic and functional extent of CAD. Consistent with a prior study using invasive FFR, in our analysis, there was no significant correlation between numerical DTS and  $FFR_{CT}$  [32].

Many patients experience MI without any prior symptoms. In a study of over 9000 patients who were free of cardiovascular disease at baseline from the Atherosclerosis Risk in Communities study, >45% of incident MI were asymptomatic in nature [33]. These individuals often lack medical treatments that may prevent subsequent adverse outcomes, including a second MI or even death [34]. In addition, the prognosis of patients with asymptomatic MI is similar, if not worse, than those with clinically evident MI [35]. Various coronary CTA studies in asymptomatic individuals have identified a significant number of patients with prognostically important CAD [36, 37]. Interestingly, in our study, there was no correlation between chest pain during the stress test and anatomic or functional CAD. A coronary CTA and  $FFR_{CT}$  diagnostic strategy may play a critical role in identifying and treating these at-risk patients.

Patients with equivocal or discordant stress test findings represent a unique patient population and often present a challenge for the treating physician. In fact, this group represents the largest portion of our stress patients with 47% of patients having an equivocal stress test. Of all the equivocal stress tests, 37% had CAD > 50% and 43% had  $FFR_{CT}$  < 0.80. Patients with discordant or equivocal stress results have an excess risk for adverse cardiac events. In a recent large

single-center study, researchers analyzed >15,000 patients undergoing stress testing and found that patients with equivocal stress tests had higher rates of major adverse cardiac events compared to patients with negative stress findings [19]. Coronary CTA and  $\text{FFR}_{\text{CT}}$  may play an important role in the diagnosis and management of patients with equivocal stress tests.

## 5. Limitations

Coronary flow reserve has been associated with exercise capacity and was not assessed in this study. Coronary microvascular dysfunction may have been a reason for reduced exercise capacity in patients who have no apparent anatomic or functional epicardial CAD. Stress testing and coronary CTA did not occur on the same day, and it remains possible that CAD could have progressed between study dates. This remains unlikely since there was only a median 49-day difference between study modalities, and no patients underwent revascularization between tests. This is a single-center retrospective study with a limited sample size. Females represented 58% of the study population, which is higher compared to many CAD clinical trials. Recently,  $\text{FFR}_{\text{CT}}$  was noted to differ between sexes as women have a higher  $\text{FFR}_{\text{CT}}$  for the same degree of stenosis [38]. In  $\text{FFR}_{\text{CT}}$ -positive CAD, women had less obstructive CAD. Further study is needed comparing gender specific differences of stress test findings to anatomic or functional extent of CAD. In addition, the average BMI of our population was  $30 \text{ kg/m}^2$ , which is more typical of the United States population compared to individuals in other geographic areas of the world, and may have impacted our findings. Finally, given the retrospective nature of this study, the choice of stress modality and subsequent referral to CTA is complex for which not all confounding variables can be accounted for and could have led to the potential of inclusion bias. Therefore, the results of this analysis are hypothesis generating and larger analyses are needed to definitively address the association of stress parameters with anatomic and functional epicardial CAD.

## 6. Conclusion

Stress testing results, metrics of functional capacity, chest pain with exercise, and low-intermediate DTS are not associated with anatomic or functional CAD by coronary CTA and  $\text{FFR}_{\text{CT}}$ .

## Data Availability

Access to data is available upon request.

## Conflicts of Interest

Dr. Nieman has received unrestricted institutional research grants from Siemens, Bayer, GE, and HeartFlow. Dr. Pontone is a consultant for GE Healthcare and has received research grants from GE Healthcare and Heartflow. Dr. Leipsic is a

consultant to HeartFlow. Dr. Rabbat is a consultant to HeartFlow.

## Acknowledgments

This study was supported by Cardiovascular Research Institute Research Grant from Loyola University Medical Center.

## Supplementary Materials

Tables 1 and 2 outline patient characteristics and stress test findings stratified by CAD severity ranges. (*Supplementary Materials*)

## References

- [1] D. B. Mark, M. A. Hlatky, Harrell FE Jr, K. L. Lee, R. M. Califf, and D. B. Pryor, "Exercise treadmill score for predicting prognosis in coronary artery disease," *Annals of internal medicine*, vol. 106, no. 6, pp. 793–800, 1987.
- [2] A. D. Kelion and E. D. Nicol, "The rationale for the primacy of coronary CT angiography in the National Institute for Health and Care Excellence (NICE) guideline (CG95) for the investigation of chest pain of recent onset," *Journal of Cardiovascular Computed Tomography*, vol. 12, no. 6, pp. 516–522, 2018.
- [3] M. R. Patel, E. D. Peterson, D. Dai et al., "Low diagnostic yield of elective coronary angiography," *New England Journal of Medicine*, vol. 362, no. 10, pp. 886–895, 2010.
- [4] G. Pontone and M. G. Rabbat, "The New Era of Computational Fluid Dynamics in CT Angiography," *JACC: Cardiovascular Imaging*, vol. 10, no. 6, pp. 674–676, 2017.
- [5] B. K. Koo, A. Erglis, J. H. Doh et al., "Diagnosis of ischemia-causing coronary stenoses by noninvasive fractional flow reserve computed from coronary computed tomographic angiograms: results from the prospective multicenter DISCOVER-FLOW (Diagnosis of Ischemia-Causing Stenoses Obtained Via Noninvasive Fractional Flow Reserve) Study," *Journal of the American College of Cardiology*, vol. 58, no. 19, pp. 1989–1997, 2011.
- [6] R. Nakazato, H. B. Park, D. S. Berman et al., "Noninvasive fractional flow reserve derived from computed tomography angiography for coronary lesions of intermediate stenosis severity results from the DeFACTO study," *Circulation: Cardiovascular Imaging*, vol. 6, no. 6, pp. 881–889, 2013.
- [7] P. S. Douglas, G. Pontone, M. A. Hlatky et al., "Clinical outcomes of fractional flow reserve by computed tomographic angiography-guided diagnostic strategies vs. usual care in patients with suspected coronary artery disease: the prospective longitudinal trial of  $\text{FFR}_{\text{CT}}$ : outcome and resource impacts study," *European heart journal*, vol. 36, no. 47, pp. 3359–3367, 2015.
- [8] M. A. Hlatky, B. de Bruyne, G. Pontone et al., "Quality-of-life and economic outcomes of assessing fractional flow reserve with computed tomography angiography: PLATFORM," *Journal of the American College of Cardiology*, vol. 66, no. 21, pp. 2315–2323, 2015.
- [9] M. Rabbat, J. Leipsic, J. Bax et al., "Fractional flow reserve derived from coronary computed tomography angiography safely defers invasive coronary angiography in patients with stable coronary artery disease," *Journal of Clinical Medicine*, vol. 9, no. 2, 2020.

- [10] G. F. Fletcher, P. A. Ades, P. Kligfield et al., "American Heart Association Exercise, Cardiac Rehabilitation, and Prevention Committee of the Council on Clinical Cardiology, Council on Nutrition, Physical Activity and Metabolism, Council on Cardiovascular and Stroke Nursing, and Council on Epidemiology and Prevention Exercise standards for testing and training," *Circulation*, vol. 128, no. 8, pp. 873–934, 2013.
- [11] P. A. Pellikka, A. Arruda-Olson, F. A. Chaudhry et al., "Guidelines for performance, interpretation, and application of stress echocardiography in ischemic heart disease: from the American Society of Echocardiography," *Journal of the American Society of Echocardiography*, vol. 33, no. 1, pp. 1–41.e8, 2020.
- [12] S. Dorbala, K. Ananthasubramaniam, I. S. Armstrong et al., "Single photon emission computed tomography (SPECT) myocardial perfusion imaging guidelines: instrumentation, acquisition, processing, and interpretation," *Journal of Nuclear Cardiology*, vol. 25, no. 5, pp. 1784–1846, 2018.
- [13] J. Leipsic, S. Abbara, S. Achenbach et al., "SCCT guidelines for the interpretation and reporting of coronary CT angiography: a report of the Society of Cardiovascular Computed Tomography Guidelines Committee," *Journal of Cardiovascular Computed Tomography*, vol. 8, no. 5, pp. 342–358, 2014.
- [14] M. J. Budoff, D. Dowe, J. G. Jollis et al., "Diagnostic Performance of 64-Multidetector Row Coronary Computed Tomographic Angiography for Evaluation of Coronary Artery Stenosis in Individuals Without Known Coronary Artery Disease: Results From the Prospective Multicenter ACCURACY (Assessment by Coronary Computed Tomographic Angiography of Individuals Undergoing Invasive Coronary Angiography) Trial," *Journal of the American College of Cardiology*, vol. 52, no. 21, pp. 1724–1732, 2008.
- [15] W. B. Meijboom, M. F. L. Meijjs, J. D. Schuijff et al., "Diagnostic Accuracy of 64-Slice Computed Tomography Coronary Angiography: A Prospective, Multicenter, Multivendor Study," *Journal of the American College of Cardiology*, vol. 52, no. 25, pp. 2135–2144, 2008.
- [16] J. M. Miller, C. E. Rochitte, M. Dewey et al., "Diagnostic performance of coronary angiography by 64-row CT," *The New England Journal of Medicine*, vol. 359, no. 22, pp. 2324–2336, 2008.
- [17] C. A. Taylor, T. A. Fonte, and J. K. Min, "Computational fluid dynamics applied to cardiac computed tomography for noninvasive quantification of fractional flow reserve: scientific basis," *Journal of the American College of Cardiology*, vol. 61, no. 22, pp. 2233–2241, 2013.
- [18] M. R. Patel, D. Dai, A. F. Hernandez et al., "Prevalence and predictors of nonobstructive coronary artery disease identified with coronary angiography in contemporary clinical practice," *American heart journal*, vol. 167, no. 6, pp. 846–852.e2, 2014.
- [19] M. A. Daubert, J. Sivak, A. Dunning et al., "Implications of abnormal exercise electrocardiography with normal stress echocardiography," *JAMA internal medicine*, vol. 180, no. 4, pp. 494–502, 2020.
- [20] D. J. Maron, J. S. Hochman, H. R. Reynolds et al., "Initial invasive or conservative strategy for stable coronary disease," *New England Journal of Medicine*, vol. 382, no. 15, pp. 1395–1407, 2020.
- [21] D. Neglia, D. Rovai, C. Caselli et al., "Detection of significant coronary artery disease by noninvasive anatomical and functional imaging," *Circulation: Cardiovascular Imaging*, vol. 8, no. 3, 2015.
- [22] I. C. Hwang, J. Y. Jeon, Y. Kim et al., "Statin therapy is associated with lower all-cause mortality in patients with non-obstructive coronary artery disease," *Atherosclerosis*, vol. 239, no. 2, pp. 335–342, 2015.
- [23] The SCOT-HEART Investigators, D. E. Newby, P. D. Adamson et al., "Coronary CT angiography and 5-year risk of myocardial infarction," *The New England Journal of Medicine*, vol. 379, no. 10, pp. 924–933, 2018.
- [24] B. de Bruyne, W. F. Fearon, N. H. J. Pijls et al., "Fractional flow reserve-guided PCI for stable coronary Artery disease," *New England Journal of Medicine*, vol. 371, no. 13, pp. 1208–1217, 2014.
- [25] J. K. Min, J. Leipsic, M. J. Pencina et al., "Diagnostic accuracy of fractional flow reserve from anatomic CT angiography," *Jama*, vol. 308, no. 12, pp. 1237–1245, 2012.
- [26] M. G. Rabbat, D. S. Berman, M. Kern et al., "Interpreting results of coronary computed tomography angiography-derived fractional flow reserve in clinical practice," *Journal of Cardiovascular Computed Tomography*, vol. 11, no. 5, pp. 383–388, 2017.
- [27] C. Ball, G. Pontone, and M. Rabbat, "Fractional flow reserve derived from coronary computed tomography angiography datasets: the next frontier in noninvasive assessment of coronary artery disease," *BioMed Research International*, vol. 2018, Article ID 2680430, 8 pages, 2018.
- [28] J. Myers, M. Prakash, V. Froelicher, D. Do, S. Partington, and J. E. Atwood, "Exercise capacity and mortality among men referred for exercise testing," *The New England Journal of Medicine*, vol. 346, no. 11, pp. 793–801, 2002.
- [29] R. K. Hung, M. H. al-Mallah, J. W. McEvoy et al., "Prognostic value of exercise capacity in patients with coronary artery disease: the FIT (Henry Ford Exercise Testing) project," *Mayo Clinic Proceedings*, vol. 89, no. 12, pp. 1644–1654, 2014.
- [30] J. F. McNeer, J. R. Margolis, K. L. Lee et al., "The role of the exercise test in the evaluation of patients for ischemic heart disease," *Circulation*, vol. 57, no. 1, pp. 64–70, 1978.
- [31] D. B. Mark, L. Shaw, F. E. Harrell et al., "Prognostic value of a treadmill exercise score in outpatients with suspected coronary artery disease," *New England Journal of Medicine*, vol. 325, no. 12, pp. 849–853, 1991.
- [32] S. Kalaycı, B. Kalaycı, E. Şahan, and A. A. Ayyılmaz, "Association between fractional flow reserve and Duke treadmill score in patients with single-vessel disease," *Kardiologia Polska (Polish Heart Journal)*, vol. 75, no. 9, pp. 877–883, 2017.
- [33] Z. M. Zhang, P. M. Rautaharju, R. J. Prineas et al., "Race and sex differences in the incidence and prognostic significance of silent myocardial infarction in the Atherosclerosis Risk in Communities (ARIC) study," *Circulation*, vol. 133, no. 22, pp. 2141–2148, 2016.
- [34] Y. B. Pride, B. J. Piccirillo, and C. M. Gibson, "Prevalence, consequences, and implications for clinical trials of unrecognized myocardial infarction," *American Journal of Cardiology*, vol. 111, no. 6, pp. 914–918, 2013.
- [35] W. B. Kannel and R. D. Abbott, "Incidence and prognosis of unrecognized myocardial infarction," *New England Journal of Medicine*, vol. 311, no. 18, pp. 1144–1147, 1984.
- [36] A. I. Guaricci, V. Lorenzoni, M. Guglielmo et al., "Prognostic relevance of subclinical coronary and carotid atherosclerosis in a diabetic and nondiabetic asymptomatic population," *Clinical cardiology*, vol. 41, no. 6, pp. 769–777, 2018.

- [37] E. di Cesare, L. Patriarca, L. Panebianco et al., "Coronary computed tomography angiography in the evaluation of intermediate risk asymptomatic individuals," *La radiologia medica*, vol. 123, no. 9, pp. 686–694, 2018.
- [38] T. A. Fairbairn, R. Dobson, L. Hurwitz-Koweek et al., "Sex Differences in Coronary Computed Tomography Angiography-Derived Fractional Flow Reserve: Lessons From ADVANCE," *JACC: Cardiovascular Imaging*, vol. 13, no. 12, pp. 2576–2587, 2020.



## Review Article

# Speckle Tracking Echocardiography: Early Predictor of Diagnosis and Prognosis in Coronary Artery Disease

**Maria Concetta Pastore** <sup>1,2</sup>, **Giulia Elena Mandoli** <sup>1</sup>, **Francesco Contorni**,<sup>1</sup> **Luna Cavigli**,<sup>1</sup> **Marta Focardi**,<sup>1</sup> **Flavio D'Ascenzi**,<sup>1</sup> **Giuseppe Patti**,<sup>2</sup> **Sergio Mondillo**,<sup>1</sup> and **Matteo Cameli** <sup>1</sup>

<sup>1</sup>Department of Medical Biotechnologies, Division of Cardiology, University of Siena, Italy

<sup>2</sup>University of Eastern Piedmont, Maggiore della Carità Hospital, Novara, Italy

Correspondence should be addressed to Matteo Cameli; [matteo.cameli@yahoo.com](mailto:matteo.cameli@yahoo.com)

Received 29 October 2020; Revised 12 December 2020; Accepted 23 January 2021; Published 3 February 2021

Academic Editor: Marco Guglielmo

Copyright © 2021 Maria Concetta Pastore et al. This is an open access article distributed under the Creative Commons Attribution License, which permits unrestricted use, distribution, and reproduction in any medium, provided the original work is properly cited.

Echocardiography represents a first level technique for the evaluation of coronary artery disease (CAD) which supports clinicians in the diagnostic and prognostic workup of these syndromes. However, visual estimation of wall motion abnormalities sometimes fails in detecting less clear or transient myocardial ischemia and in providing accurate differential diagnosis. Speckle tracking echocardiography (STE) is a widely available noninvasive tool that could easily and quickly provide additive information over basic echocardiography, since it is able to identify subtle myocardial damage and to localize ischemic territories in accordance to the coronary lesions, obtaining a clear visualization with a “polar map” useful for differential diagnosis and management. Therefore, it has increasingly been applied in acute and chronic coronary syndromes using rest and stress echocardiography, showing good results in terms of prediction of CAD, clinical outcome, left ventricular remodeling, presence, and quantification of new/residual ischemia. The aim of this review is to illustrate the current available evidence on STE usefulness for the assessment and follow-up of CAD, discussing the main findings on bidimensional and tridimensional strain parameters and their potential application in clinical practice.

## 1. Background

It is widely known that echocardiography is an essential supporting tool for clinicians in the evaluation of coronary artery disease (CAD). Its application could vary between acute and chronic coronary syndromes (ACS and CCS); however, it has shown not only to aid diagnosis but also to provide useful prognostic information in this clinical setting.

The gradual introduction of speckle tracking echocardiography (STE) into clinical practice and its validation for diagnosis and risk stratification in different cardiac disease [1–4] with a great feasibility [5] have allowed to appreciate its potential additive value also for patients with CAD [6].

In fact, speckle tracking analysis is capable to assess typical ischemic subendocardial damage through several parameters: longitudinal strain (LS), which is the most used STE parameter to assess the early affection of subendocardial

fibers of all cardiac chambers; bull's eye representation of left ventricular global LS (LVGLS) that provides a regional evaluation of LV injury according to coronary vascularization territories and the specific analysis of endocardial wall deformation properties with the three-layer analysis [7]. These tools could be useful to promptly guide diagnosis in uncertain cases of ACS and to provide early detection of CCS. Moreover, speckle tracking analysis could be performed on stress echocardiography (SE) images to assess subtle myocardial damage in case of doubtful stress test results or to assess myocardial viability [8]. STE was also shown to be a marker of myocardial fibrosis [9]; therefore, it could represent a non-invasive marker of myocardial postischemic scar.

The present review is aimed at providing an overview of the different clinical applications of sSTE for the evaluation of CAD, highlighting benefits and challenges of its inclusion in the diagnostic and prognostic workup of ACS and CCS.

## 2. CAD Diagnosis

The latest European Society of Cardiology (ESC) guidelines for the diagnosis and management of non-ST-elevation ACS [10] (NSTEMI-ACS) and CCS [11] suggest the use of speckle tracking to support diagnosis in patients referred to echocardiography for clinical suspicion of ischemic disease and absence of visual wall motion abnormalities. In fact, high sensitivity and specificity (86% and 73%, respectively) were reported for cutoff values of LVGLS  $> -18.8\%$  and of LV global circumferential strain (GCS)  $> -21.7\%$  (87% and 76%, respectively) to detect significant coronary stenosis in patients with chest pain and inconclusive electrocardiographic (ECG) and blood test results [12], providing an additive value to the wall motion score index (WMSI).

Accordingly, a meta-analysis including 1385 patients analyzed LVGLS ability to reveal CAD, showing satisfactory results for this noninvasive marker. The mean values of LVGLS for those with and without CAD were  $-16.5\%$  [95% confidence interval (CI):  $-15.8\%$  to  $-17.3\%$ ] and  $-19.7\%$  [95% CI:  $-18.8\%$  and  $-20.7\%$ ]. Moreover, abnormal LVGLS detected moderate-to-severe CAD with a pooled 74.4% sensitivity, 72.1% specificity, 2.9 positive likelihood ratio, and 0.35 negative likelihood ratio. The area under the curve (AUC) and diagnostic odds ratio (OR) were 0.81 and 8.5, respectively [13].

What is more, LVGLS bull's eye polar maps offer an easy and quick assessment of regional distribution of myocardial necrosis through regional LS: the division in 17 wall segments from the apex to base and the visualization of a circumscribed blue area in specific segments allow to determine the distribution of blood flow abnormalities according to the culprit coronary artery (Figure 1). Moreover, regional LS can be useful for the differential diagnosis between ACS and Takotsubo syndrome, which has typical LV strain patterns of the polar map with exclusive involvement of apical segment, and between ACS and acute myocardial infarction (AMI) since the impaired areas do not follow a typical coronary topographic localization [12].

Some authors claim that the analysis of LV regional function by segmental LS is not recommended because of less reliability and large intervendor and interobserver variabilities [14]. Therefore, it would be reasonable to use regional strain distribution to overall assess typical patterns in order to guide diagnosis, rather than evaluating the numerical segment-specific strain values, and prefer using LVGLS as the diagnostic index [1]. Moreover, high heart rate, lack of ECG tracing, and poor acoustic window (a frequent circumstance in acute settings with limited patients' movement and collaboration) strongly limit its application in the acute phase.

Therefore, in the last years, advanced imaging modalities have been proposed for the evaluation of CAD: while cardiac computed tomography (CCT) use has been recommended in the last ESC guidelines [10, 11] and National Institute for Health and Care Excellence (NICE) for younger patients with chest pain and low pretest probability of CAD, due to its greater anatomic insights and high negative predictive value (NPV) [15], cardiac magnetic resonance could be preferred for prognostic purposes in ACS and CCS [16]. In fact, in a

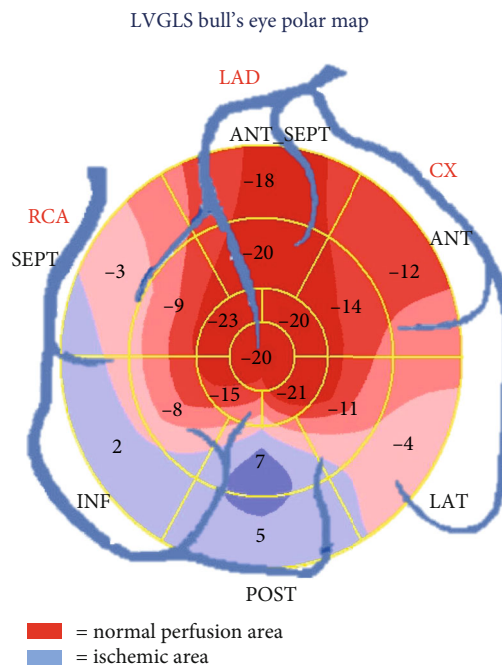


FIGURE 1: Bull's eye polar map representation of regional global longitudinal strain according to specific territories of coronary artery vascularization on a 17-segments model. The "blue" segments represent the ischemic area. ANT: anterior; SEPT: septal; ANT\_SEPT: anteroseptal region; CX: circumflex coronary artery; INF: inferior; LAD: left anterior descending coronary artery; LAT: lateral; POST: posterior; RCA: right coronary artery.

cohort of 206 patients, the application of CCT, as first- or second-line investigation, allowed to spare 42.6% unnecessary invasive coronary angiography (ICA) and 63.7% of additional functional test (when used as first-line exam) [17]. However, CCT pitfalls still remain high costs and have low availability and a need of a specific trained team of operators and clinicians.

Of note, 103 patients with chest pain who underwent multimodality imaging evaluation with stress/rest echocardiography and CCT and LVGLS showed comparable results with CCT for the exclusion of CAD, since patients who had abnormal CCT had lower resting and peak stress GLS than those with normal CCT ( $14.85\% \pm 3.05$  vs  $17.99\% \pm 2.88$ ,  $p < 0.001$ ;  $14.89\% \pm 3.35$  vs  $18.44\% \pm 4.27$ ,  $p = 0.007$ , respectively) [18].

**2.1. Acute Coronary Syndromes.** Being low time-consuming and easy to perform, STE could be applied also in acute settings, either before ICA, in case of uncertain diagnosis, or after revascularization for further risk stratification, if available. In patients hospitalized in a coronary care unit, the reduction of regional LV LS has shown to identify epicardial coronary lesions detected with subsequent ICA; moreover, its calculation after revascularization showed to predict the extension of myocardial necrosis due to the recent ischemia, of LV remodeling, and of postprocedural short-term and long-term complications, such as heart failure (HF) [19–22].

Noteworthy, LVGLS was demonstrated to be more accurate than WMSI in identifying NSTEMI-ACS patients with acute coronary occlusion who may benefit from urgent

reperfusion therapy [23]. This represents an important gateway function of STE, which has been considered in the newest NSTEMI-ACS guidelines [10].

Particularly, LV LS polar maps are able to define the extension and localization of transmural necrosis with nonviable myocardium after AMI [24].

A study investigating the diagnostic power of LVGLS and territorial LV LS to predict CAD in patients with suspected NSTEMI-ACS and normal global/regional systolic function showed that GLS was significantly impaired in patients with significant coronary artery stenosis than those without ( $16.7 \pm 3.4\%$  vs.  $22.4 \pm 2.9\%$ ,  $p < 0.001$ ) [25] and that territorial LS was able to identify the localization of coronary stenosis (left anterior descending artery (LAD), left circumflex artery (CX), and right coronary artery (RCA)); this suggests an incremental diagnostic value of GLS over the visual echocardiographic assessment of wall motion. Moreover,  $GLS > -19.7\%$  showed AUC = 0.92, 81% sensitivity, and 88% specificity for detecting a significant stenosis ( $p < 0.001$ ).

Myocardial strain by echocardiography may also facilitate the exclusion of significant coronary artery stenosis among patients presenting with suspected NSTEMI-ACS with unremarkable ECG findings and normal cardiac biomarkers [1]. In a study on patients referred to the emergency department with suspected NSTEMI-ACS, LVGLS was superior to conventional echocardiographic parameters in distinguishing patients with and without significant coronary artery stenosis ( $>50\%$  luminal narrowing), with high sensitivity and NPV (AUC = 0.87, 93% sensitivity and 78% specificity, 0.74 positive predictive value (PPV), 0.92 NPV) [26]. Another research revealed that GLS and GRACE ACS risk scores were independent predictors of CAD at multivariate analysis (GLS: OR = 0.51,  $p < 0.001$ ; GRACE score: OR = 0.93,  $p = 0.007$ ) in patients with typical chest pain with unstable angina characteristics and a typical rise and/or fall of cardiac biomarkers, aiding in the diagnosis of NSTEMI-ACS [27].

LVGLS diagnostic value and capability to define myocardial infarction size were assessed in a meta-analysis including eleven studies and 765 patients, which compared LVGLS to late gadolinium enhancement (LGE) as a reference method [28]. Pooled estimates of GLS revealed a sensitivity and specificity of 77% and 86%, respectively, with an AUC = 0.70. As for the transmural extent of the infarction (50% of myocardium involved was used as cutoff value), GLS showed a sensitivity and specificity of 76% and 79%, respectively, and an AUC of 0.65. These results suggest that STE could also be used as noninvasive diagnostic parameter to assess myocardial infarction area.

In addition, the analysis of LV torsion by STE has shown surprising results in patients with AMI: there is a direct correlation between torsion values and the area of the extension of myocardial infarction [29]; experimental models showed how LV torsion properties was preserved or mildly reduced for subendocardial ischemia, while being largely reduced in case of transmural ischemia. Of note, it was also considerably reduced 10 minutes after LAD occlusion ( $p < 0.05$ ) [30–32]. Accordingly, other authors described a clear improvement of LV torsion after percutaneous coronary intervention (PCI) [33].

**2.1.1. Takotsubo Syndrome.** In Takotsubo syndrome (TTS) there is a transient reduction of myocardial perfusion without coronary atherosclerotic lesions, in which etiology, probably associated with emotional stress and high catecholamine and serotonin levels [34], is still a matter of research [35]; this could cause temporary LV systolic dysfunction which could mimic ACS. Typically, kinetic abnormalities are focused on the apical region (with hypo-, a-, or dyskinesia of midapical myocardial segments, sometimes associated with hypokinetic mid-segments) preserving the basal region (identifying the so-called “apical ballooning”), last few days, and then complete recovery [36]. Echocardiography has a pivotal role in identifying and in monitoring this regional kinetic impairment and overall cardiac function, in order to guide the diagnostic and therapeutic approach.

As for STE in TTS, its reduction is “circular” rather than being confined to a specific coronary region and LV twisting/untwisting properties are impaired in the acute phase [36].

It has been shown to accurately identify the recovery of myocardial dysfunction in patients with TTS 1 month after the acute phase as compared to patients with AMI [37]. However, more data are required in this field.

**2.2. Stable CAD.** To date, stable CAD was the major setting of investigation of STE among myocardial ischemic disease. Particularly, the importance of the reduction of LVGLS has been shown with rest and SE in both symptomatic and asymptomatic patients for the prediction of significant CAD [8, 38, 39].

As for rest echocardiography,  $GLS > -18\%$  was prevalent in those with significant coronary lesions among 216 patients undergoing ICA for suspected CAD ( $p < 0.0001$ ), with a 91.1% sensitivity, 63% specificity, 80.4% PPV, 81% NPV, and 80.5% accuracy for the detection of significant CAD [40]. In a similar cohort, a stratification of results for one- (AUC 0.95 for  $GLS > -18.44\%$ ), two- (AUC 0.9 for  $GLS > -17.35\%$ ), and three- (AUC 0.68 for  $GLS > -15.33\%$ ) vessel CAD was performed; moreover, segmental LV LS predicted the localization of the affected vessel ( $p \leq 0.001$ ) and had an inverse correlation with SYNTAX score that was significant for high and intermediate score ( $p \leq 0.001$ ) and nonsignificant for low score ( $p = 0.05$ ) [41]. Another study of 211 subjects excluding patients with diabetes mellitus assessed the accuracy of  $GLS > -19\%$  to identify coronary-specific critical stenosis [stenosis  $\geq 70\%$  in  $\geq 1$  epicardial coronary artery ( $\geq 50\%$  in left main coronary artery)]; AUC to detect ICA stenosis was 0.818 for CX, 0.764 for LAD, and 0.723 for RCA, respectively [42].

These results confirmed the additive value of STE for the reliable detection and localization of ischemic myocardium according to coronary perfusion territories also for the study of CCS.

Radwan and Hussein showed a decrease of GLS parallel with an increasing number of coronary vessels involved in patients with stable angina and a significant positive correlation between GLS and LV ejection fraction (EF) ( $r = 0.33$ ;  $p = 0.036$ ); they presented a slightly inferior cutoff for GLS than other studies ( $GLS > -15.6\%$  had AUC 0.88, 95% for the prediction of significant CAD;  $p \leq 0.001$ ), probably due to the higher cutoff of coronary stenosis considered to define significant CAD ( $>70\%$  narrowing) [43].



Furthermore, two studies analyzed GLS performance in patients with normal global and/or regional wall motion on basic rest echocardiography who subsequently underwent ICA. The first study demonstrated a significant inverse correlation between GLS and SYNTAX score values ( $r^2 = 0.38$ ,  $p < 0.001$ ) and identified an optimal cutoff value of  $GLS > -13.95\%$  to detect high severity coronary stenosis (sensitivity = 71%, specificity = 90%,  $p < 0.001$ ) [44]; the second one found an impaired systolic function by GLS and radial strain despite normal wall motion in patients with multivessel CAD [45].

Biering-Sørensen et al. studied 296 patients with stable angina pectoris, no previous CAD, and normal LV EF, finding that GLS was an independent predictor of CAD after multivariable adjustment for baseline data, exercise test, and conventional echocardiography (OR = 1.25,  $p = 0.016$  per 1% decrease) and was able to provide an additive accuracy value to exercise test alone (AUC = 0.84 for exercise test + GLS versus 0.78 for exercise test;  $p = 0.007$ ) [46]. Again, regional LS identified which coronary artery was stenotic, which was also confirmed in another study conducted in younger patients (mean age  $51 \pm 8.7$  years) with suspected CAD [47].

**2.2.1. Three-Layer Analysis.** As previously mentioned, the additional analysis of three myocardial wall layers (epicardial, midwall, and endocardial strains) by STE could be enlightening in patients with CAD, due to the peculiar distribution of ischemic damage starting from endocardium and then reaching the epicardium in the case of transmural myocardial infarction, also providing further insights for differential diagnosis (e.g., endocardial/transmural ischemia, endocardial ischemia/no ischemia, and acute myocarditis).

Therefore, several authors focused on the use of a layer-specific strain in patients with CAD, with greater utilization of circumferential and radial strain for a more reliable delineation of the layers.

Particularly, Liu et al. applied receiver operating characteristic (ROC) curves to assess the performance of three-layer STE analysis in patients with NSTEMI-ACS, showing that endocardial GLS and territorial LAD LS were significantly better markers (AUC = 0.91 and 0.87, respectively) of significant LAD stenosis than that in the mid-myocardial and epicardial layers in these patients [48].

Three studies also evaluated whether layer-specific circumferential strain analysis can identify scars and transmural myocardial infarction, reaching good results also after comparison with CMR [49–51].

Conversely, other authors found that epicardial and mid-myocardial LVGLS had a significantly higher diagnostic performance compared to endocardial GLS for the prediction of significant CAD (>70% coronary stenosis) in 285 patients with clinically suspected stable angina, normal EF, and no previous cardiac history [39].

Therefore, the use of three-layer analysis by STE for the assessment of coronary lesions is still controversial and its results should be taken with caution.

As an attempt to enhance diagnostic accuracy in stable CAD patients, many authors combined the use of physical/pharmacological SE and three-layer STE.

**2.2.2. Stress Echocardiography.** The application of STE to stress echocardiography is still debated, since its feasibility could be limited by high heart rate and poor acoustic window due to patients' position; in fact, it lacks standardization and/or reference cutoffs and strongly depends on the operator's experience [1]. However, to date, there is mounting evidence supporting its use in clinical practice [3, 52].

The first studies with dobutamine SE showed that LV strain was comparable to WMSI for the diagnosis of CAD [53]. Later, LV strain showed a greater predictive value than WMSI for significant coronary artery stenoses in patients with stable CAD undergoing dobutamine SE: in one study, reduced GLS during high dobutamine dose had an AUC of 0.81 (sensitivity 89.4%, specificity 64.7%) vs. 0.78 for WMSI [54]; in another study, GLS had an AUC of 0.95 (sensitivity 94%, specificity 92%) to identify significant CAD (defined as  $\geq 70\%$  diameter stenosis on coronary angiography validated as hemodynamically significant by adenosine CMR) [55]. Furthermore, recovery LVGLS was the strongest predictor of obstructive CAD and was associated with positron emission tomography findings (extent, localization, and depth of myocardial ischemia) [56].

Accordingly, Park et al. found that endocardial LVGLS  $> -16\%$  at recovery phase during dobutamine SE was an important predictor of significant CAD, considerably increasing sensitivity, specificity, PPV, and NPV of visual assessment alone (91%, 91%, 79%, and 96%, respectively, vs. 48%, 83%, 52%, and 81%, respectively) [57].

Nishi et al. demonstrated an association between layer-specific regional LV LS during exercise stress and functionally significant CAD as confirmed by invasive fractional flow reserve in stable patients. Moreover, the combination of endocardial LV LS and percent change in the endocardial-to-epicardial LV LS ratio at early recovery phase offered an incremental diagnostic value to visual estimation of LV wall motion for the detection of the ischemic territory (AUC = 0.75 vs. 0.61 of visual estimation alone,  $p = 0.006$ ) [58].

In 132 patients undergoing adenosine SE and ICA, endocardial, midventricular, and epicardial LVGLS had similar diagnostic values, with high specificity, even though showing modest sensitivity, which could limit its clinical application [59].

An important use of STE during stress echocardiography in clinical practice could be the assessment of subtle myocardial injury in patients with cardiovascular risk factors [60].

Interestingly, two researches evaluated the use of STE during SE in almost-entirely women cohorts: the first one found significantly impaired values of GCS, global radial strain and strain rate, and GLS in patients with angiographically confirmed CAD and a positive exercise stress echocardiography as compared with controls, showing that a combination of GLS, GCS, and standard deviation of the longitudinal strain time-to-peak had very high accuracy for the detection of CAD (AUC = 0.96, sensitivity 97%, specificity 86%) [61]. The other study assessed whether STE during SE could help in the diagnosis of microvascular angina, showing that the most discriminative parameter for microvascular angina during SE was GCS [62].

**2.2.3. The Choice between Global and Regional Strain.** Even though the abovementioned studies showed a valuable

diagnostic power of LVGLS for the study of CAD, since a reduction of LVGLS in patients with typical angina is highly suggestive of CAD, the key for the diagnosis of stable CAD is represented by the additive value of regional strain analysis. However, it is characterized by high variability making its interpretation more challenging and requiring experience, also considering that its sensitivity could vary among different LV segments depending on their location and their echocardiographic visualization (often limited by poor acoustic window) [63]. This is why many authors chose to use more easily and rapidly performing LVGLS that we endorse in order to avoid under- or overestimation of myocardial damage; however, we recommend the integration of STE with clinical data to enhance diagnostic probability.

### 3. Prognosis

The evaluation of patients with acute and chronic CAD using STE has shown to improve the prognostic assessment of these patients, particularly those with preserved EF, as STE is able to predict cardiac dysfunction prior to EF reduction [64]. This is a crucial point, since the development of HF and cardiac death as a consequence of AMI strongly depends on the extent of myocardial damage.

First of all, STE has shown an association with after-ACS event clinical outcome in different studies: a LVGLS  $> -13\%$  measured during the index hospitalization was a predictor of event-free survival in a cohort of both STE-ACS and NSTEMI-ACS [65], while LVGLS  $> -14\%$  predicted admissions for acute HF and cardiovascular mortality in patients with AMI [66].

In 70 patients with NSTEMI-ACS  $< 72$  hours, an impaired baseline LVGLS and its lack of improvement 24 hours after coronary revascularization were associated with negative LV remodeling (defined as lack of improvement of LV function, with increase in LV end-diastolic volume  $\geq 15\%$ ) (OR = 4.3,  $p < 0.0001$ ; OR = 1.45,  $p < 0.01$ , respectively) [21].

Moreover, in a large study of patients with recent AMI, LVGLS and strain rate were significantly and independently correlated with all-cause mortality, reinfarction, revascularization, and HF hospitalization at 3-year follow-up (OR = 4.5 for LVGLS  $< -15.1\%$  and 4.4 for LV strain rate  $> -1.06 \text{ s}^{-1}$ ), and LVGLS was superior to LV EF and WMSI after multivariate analysis [67].

Furthermore, van Mourik et al. demonstrated the additional value of STE over visual echocardiographic evaluation for the accuracy in the detection of postinfarct scars in a cohort of patients analyzed around 110 days after STE-ACS [68]. An early assessment of residual ischemic injury and myocardial viability after AMI can help to optimize the therapeutic management in order to prevent serious complications, such as LV remodeling with development or progressive worsening of HF, arrhythmias and sudden cardiac death, or to identify patients to refer for cardiac surgery, LV mechanical assistance treatment, or preventive intracardiac defibrillator implantation.

Importantly, the evaluation of transmural myocardial ischemia and the degree of endocardial damage play an important role in the prognosis of CAD not only in the acute

phase but also during follow-up, in which STE could be of great utility for its high availability and rapidity of execution.

In fact, Joyce et al. used STE for the evaluation of 105 first STE-ACS patients treated with primary PCI at baseline and during follow-up (together with 3-month SE and 1-year ICA); they found that patients with significant angiographic CAD at 1-year had greater worsening in global LVGLS during SE from rest to peak ( $-16.8 \pm 0.5\%$  to  $-12.6 \pm 0.5\%$ ) compared with patients without significant CAD ( $-16.6 \pm 0.4\%$  to  $-14.3 \pm 0.3\%$ ), with an optimal cutoff of global variation  $\geq 1.9\%$  (AUC 0.70; sensitivity, 87%; specificity, 46%); higher segmental  $\Delta$ GLS was independently associated with significant CAD (OR 1.1) [69].

Also, a prospective study comparing 94 patients with a first AMI and 137 patients with stable CAD, all of whom had undergone coronary revascularization, showed that in stable CAD patients, the addition of endocardial LVGLS  $> -20\%$  to baseline characteristics and EF into a regression model significantly improved the prediction of cardiac events (AUC = 0.86, sensitivity: 79%, specificity: 84%); conversely, the same analysis in AMI patients was unsuccessful to increase the predictive power for cardiac events [70].

Notably, in a small population of after-STE-ACS, three-layer STE was applied to assess the strain gradient between the three layers as a marker of irreversible transmural damage and of myocardial viability, with ROC curves endocardial LS having an AUC = 0.69 and strain gradient having an AUC = 0.73 for myocardial viability [71].

### 4. Postsystolic Shortening

Some authors consider the calculation of postsystolic shortening (PSS) during strain analysis in patients with CAD as equally or more important to commonly used LV strain, since its presence is a characteristic feature of myocardial ischemic dysfunction [72].

PSS is defined as myocardial shortening that occurs after end-systole and is observed mainly during isovolumic relaxation [73]. This relies on the fact that regional contraction of the myocardium depends not only by inherent contractility of the concerned myocardium but also by tension from the surrounding myocardium. Therefore, in case of reduced regional contractility because of ischemia, the amplitude of shortening during ejection time decreases, and early systolic lengthening (ESL) and PSS are observed in the ischemic myocardium.

In some case of myocardial ischemia when regional wall motion abnormalities are not seen on visual assessment, the analysis of the LV strain curve show PSS, appearing as the peak of regional LS that occurs after aortic valve closure (AVC).

The mostly used parameter to quantify PSS is postsystolic index, which is calculated as follows:  $([\text{peak postsystolic strain}] - [\text{end-systolic strain}] / (\text{peak strain or maximum strain change during the cardiac cycle}))$ , showing the ratio of the amplitude of PSS to total shortening. The time from aortic valve closure to peak postsystolic strain is used as another parameter [74].

TABLE 1: Medium cutoff values of strain parameters for diagnosis and prognostic assessment of coronary artery disease based on the available literature.

	Diagnosis		Prognosis	
	Acute	Chronic	Acute	Chronic
GLS	-17.82% [12, 13, 26, 27]	-17.41% [37, 39, 41–43] SE: -16.75% [55, 56, 58]	-13.32% [20, 21, 64–66]	—
GCS	-17.35% [12, 19]	—	-13% [19]	-20% [69]
GRS	—	—	—	—
Regional LS	—	-20.45% [44, 64]	—	—
Torsion	1.39 degrees/cm	—	—	—
PSS	-13.9% [73]	—	—	—
PALS	—	—	—	—
fwRVLS	—	—	—	—
3D strain echocardiography	3D GLS: -11.75% [89, 90] 3D GAS: -21% [90]		—	—

fwRVLS: free-wall RVLS; GAS: global area strain; GCS: global circumferential strain; GLS: global longitudinal strain; GRS: global radial strain; PALS: peak atrial longitudinal strain; PSS: post systolic-shortening; SE: stress echocardiography.

The assessment of PSS is valuable in identifying acute ischemia, because PSS occurs in the myocardium with regional contractile dysfunction [75]. It was found to be a reliable index for the diagnosis of CAD, at rest and during SE [46], and also to be associated with prognosis in patients with stable angina [76].

## 5. Other Cardiac Chambers

Even though the most studied cardiac chamber for the evaluation of CAD is the LV, representing the largest part of myocardium and being responsible of cardiac pump function and output, the other cardiac chambers could be either directly involved in ischemic cardiac damage (particularly, left atrium (LA) in the case of CX lesions and right ventricle (RV) in the case of RCA) or secondarily affected due to post-ischemic acute or chronic HF [77].

As the application of STE to LA and RV has been increasingly performed for the evaluation of HF, valvular disease, hypertension, etc. [78–80] showing great feasibility regardless of the operator's experience [81], it has also recently been extended to patients with CAD.

**5.1. Left Atrial Strain in CAD.** In 68 patients with AMI treated with emergent or urgent PCI, peak atrial longitudinal strain (PALS) was lower in patients with a CX culprit lesion than those with culprit lesions in other vessels, whereas the LA volume index did not show any difference. This confirms the importance of LA strain over dimensional measures for the early diagnosis of myocardial damage [82].

In a small study involving patients with stable CAD undergoing ICA, PALS and peak atrial contraction strain (PACS) were significantly reduced in patients with SYNTAX score  $\geq 33$ ; notably, these parameters had a close negative correlation with such parameter ( $r = 0.861$ ;  $p < 0.001$ ) [83]. LA strain was also related to clinical outcome in a cohort of patients with AMI undergoing PCI [84].

Meanwhile, in patients with typical Takotsubo syndrome who underwent transthoracic-Doppler echocardiography dur-

ing the acute phase and at follow-up ( $32 \pm 18$  days later), PALS was transiently impaired at baseline and was associated to in-hospital complications. Moreover, LA strain improved parallel to the dynamic improvement of LV GLS, following the typical feature of a transient myocardial damage of the disease [85].

**5.2. Right Ventricular Strain in CAD.** As previously mentioned, RV dysfunction was found by STE in 87 patients with CAD involving RCA, in whom free wall RV LS was an independent predictor of RCA involvement at multivariate analysis (OR = 1.07; 95%;  $p = 0.02$ ) [86]. Therefore, it could be used as a reliable marker of RV dysfunction in patients with inferior AMI.

Moreover, RV involvement has shown significant prognostic consequences in CAD: patients with acute MI complicated by cardiogenic shock showed a worse prognosis if RV dysfunction by echocardiography was present [87]. Antoni et al. also showed that a reduction of RV strain was an independent predictor of death, reinfarction, and HF hospitalization (hazard ratio = 1.08) in patients with AMI treated with PCI; finally, RV strain provided an incremental value to clinical information, infarct characteristics, LV function, and RVFAC [88].

## 6. 3D Strain

The advances in cardiac imaging and the development of new devices have led to more availability of three-dimensional (3D) echocardiography, which provides further insights on cardiac anatomy and is considered superior to 2D echocardiography for the assessment of cardiac geometry. However, 3D strain value in clinical practice is still debatable, also due to vendor-dependency and the lack of standardization.

However, recent studies suggested a potential role of 3D strain for the evaluation of patients with stable and unstable CAD.

A recent investigation involving 255 STE-ACS patients undergoing PCI demonstrated that 3D-LVGLS was the strongest predictor of LV reverse remodeling (OR = 1.43,  $p$

TABLE 2: Benefits and drawbacks of using speckle tracking echocardiography for the evaluation of coronary artery disease.

Advantages	Disadvantages
Noninvasive	Lack of standardization and defined cutoff values
Availability and repeatability	Operator-dependence
Rapidity	Acoustic window-dependence
Portability	Challenging in case of high heart rate and arrhythmias
Low costs	Lower spatial resolution than other imaging methods
Semiautomatic and angle-independent (more reliable than 2D-echo)	
Early diagnosis with regional localization of myocardial injury	
Differential diagnosis with bull eye-specific patterns	

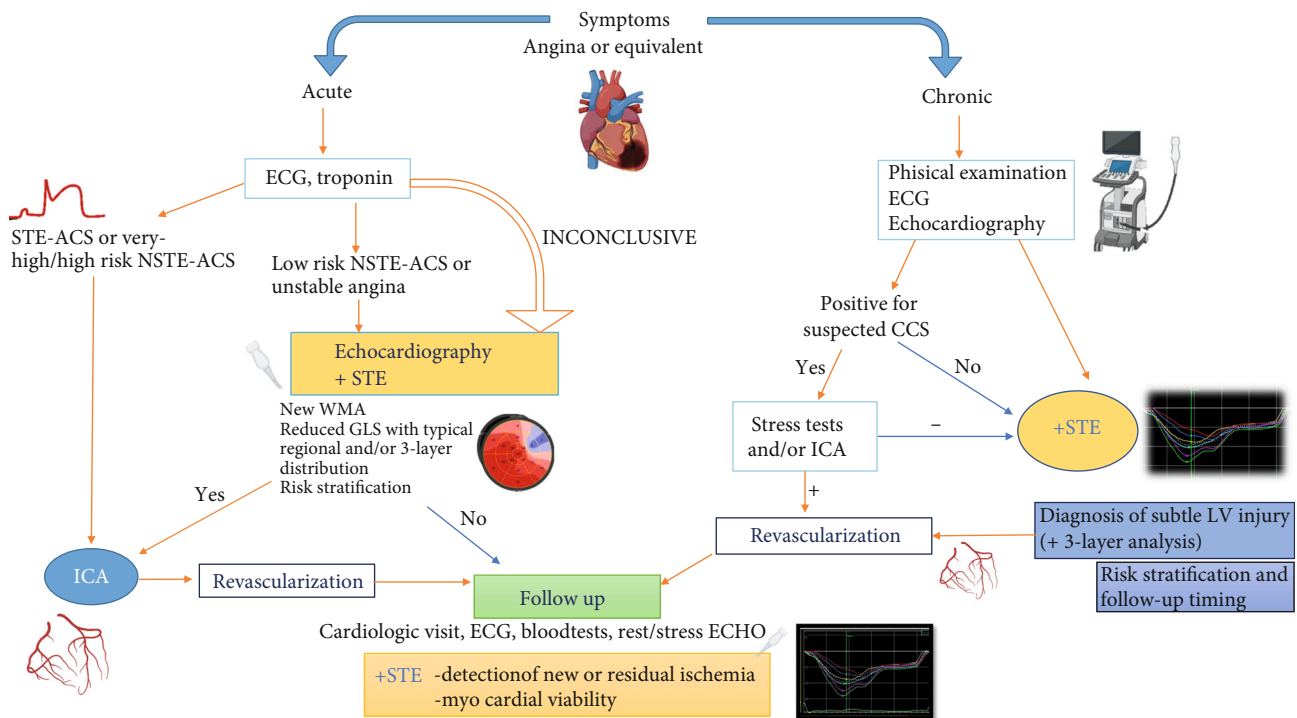


FIGURE 2: Potential integration of speckle tracking echocardiography as additive tool in diagnostic and follow-up algorithms of acute and chronic coronary syndromes. Large prospective studies are needed to validate this algorithm and investigate its impact on clinical outcome.

= 0.02) and major adverse cardiac events (OR = 1.44,  $p < 0.0001$ ), being superior to bidimensional LVGLS for the prediction of outcome [89]. Similar results on 3D strain as the index of future LV reverse remodeling were showed in another STE-ACS cohort [90].

Moreover, in patients with NSTEMI-ACS, 3D STE performed prior to ICA showed that 3D GLS  $> -13.50\%$  could detect those with significant coronary disease (AUC = 0.84) [91].

Finally, in 130 patients with stable angina pectoris, 3D GLS was correlated with Gensini score, with 88.9% sensitivity and 92.9% specificity being observed for a GLS  $> -10\%$ ; while global area strain (GAS), a new feature of 3D echocardiography which integrates longitudinal and circumferential deformation, had 97.2% sensitivity and 88.1% specificity for a cutoff value  $> -21\%$  to detect critical CAD (estimated as Gensini score  $\geq 20$ ) [92].

Despite these promising results, the diagnostic value of 3D GLS was lower than that of 2D GLS in a recent meta-

analysis on the detection of myocardial infarction size [28]; this suggests that more consolidated researches are warranted to define the 3D usefulness in this clinical setting.

### 7. Limitations

The major limitation of STE is the lack of defined cutoff values for its confident use in different clinical settings. Table 1 shows medium cutoff values of several strain parameters proposed in the aforementioned studies on patients with CAD; however, these values need an external validation to become generalizable; LA and RV strain cutoffs require further research to be identified. Vendor dependency could be considered partially solved after the publication of the European Association of Cardiovascular Imaging (EACVI) standardization documents for all chambers' deformation imaging [93]. Also, negative values of LV and RV strain are currently matter of discussion, since the use of negative



values could result in some confusion, especially when it comes to expressing majority and minority criteria, or could expose to important mistakes during the data collection for missing minus typing. We agree with this opinion and understand the choice of some authors to report absolute values in their research papers; however, in our personal practice, we still prefer to use negative values of ventricular strain since it currently is the most standardized method based on the international committee documents. Moreover, the use of a negative sign is important to differentiate ventricular strain, which describes contractile function, being negative in order to reflect myocardial fiber shortening, from left atrial strain, which describes relaxation properties as myocardial fiber distension.

Furthermore, STE maintains the common limitations of bidimensional echocardiographic measures, such as image quality, operator dependency, and load dependency (lower than LV EF). These limitations could be overcome by the use of 3D echocardiography. However, validated data and standardization among different vendors are necessary to extend its applicability beyond research purposes. Table 2 resumes the benefits and drawbacks of using STE for the study of CAD.

## 8. Conclusions

Beyond ECG and biomarkers, echocardiography is a milestone for the evaluation of CAD in acute and chronic settings. STE could provide an additive value over visual wall motion assessment both for diagnostic and prognostic assessment, and the inclusion of LVGLS in clinical diagnostic workup of these patients is supported by plenty of evidence and clear advantages outweighing the intrinsic limitations of STE technique (Figure 2). However, further studies are needed to confirm the potential value of other chambers' strain. Future experts' consensus to identify reference values of LV strain parameters in CAD is highly expectable for a definitive standardization of their use.

## Conflicts of Interest

The authors declare that they have no conflicts of interest.

## References

- [1] A. F. Yu, J. Raikhelkar, E. C. Zabor et al., "Two-dimensional speckle tracking echocardiography detects subclinical left ventricular systolic dysfunction among adult survivors of childhood, adolescent, and young adult cancer," *BioMed Research International*, vol. 2016, Article ID 9363951, 8 pages, 2016.
- [2] F. Franchi, A. Faltoni, M. Cameli et al., "Influence of positive end-expiratory pressure on myocardial strain assessed by speckle tracking echocardiography in mechanically ventilated patients," *BioMed Research International*, vol. 2013, Article ID 918548, 8 pages, 2013.
- [3] M. C. Pastore, G. E. Mandoli, H. S. Aboumarie et al., "Basic and advanced echocardiography in advanced heart failure: an overview," *Heart Failure Reviews*, vol. 25, no. 6, pp. 937–948, 2020.
- [4] D. A. Morris, X. X. Ma, E. Belyavskiy et al., "Left ventricular longitudinal systolic function analysed by 2D speckle-tracking echocardiography in heart failure with preserved ejection fraction: a meta-analysis," *Open Heart*, vol. 4, no. 2, article e000630, 2017.
- [5] S. Buccheri, I. Monte, S. Mangiafico, V. Bottari, S. Leggio, and C. Tamburino, "Feasibility, reproducibility, and agreement between different speckle tracking echocardiographic techniques for the assessment of longitudinal deformation," *BioMed Research International*, vol. 2013, Article ID 297895, 9 pages, 2013.
- [6] M. Takeuchi and V. C. Wu, "Application of left ventricular strain to patients with coronary artery disease," *Current Opinion in Cardiology*, vol. 33, no. 5, pp. 464–469, 2018.
- [7] M. Cameli, G. E. Mandoli, C. Sciacaluga, and S. Mondillo, "More than 10 years of speckle tracking echocardiography: still a novel technique or a definite tool for clinical practice?," *Echocardiography*, vol. 36, no. 5, pp. 958–970, 2019.
- [8] G. E. Mandoli, M. C. Pastore, K. Vassiljevaite et al., "Speckle tracking stress echocardiography: a valuable diagnostic technique or a burden for everyday practice?," *Echocardiography*, vol. 37, no. 12, pp. 2123–2129, 2020.
- [9] M. Cameli, S. Mondillo, F. M. Righini et al., "Left ventricular deformation and myocardial fibrosis in patients with advanced heart failure requiring transplantation," *Journal of Cardiac Failure*, vol. 22, no. 11, pp. 901–907, 2016.
- [10] J.-P. Collet, H. Thiele, E. Barbato et al., "2020 ESC Guidelines for the management of acute coronary syndromes in patients presenting without persistent ST-segment elevation," *European Heart Journal*, vol. ehaa575.
- [11] J. Knuuti, W. Wijns, A. Saraste, D. Capodanno, E. Barbato, and C. Funck-Brentano, "2019 ESC guidelines for the diagnosis and management of chronic coronary syndromes," *European Heart Journal*, vol. 41, no. 3, pp. 407–477, 2020.
- [12] J. Schroeder, S. Hamada, N. Gründlinger et al., "Myocardial deformation by strain echocardiography identifies patients with acute coronary syndrome and nondiagnostic ECG presenting in a chest pain unit: a prospective study of diagnostic accuracy," *Clinical Research in Cardiology*, vol. 105, pp. 1–9, 2015.
- [13] K. Liou, K. Negishi, S. Ho, E. A. Russell, G. Cranney, and S. Y. Ooi, "Detection of obstructive coronary artery disease using peak systolic global longitudinal strain derived by two-dimensional speckle-tracking: a systematic review and meta-analysis," *Journal of the American Society of Echocardiography*, vol. 29, no. 8, pp. 724–735.e4, 2016.
- [14] C. Zito, L. Longobardo, R. Citro et al., "Ten years of 2D longitudinal strain for early myocardial dysfunction detection: a clinical overview," *BioMed Research International*, vol. 2018, Article ID 8979407, 14 pages, 2018.
- [15] N. Carrabba, A. Migliorini, S. Pradella et al., "Old and new NICE guidelines for the evaluation of new onset stable chest pain: a real world perspective," *BioMed Research International*, vol. 2018, Article ID 3762305, 7 pages, 2018.
- [16] O. Catalano, G. Moro, A. Mori et al., "Cardiac magnetic resonance in stable coronary artery disease: added prognostic value to conventional risk profiling," *BioMed Research International*, vol. 2018, Article ID 2806148, 10 pages, 2018.
- [17] N. Carrabba, M. Berteotti, G. Taborchi et al., "Integration of CTA in the diagnostic workup of new onset chest pain in clinical practice," *BioMed Research International*, vol. 2019, Article ID 2647079, 8 pages, 2019.



- [18] M. Bertini, S. A. Mollema, V. Delgado et al., "Impact of time to reperfusion after acute myocardial infarction on myocardial damage assessed by left ventricular longitudinal strain," *The American Journal of Cardiology*, vol. 104, no. 4, pp. 480–485, 2009.
- [19] B. Sjøli, S. Ørn, B. Grenne, H. Ihlen, T. Edvardsen, and H. Brunvand, "Diagnostic capability and reproducibility of strain by Doppler and by speckle tracking in patients with acute myocardial infarction," *JACC: Cardiovascular Imaging*, vol. 2, no. 1, pp. 24–33, 2009.
- [20] J. Lacalzada, A. de la Rosa, M. M. Izquierdo et al., "Left ventricular global longitudinal systolic strain predicts adverse remodeling and subsequent cardiac events in patients with acute myocardial infarction treated with primary percutaneous coronary intervention," *The International Journal of Cardiovascular Imaging*, vol. 31, no. 3, pp. 575–584, 2015.
- [21] A. D'Andrea, R. Cocchia, P. Caso et al., "Global longitudinal speckle-tracking strain is predictive of left ventricular remodeling after coronary angioplasty in patients with recent non-ST elevation myocardial infarction," *International Journal of Cardiology*, vol. 153, no. 2, pp. 185–191, 2011.
- [22] M. Ersbøll, N. Valeur, U. M. Mogensen et al., "Relationship between left ventricular longitudinal deformation and clinical heart failure during admission for acute myocardial infarction: a two-dimensional speckle-tracking study," *Journal of the American Society of Echocardiography*, vol. 25, no. 12, pp. 1280–1289, 2012.
- [23] C. Eek, B. Grenne, H. Brunvand et al., "Strain echocardiography predicts acute coronary occlusion in patients with non-ST-segment elevation acute coronary syndrome," *European Journal of Echocardiography*, vol. 11, no. 6, pp. 501–508, 2010.
- [24] D. Mele, A. Fiorencis, E. Chiodi, C. Gardini, G. Benea, and R. Ferrari, "Polar plot maps by parametric strain echocardiography allow accurate evaluation of non-viable transmural scar tissue in ischaemic heart disease," *European Heart Journal Cardiovascular Imaging*, vol. 17, no. 6, pp. 668–677, 2016.
- [25] T. Caspar, H. Samet, M. Ohana et al., "Longitudinal 2D strain can help diagnose coronary artery disease in patients with suspected non-ST-elevation acute coronary syndrome but apparent normal global and segmental systolic function," *International Journal of Cardiology*, vol. 236, pp. 91–94, 2017.
- [26] T. Dahlslett, S. Karlsen, B. Grenne et al., "Early assessment of strain echocardiography can accurately exclude significant coronary artery stenosis in suspected non-ST-segment elevation acute coronary syndrome," *Journal of the American Society of Echocardiography*, vol. 27, no. 5, pp. 512–519, 2014.
- [27] A. Atici, H. A. Barman, E. Durmaz et al., "Predictive value of global and territorial longitudinal strain imaging in detecting significant coronary artery disease in patients with myocardial infarction without persistent ST-segment elevation," *Echocardiography*, vol. 36, no. 3, pp. 512–520, 2019.
- [28] K. Y. Diao, Z. G. Yang, M. Ma et al., "The diagnostic value of global longitudinal strain (GLS) on myocardial infarction size by echocardiography: a systematic review and meta-analysis," *Scientific Reports*, vol. 7, no. 1, pp. 1–8, 2017.
- [29] G. Nucifora, N. A. Marsan, M. Bertini et al., "Reduced left ventricular torsion early after myocardial infarction is related to left ventricular remodeling," *Circulation. Cardiovascular Imaging*, vol. 3, no. 4, pp. 433–442, 2010.
- [30] C. A. Gibbons Kroeker, J. V. Tyberg, and R. Beyar, "Effects of ischemia on left ventricular apex rotation," *Circulation*, vol. 92, no. 12, pp. 3539–3548, 1995.
- [31] M. L. Knudtson, P. D. Galbraith, K. L. Hildebrand, J. V. Tyberg, and R. Beyar, "Dynamics of left ventricular apex rotation during angioplasty: a sensitive index of ischemic dysfunction," *Circulation*, vol. 96, no. 3, pp. 801–808, 1997.
- [32] J. Huang, Z. N. Yan, L. Fan, Y. F. Rui, and X. T. Song, "Left ventricular longitudinal function assessment in rabbits after acute occlusion of left anterior descending coronary artery by two-dimensional speckle tracking imaging," *BMC Cardiovascular Disorders*, vol. 17, no. 1, p. 219, 2017.
- [33] L. Spinelli, C. Morisco, E. Assante di Panzillo, R. Izzo, and B. Trimarco, "Reverse left ventricular remodeling after acute myocardial infarction: the prognostic impact of left ventricular global torsion," *The International Journal of Cardiovascular Imaging*, vol. 29, no. 4, pp. 787–795, 2013.
- [34] C. Rouzaud Laborde, C. Delmas, J. Mialet-Perez et al., "First evidence of increased plasma serotonin levels in Tako-Tsubo cardiomyopathy," *BioMed Research International*, vol. 2013, Article ID 847069, 5 pages, 2013.
- [35] S. Moscatelli, F. Montecucco, F. Carbone et al., "An emerging cardiovascular disease: takotsubo syndrome," *BioMed Research International*, vol. 2019, Article ID 6571045, 9 pages, 2019.
- [36] J. R. Ghadri, I. S. Wittstein, A. Prasad et al., "International expert consensus document on takotsubo syndrome (Part II): diagnostic workup, outcome, and management," *European Heart Journal*, vol. 39, no. 22, pp. 2047–2062, 2018.
- [37] P. Meimoun, S. Abouth, J. Boulanger, A. Luyck-Bore, S. Martis, and J. Clerc, "Relationship between acute strain pattern and recovery in tako-tsubo cardiomyopathy and acute anterior myocardial infarction: a comparative study using two-dimensional longitudinal strain," *The International Journal of Cardiovascular Imaging*, vol. 30, no. 8, pp. 1491–1500, 2014.
- [38] M. P. Mahjoob, S. Alipour Parsa, A. Mazarei, M. Safi, I. Khaheshi, and S. Esmaeeli, "Rest 2D speckle tracking echocardiography may be a sensitive but nonspecific test for detection of significant coronary artery disease," *Acta Biomed*, vol. 88, no. 4, pp. 457–461, 2018.
- [39] C. A. Hagemann, S. Hoffmann, R. A. Hagemann et al., "Usefulness of layer-specific strain in diagnosis of coronary artery disease in patients with stable angina pectoris," *The International Journal of Cardiovascular Imaging*, vol. 35, no. 11, pp. 1989–1999, 2019.
- [40] J. O. Choi, S. W. Cho, Y. B. Song et al., "Longitudinal 2D strain at rest predicts the presence of left main and three vessel coronary artery disease in patients without regional wall motion abnormality," *European Journal of Echocardiography*, vol. 10, no. 5, pp. 695–701, 2009.
- [41] S. Moustafa, K. Elrabat, F. Swailem, and A. Galal, "The correlation between speckle tracking echocardiography and coronary artery disease in patients with suspected stable angina pectoris," *Indian Heart Journal*, vol. 70, no. 3, pp. 379–386, 2018.
- [42] H. J. Zuo, X. T. Yang, Q. G. Liu et al., "Global longitudinal strain at rest for detection of coronary artery disease in patients without diabetes mellitus," *Current Medical Science*, vol. 38, no. 3, pp. 413–421, 2018.
- [43] H. Radwan and E. Hussein, "Value of global longitudinal strain by two dimensional speckle tracking echocardiography in predicting coronary artery disease severity," *The Egyptian Heart Journal*, vol. 69, no. 2, pp. 95–101, 2017.











- [44] A. Vrettos, D. Dawson, C. Grigoratos, and P. Nihoyannopoulos, "Correlation between global longitudinal peak systolic strain and coronary artery disease severity as assessed by the angiographically derived SYNTAX score," *Echo Research and Practice*, vol. 3, no. 2, pp. 29–34, 2016.
- [45] M. Y. Xie, Q. Lv, J. Wang, and J. B. Yin, "Assessment of myocardial segmental function with coronary artery stenosis in multi-vessel coronary disease patients with normal wall motion," *European Review for Medical and Pharmacological Sciences*, vol. 20, no. 8, pp. 1582–1589, 2016.
- [46] T. Biering-Sørensen, S. Hoffmann, R. Mogelvang et al., "Myocardial strain analysis by 2-dimensional speckle tracking echocardiography improves diagnostics of coronary artery stenosis in stable angina pectoris," *Circulation. Cardiovascular Imaging*, vol. 7, no. 1, pp. 58–65, 2014.
- [47] A. M. Anwar, "Accuracy of two-dimensional speckle tracking echocardiography for the detection of significant coronary stenosis," *Journal of Cardiovascular Ultrasound*, vol. 21, no. 4, pp. 177–182, 2013.
- [48] C. Liu, J. Li, M. Ren et al., "Multilayer longitudinal strain at rest may help to predict significant stenosis of the left anterior descending coronary artery in patients with suspected non-ST-elevation acute coronary syndrome," *International Journal of Cardiac Imaging*, vol. 32, no. 12, pp. 1675–1685, 2016.
- [49] M. Becker, C. Ocklenburg, E. Altiok et al., "Impact of infarct transmuralty on layer-specific impairment of myocardial function: a myocardial deformation imaging study," *European Heart Journal*, vol. 30, no. 12, pp. 1467–1476, 2009.
- [50] E. Altiok, M. Neizel, S. Tiemann et al., "Layer-specific analysis of myocardial deformation for assessment of infarct transmuralty: comparison of strain encoded cardiovascular magnetic resonance with 2D speckle tracking echocardiography," *European Heart Journal Cardiovascular Imaging*, vol. 14, no. 6, pp. 570–578, 2013.
- [51] M. Tarascio, L. A. Leo, C. Klersy, R. Murzilli, T. Moccetti, and F. F. Faletra, "Speckle-tracking layer-specific analysis of myocardial deformation and evaluation of scar transmuralty in chronic ischemic heart disease," *Journal of the American Society of Echocardiography*, vol. 30, no. 7, pp. 667–675, 2017.
- [52] M. Cameli, T. Bombardini, A. Dokollari et al., "Longitudinal strain stress-echo evaluation of aged marginal donor hearts: feasibility in the Adonhers project," *Transplantation Proceedings*, vol. 48, no. 2, pp. 399–401, 2016.
- [53] N. Gaibazzi, F. Pigazzani, C. Reverberi, and T. R. Porter, "Rest global longitudinal 2D strain to detect coronary artery disease in patients undergoing stress echocardiography: a comparison with wall-motion and coronary flow reserve responses," *Echo Research and Practice*, vol. 1, no. 2, pp. 61–70, 2014.
- [54] E. Rumbinaite, D. Zaliaduonyte-Peksiene, T. Lapinskas et al., "Early and late diastolic strain rate vs global longitudinal strain at rest and during dobutamine stress for the assessment of significant coronary artery stenosis in patients with a moderate and high probability of coronary artery disease," *Echocardiography*, vol. 33, no. 10, pp. 1512–1522, 2016.
- [55] E. Rumbinaite, D. Žaliaduonytė-Pekšienė, M. Vieželis et al., "Dobutamine-stress echocardiography speckle-tracking imaging in the assessment of hemodynamic significance of coronary artery stenosis in patients with moderate and high probability of coronary artery disease," *Medicina*, vol. 52, no. 6, pp. 331–339, 2016.
- [56] V. Uusitalo, M. Luotolahti, M. Pietilä et al., "Two-dimensional speckle-tracking during dobutamine stress echocardiography in the detection of myocardial ischemia in patients with suspected coronary artery disease," *Journal of the American Society of Echocardiography*, vol. 29, no. 5, pp. 470–479.e3, 2016.
- [57] J. H. Park, J. S. Woo, S. Ju et al., "Layer-specific analysis of dobutamine stress echocardiography for the evaluation of coronary artery disease," *Medicine*, vol. 95, no. 32, article e4549, 2016.
- [58] T. Nishi, N. Funabashi, K. Ozawa et al., "Regional layer-specific longitudinal peak systolic strain using exercise stress two-dimensional speckle-tracking echocardiography for the detection of functionally significant coronary artery disease," *Heart and Vessels*, vol. 34, no. 8, pp. 1394–1403, 2019.
- [59] J. A. Ejlersen, S. H. Poulsen, J. Mortensen, and O. May, "Diagnostic value of layer-specific global longitudinal strain during adenosine stress in patients suspected of coronary artery disease," *The International Journal of Cardiovascular Imaging*, vol. 33, no. 4, pp. 473–480, 2017.
- [60] B. Loncarevic, D. Trifunovic, I. Soldatovic, and B. Vujisic-Tesic, "Silent diabetic cardiomyopathy in everyday practice: a clinical and echocardiographic study," *BMC Cardiovascular Disorders*, vol. 16, no. 1, p. 242, 2016.
- [61] R. T. Hubbard, M. C. Arciniegas Calle, S. Barros-Gomes et al., "2-dimensional speckle tracking echocardiography predicts severe coronary artery disease in women with normal left ventricular function: a case-control study," *BMC Cardiovascular Disorders*, vol. 17, no. 1, p. 231, 2017.
- [62] G. E. Mandoli, M. Cameli, S. Minardi, F. Crudele, S. Lunghetti, and S. Mondillo, "Layer-specific strain in dipyridamole stress echo: a new tool for the diagnosis of microvascular angina," *Echocardiography*, vol. 35, no. 12, pp. 2005–2013, 2018.
- [63] R. Hoffmann, H. Lethen, T. Marwick et al., "Analysis of inter-institutional observer agreement in interpretation of dobutamine stress echocardiograms," *Journal of the American College of Cardiology*, vol. 27, no. 2, pp. 330–336, 1996.
- [64] M. C. Pastore, G. De Carli, G. E. Mandoli et al., "The prognostic role of speckle tracking echocardiography in clinical practice: evidence and reference values from the literature," *Heart Failure Reviews*, 2020.
- [65] S. W. Choi, J. H. Park, B. J. Sun et al., "Impaired two-dimensional global longitudinal strain of left ventricle predicts adverse long-term clinical outcomes in patients with acute myocardial infarction," *International Journal of Cardiology*, vol. 196, pp. 165–167, 2015.
- [66] M. Ersbøll, N. Valeur, U. M. Mogensen et al., "Prediction of all-cause mortality and heart failure admissions from global left ventricular longitudinal strain in patients with acute myocardial infarction and preserved left ventricular ejection fraction," *Journal of the American College of Cardiology*, vol. 61, no. 23, pp. 2365–2373, 2013.
- [67] M. L. Antoni, S. A. Mollema, V. Delgado et al., "Prognostic importance of strain and strain rate after acute myocardial infarction," *European Heart Journal*, vol. 31, no. 13, pp. 1640–1647, 2010.
- [68] M. J. W. van Mourik, D. V. J. Zaar, M. W. Smulders et al., "Adding speckle-tracking echocardiography to visual assessment of systolic wall motion abnormalities improves the detection of myocardial infarction," *Journal of the American Society of Echocardiography*, vol. 32, no. 1, pp. 65–73, 2019.
- [69] E. Joyce, G. E. Hoogslag, I. Al Amri et al., "Quantitative dobutamine stress echocardiography using speckle-tracking analysis versus conventional visual analysis for detection of significant coronary artery disease after ST-segment elevation

- myocardial infarction,” *Journal of the American Society of Echocardiography*, vol. 28, no. 12, pp. 1379–1389.e1, 2015.
- [70] J. Scharrenbroich, S. Hamada, A. Keszei et al., “Use of two-dimensional speckle tracking echocardiography to predict cardiac events: comparison of patients with acute myocardial infarction and chronic coronary artery disease,” *Clinical Cardiology*, vol. 41, no. 1, pp. 111–118, 2018.
- [71] S. Kim, D. H. Cho, M. N. Kim et al., “Transmural difference in myocardial damage assessed by layer-specific strain analysis in patients with ST elevation myocardial infarction,” *Scientific Reports*, vol. 10, no. 1, article 11104, 2020.
- [72] O. A. Smiseth, H. Torp, A. Opdahl, K. H. Haugaa, and S. Urheim, “Myocardial strain imaging: how useful is it in clinical decision making?,” *European Heart Journal*, vol. 37, no. 15, pp. 1196–1207, 2016.
- [73] M. Cameli, S. Mondillo, M. Galderisi et al., “Speckle tracking echocardiography: a practical guide,” *Giornale Italiano di Cardiologia*, vol. 18, no. 4, pp. 253–269, 2017.
- [74] S. Shimoni, G. Gendelman, O. Ayzenberg et al., “Differential effects of coronary artery stenosis on myocardial function: the value of myocardial strain analysis for the detection of coronary artery disease,” *Journal of the American Society of Echocardiography*, vol. 24, no. 7, pp. 748–757, 2011.
- [75] P. Brainin, S. Hoffmann, T. Fritz-Hansen, F. J. Olsen, J. S. Jensen, and T. Biering-Sørensen, “Usefulness of postsystolic shortening to diagnose coronary artery disease and predict future cardiovascular events in stable angina pectoris,” *Journal of the American Society of Echocardiography*, vol. 31, no. 8, pp. 870–879.e3, 2018.
- [76] T. Asanuma and S. Nakatani, “Myocardial ischaemia and post-systolic shortening,” *Heart*, vol. 101, no. 7, pp. 509–516, 2015.
- [77] M. Cameli, M. C. Pastore, M. Y. Henein, and S. Mondillo, “The left atrium and the right ventricle: two supporting chambers to the failing left ventricle,” *Heart Failure Reviews*, vol. 24, no. 5, pp. 661–669, 2019.
- [78] Y. Ikejder, M. Sebbani, I. Hendy, M. Khramz, A. Khatouri, and L. Bendriss, “Impact of arterial hypertension on left atrial size and function,” *BioMed Research International*, vol. 2020, Article ID 2587530, 14 pages, 2020.
- [79] G. E. Mandoli, M. C. Pastore, G. Benfari et al., “Left atrial strain as a pre-operative prognostic marker for patients with severe mitral regurgitation,” *International Journal of Cardiology*, vol. 324, pp. 139–145, 2021.
- [80] M. Cameli, M. C. Pastore, G. E. Mandoli et al., “Prognosis and risk stratification of patients with advanced heart failure (from PROBE),” *The American Journal of Cardiology*, vol. 124, no. 1, pp. 55–62, 2019.
- [81] M. Cameli, M. H. Miglioranza, J. Magne et al., “Multicentric atrial strain comparison between two different modalities: MASCOT HIT study,” *Diagnostics*, vol. 10, no. 11, p. 946, 2020.
- [82] D. H. Lee, T. H. Park, J. E. Lee et al., “Left atrial function assessed by left atrial strain in patients with left circumflex branch culprit acute myocardial infarction,” *Echocardiography*, vol. 32, no. 7, pp. 1094–1100, 2015.
- [83] K. M. Said, A. I. Nassar, A. Fouad, A. A. Ramzy, and M. F. F. Abd Allah, “Left atrial deformation analysis as a predictor of severity of coronary artery disease,” *The Egyptian Heart Journal*, vol. 70, no. 4, pp. 353–359, 2018.
- [84] M. L. Antoni, E. A. ten Brinke, J. Z. Atary et al., “Left atrial strain is related to adverse events in patients after acute myocardial infarction treated with primary percutaneous coronary intervention,” *Heart*, vol. 97, no. 16, pp. 1332–1337, 2011.
- [85] P. Meimoun, V. Stracchi, J. Boulanger et al., “The left atrial function is transiently impaired in Tako-tsubo cardiomyopathy and associated to in-hospital complications: a prospective study using two-dimensional strain,” *The International Journal of Cardiovascular Imaging*, vol. 36, no. 2, pp. 299–307, 2020.
- [86] W. T. Chang, W. C. Tsai, Y. W. Liu et al., “Changes in right ventricular free wall strain in patients with coronary artery disease involving the right coronary artery,” *Journal of the American Society of Echocardiography*, vol. 27, no. 3, pp. 230–238, 2014.
- [87] L. S. Rallidis, G. Makavos, and P. Nihoyannopoulos, “Right ventricular involvement in coronary artery disease: role of echocardiography for diagnosis and prognosis,” *Journal of the American Society of Echocardiography*, vol. 27, no. 3, pp. 223–229, 2014.
- [88] M. L. Antoni, R. W. C. Scherptong, J. Z. Atary et al., “Prognostic value of right ventricular function in patients after acute myocardial infarction treated with primary percutaneous coronary intervention,” *Circulation. Cardiovascular Imaging*, vol. 3, no. 3, pp. 264–271, 2010.
- [89] N. Iwahashi, J. Kirigaya, T. Abe et al., “Impact of three-dimensional global longitudinal strain for patients with acute myocardial infarction,” *European Heart Journal Cardiovascular Imaging*, vol. jeaa241, 2020.
- [90] J. Zhong, P. Liu, S. Li et al., “A comparison of three-dimensional speckle tracking echocardiography parameters in predicting left ventricular remodeling,” *Journal of Healthcare Engineering*, vol. 2020, Article ID 8847144, 9 pages, 2020.
- [91] A. K. Biswas, T. Haque, D. Banik, S. R. Choudhury, S. R. Khan, and F. T. Malik, “Identification of significant coronary artery disease in patients with non-ST segment elevation acute coronary syndrome by myocardial strain analyses using three-dimensional speckle tracking echocardiography,” *Echocardiography*, vol. 35, no. 12, pp. 1988–1996, 2018.
- [92] M. Dogdus, E. Simsek, and C. S. Cinar, “3D-speckle tracking echocardiography for assessment of coronary artery disease severity in stable angina pectoris,” *Echocardiography*, vol. 36, no. 2, pp. 320–327, 2019.
- [93] L. P. Badano, T. J. Kolias, D. Muraru et al., “Standardization of left atrial, right ventricular, and right atrial deformation imaging using two-dimensional speckle tracking echocardiography: a consensus document of the EACVI/ASE/Industry Task Force to standardize deformation imaging. Eur Heart J Cardiovasc Imaging. 2018;19(6):591-600,” *Erratum in: Eur Heart J Cardiovasc Imaging*, vol. 19, no. 7, pp. 830–833, 2018.



## Review Article

# Stress CMR in Known or Suspected CAD: Diagnostic and Prognostic Role

**Francesca Baessato** <sup>1</sup>, **Marco Guglielmo** <sup>2</sup>, **Giuseppe Muscogiuri** <sup>2</sup>, **Andrea Baggiano** <sup>2</sup>,  
**Laura Fusini** <sup>2</sup>, **Stefano Scafuri** <sup>2</sup>, **Mario Babbaro** <sup>2</sup>, **Rocco Mollace** <sup>2</sup>,  
**Ada Collevocchio**,<sup>3</sup> **Andrea I. Guaricci** <sup>4</sup>, and **Gianluca Pontone** <sup>2</sup>

<sup>1</sup>Department of Cardiology, San Maurizio Regional Hospital, Bolzano, Italy

<sup>2</sup>Cardiovascular Imaging Department, Centro Cardiologico Monzino IRCCS, Milan, Italy

<sup>3</sup>Department of Cardiac, Thoracic, Vascular Sciences and Public Health, University of Padua, Padua, Italy

<sup>4</sup>Institute of Cardiovascular Disease, Department of Emergency and Organ Transplantation, University Hospital Policlinico of Bari, Bari, Italy

Correspondence should be addressed to Gianluca Pontone; [gianluca.pontone@cardiologicomonzino.it](mailto:gianluca.pontone@cardiologicomonzino.it)

Received 30 October 2020; Revised 23 December 2020; Accepted 4 January 2021; Published 15 January 2021

Academic Editor: Luca Liberale

Copyright © 2021 Francesca Baessato et al. This is an open access article distributed under the Creative Commons Attribution License, which permits unrestricted use, distribution, and reproduction in any medium, provided the original work is properly cited.

The recently published 2019 guidelines on chronic coronary syndromes (CCS) focus on the need for noninvasive imaging modalities to accurately establish the diagnosis of coronary artery disease (CAD) and assess the risk of clinical scenario occurrence. Appropriate patient management should rely on controlling symptoms, improving prognosis, and guiding each therapeutic strategy as well as monitoring disease progress. Among the noninvasive imaging modalities, cardiovascular magnetic resonance (CMR) has gained broad acceptance in past years due to its unique features in providing a complete assessment of CAD through data on cardiac anatomy and function and myocardial viability, with high spatial and temporal resolution and without ionizing radiation. In detail, evaluation of the presence and extent of myocardial ischemia through stress CMR (S-CMR) has shown a high rule-in power in detecting functionally significant coronary artery stenosis in patients suspected of CCS. Moreover, S-CMR technique may add significant prognostic value, as demonstrated by different studies which have progressively evidenced the valuable power of this multiparametric imaging modality in predicting adverse cardiac events. The latest scientific progress supports a greater expansion of S-CMR with improvement of quantitative myocardial perfusion analysis, myocardial strain, and native mapping within the same examination. Although further study is warranted, these techniques, which are currently mostly restricted to the research field, are likely to become increasingly prevalent in the clinical setting with the scope of increasing accuracy in the selection of patients to be sent to invasive revascularization. This review investigates the diagnostic and prognostic role of S-CMR in the context of CAD, by analysing a strong, long-standing, scientific evidence together with an appraisal of new advanced techniques which may potentially enrich CAD management in the next future.

## 1. Introduction

Coronary artery disease (CAD) is a widespread clinical phenomenon associated with different clinical entities, which involves a large burden on the healthcare system with an increasing need for objective diagnostic tests to both confirm the diagnosis and assess the event risk [1–4]. In 2019, the European Society of Cardiology (ESC) published the guidelines on the diagnosis and management of chronic coronary

syndromes (CCS), which represent a relevant step by introducing innovative changes mostly in the diagnostic workup of suspected obstructive CAD. Noninvasive imaging methods, either functional tests or anatomical imaging, represent indispensable tools for appropriate management of patients with known or suspected CAD, by providing adequate detection of the disease, guiding therapy, and predicting outcome. Stress CMR (S-CMR) is a functional imaging test that has been widely recognized in the past few years as an accurate, well-

validated, nonionizing technique [5–7]. The possibility of a multiparametric approach in each S-CMR study, from reproducible evaluation of cardiac function and scar detection to an accurate definition of myocardial ischemia in hemodynamically relevant coronary stenosis and microvascular dysfunction, has made S-CMR an appealing noninvasive modality for comprehensive assessment of CAD.

## 2. Clinical Applications and Technical Approach

According to the latest version of the guidelines, the diagnostic approach of CAD should be primarily based on the clinical likelihood of the disease, and the choice for the initial diagnostic test, either noninvasive imaging as a “gatekeeper” to invasive coronary angiography (ICA) or direct ICA, should be based on clinical risk assessment, patient characteristics, local expertise, and test availability [8].

Noninvasive imaging methods, either functional tests, such as S-CMR, or anatomical imaging, such as cardiac computed tomography angiography (CCTA), are recommended in Class Ib as the initial tests for diagnosing CAD in symptomatic patients in whom obstructive CAD cannot be excluded by clinical assessment alone [9]. Of note, each imaging test has a different performance in ruling in or ruling out obstructive CAD, which should also be taken into account in the initial workup.

Functional imaging methods include myocardial perfusion imaging with single-photon emission computed tomography (SPECT), positron emission computed tomography (PET), stress echocardiography, and S-CMR. These modalities, although possibly missing subclinical atherosclerosis, typically have better rule-in power and have shown higher specificity for the detection of hemodynamically significant coronary stenosis than anatomical imaging with CCTA, by leading to fewer referrals for ICA compared with a strategy relying on anatomical imaging or exercise ECG only [10].

S-CMR can detect myocardial ischemia, thus functionally significant CAD, through evaluation of perfusion defects or ischemic wall motion abnormalities (WMA) provoked by exercise or pharmacological stress. S-CMR protocol should be performed according to the latest update of the S-CMR guidelines [11] and briefly implies a rest and stress phase, with final late gadolinium enhancement (LGE) sequences.

Vasodilators are the most commonly used stress agents (adenosine, dipyridamole, and regadenoson) which commonly induce myocardial ischemia through a “steal phenomenon” and loss of autoregulation mechanism, thus leading to perfusion defects [12]. In case of perfusion imaging, a first-pass perfusion technique using a saturation-prepared T1-weighted fast gradient echo sequence is performed at peak myocardial stress during contemporary gadolinium contrast agent injection. If dipyridamole is used, additional cine sequences are exploited due to its longer half-life [13].

In opposition, inotropic agents, such as dobutamine, act by improving heart rate and only cine sequences are acquired at maximal stress for detection of regional WMA to unmask myocardial ischemia. Hence, each S-CMR examination can be classified as either normal (absence of stress perfusion

defect in at least 1 myocardial segment free from LGE) or positive for ischemia (reversible myocardial perfusion defect alone or combined with WMA in at least 1 myocardial segment without corresponding LGE, as shown in Figure 1).

Actually, the recent 2019 guidelines recommend S-CMR (Class Ib) preferentially in patients with higher clinical likelihood of CAD or with a history of revascularization, in whom a functional evaluation of ischemia together with myocardial viability would be most useful, as also supported by cost-effectiveness data [14]. On the other hand, anatomical imaging with CCTA is recommended as first-line test (Class Ib) in suitable patients with low to intermediate clinical likelihood of CAD or no history of CAD, due to its highest rule-out capability [9].

This represents a relevant change compared to the previous version of the guidance, where stress imaging was recommended in patients with stable CAD as the first preferred diagnostic option (Class Ib), while CCTA was given only a Class IIa indication as an alternative test for ruling out significant CAD in selected patients [15].

If recent strong evidences [16, 17] have favoured in Europe a relevant spin-off of CCTA in the field of CCS against functional imaging [18, 19], numerous data have underlined the excellent sensibility and specificity of S-CMR in CAD diagnosis and patient risk classification with a long-standing scientific evidence [20, 21].

## 3. Diagnostic Role of Stress CMR

Numerous studies have reported a high diagnostic accuracy of noninvasive imaging modalities in detecting significant obstructive CAD against clinical gold standards, angiographically determined luminal coronary stenosis and fractional flow reserve (FFR) [22–28].

Concerning S-CMR, there is a wide body of scientific evidence that has strengthened its position, and S-CMR has shown excellent diagnostic performance in the detection of CAD, both for hemodynamically significant coronary stenosis and microvascular dysfunction [29, 30]. Many of these studies regarding the diagnostic performance of S-CMR are listed in Table 1.

In 2001, Schwitter et al. presented one of the first multi-slice approach studies on perfusion S-CMR in an unselected study population and demonstrated for S-CMR a sensitivity and specificity of 91% and 94%, respectively, for the detection of CAD by S-CMR using PET as gold standard, and a sensitivity and specificity of 87% and 85%, respectively, using quantitative coronary angiography (stenosis > 50%) as gold standard [31]. These results initially sustained the role of perfusion CMR as a reliable modality for the detection of CAD in comparison to other perfusion modalities, with the additional capacity of identifying even subendocardial defects, which are currently missed by SPECT.

A large meta-analysis by Nandalur et al. involving 1183 patients further enhanced the emerging role of S-CMR in the diagnosis of CAD by showing a sensitivity of 91% and a specificity of 81% for perfusion CMR and a sensitivity of 83% and specificity of 86% for stress-induced WMA in a per patient analysis, respectively [32].

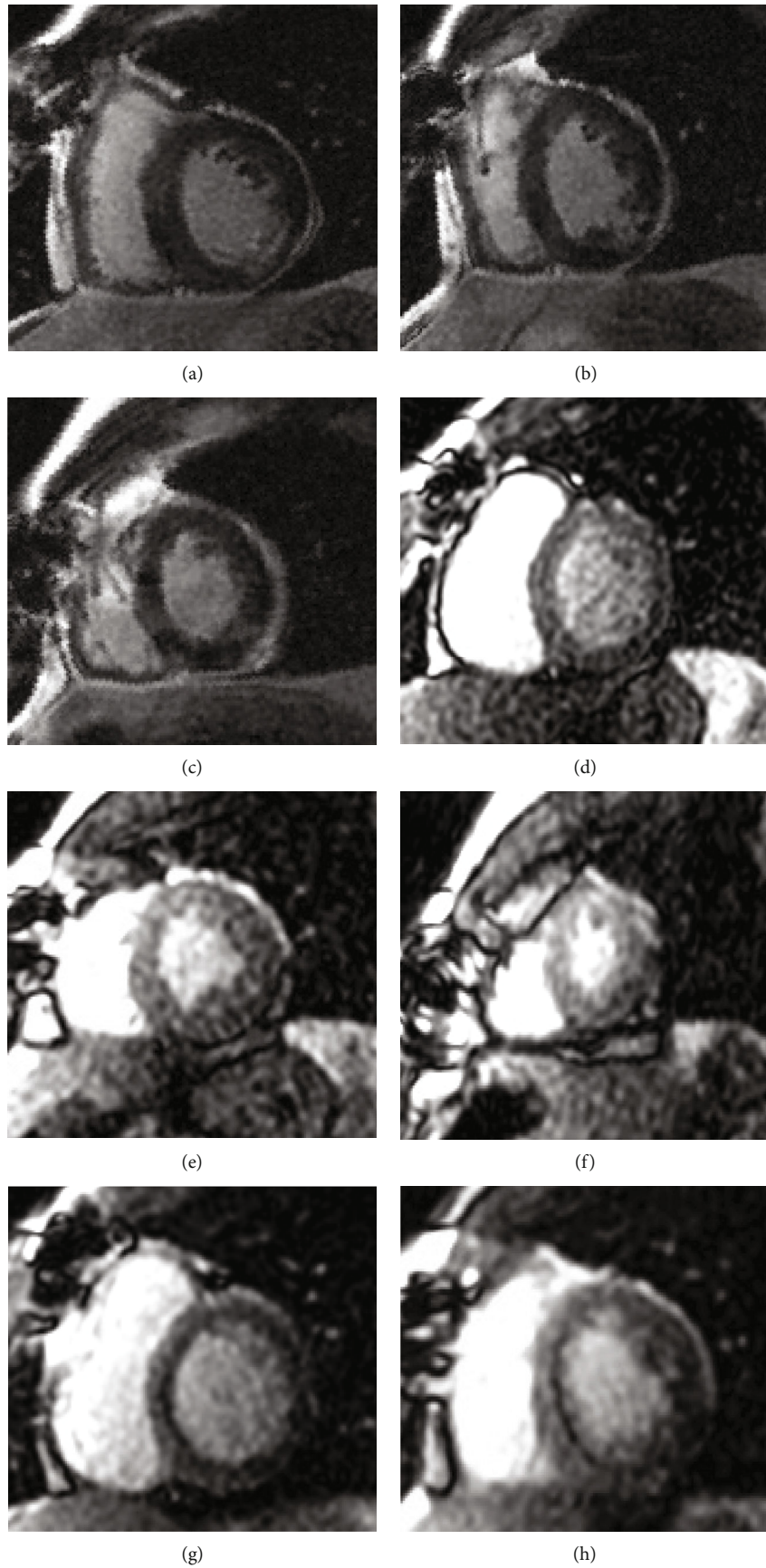
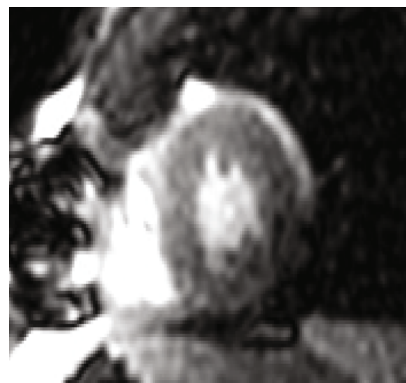


FIGURE 1: Continued.



(i)

FIGURE 1: A 60-year-old woman: new-onset angina in previous myocardial infarction and PCI of right coronary artery; LGE sequences (a–c) showed subendocardial inferolateral fibrosis (ischemic pattern); after regadenoson administration, matching rest (d–f) and stress perfusion sequences (g–i) septal reversible perfusion defect was detected. Invasive coronary angiography confirmed subocclusive left descending anterior coronary artery stenosis.

TABLE 1: Characteristics of defined studies regarding the diagnostic performance of stress perfusion cardiovascular magnetic resonance.

Author	Reference	N	Sensitivity (%)	Specificity (%)	Year
Schwitzer et al. [31]	S-CMR vs. ICA	48	87%	85%	2001
Nandalur et al. [32]	S-CMR vs. ICA (meta-analysis)	1183	91%	81%	2007
Schwitzer et al. [33]	S-CMR and SPECT vs. ICA	234	67%	85%	2008
Greenwood et al. [36]	S-CMR and SPECT vs. ICA	752	86%	83%	2012
Schwitzer et al. [35]	S-CMR and SPECT vs. ICA	533	75%	59%	2013
Greenwood et al. [37]	S-CMR and SPECT vs. ICA	235	88%	83%	2014
Takx et al. [41]	S-CMR vs. FFR-ICA (meta-analysis)	798	89%	87%	2015
Danad et al. [38]	S-CMR vs. FFR-ICA (meta-analysis)	3788	90%	94%	2017
Pontone et al. [42]	S-CMR vs. FFR-ICA (meta-analysis)	1085	87%	88%	2019

S-CMR: stress cardiovascular magnetic resonance; ICA: invasive coronary angiography; SPECT: single-photon emission computed tomography; FFR-ICA: fractional flow reserve derived from invasive coronary angiography.

Different trials investigated the diagnostic accuracy of S-CMR versus SPECT, a still worldwide used technique that historically has represented the gold standard for myocardial perfusion assessment.

The MR-IMPACT trial in 2008 was a multicentre, multi-vendor, randomized trial that determined in 241 patients the diagnostic performance of adenosine perfusion-CMR in comparison to SPECT for the detection of CAD, with ICA as the reference standard. Perfusion-CMR at the optimal contrast dose had similar performance as SPECT studies in patients with the same dose (area under ROC curve (AUC):  $0.86 \pm 0.06$  vs.  $0.75 \pm 0.09$  for SPECT,  $p = 0.12$ ), but with even superior diagnostic performance when compared to the entire SPECT population (AUC:  $0.67 \pm 0.05$ ,  $n = 212$ ;  $p = 0.013$ ). Schwitzer et al. were therefore able to demonstrate how S-CMR could at least represent a valuable alternative to SPECT for CAD detection [33].

These evidences were later supported by the larger MR-IMPACT II trial, which involved 533 patients among 33 centres. Patients were evaluated by S-CMR and gated-SPECT before ICA. Both tests showed a nonsignificant difference in

terms of percentage of not-evaluable tests (5.6% versus 3.7%, respectively,  $p = 0.21$ ) while S-CMR showed a superior sensitivity in detecting CAD compared to SPECT (sensitivity score of 0.69 and 0.59, respectively,  $p = 0.024$ ), but with a lower specificity (specificity scores of 0.61 and 0.72, respectively,  $p = 0.038$ ) [34]. The overall superiority of S-CMR over SPECT and gated-SPECT for the detection of CAD was demonstrated (AUC 0.75 vs. 0.65 vs. 0.69) with significant difference ( $p = 0.0004$  and  $p = 0.018$ ) [35].

Of note, MR-IMPACT trials were performed on a selected population with a relatively high pretest probability of disease, which is not the typical population referred for noninvasive stress tests in clinical practice. However, all tests were performed in all patients to avoid testing bias.

A powerful and direct comparison between S-CMR and SPECT was additionally provided by the CE-MARC study in 2012. This was a large, prospective, multicentre trial that involved a cohort of 628 patients with suspected angina, who prospectively underwent S-CMR, SPECT, and ICA (reference standard) examinations in a period of 4 weeks with later follow-up till 5 years. Of note, the S-CMR examination



included a multiparametric protocol with rest and stress (adenosine) perfusion, cine imaging, 3D coronary MR angiography, and LGE. In this study, Greenwood et al. demonstrated a significantly higher sensitivity and negative predictive value of S-CMR compared to SPECT (86% vs. 66%, 90% vs. 79%, respectively,  $p < 0.0001$ ), but with similar specificity and positive predictive values (83% vs. 82%, 77% vs. 71%, respectively,  $p = 0.916$  and  $p = 0.061$ ) for detecting significant coronary artery stenosis. Furthermore, S-CMR showed a higher AUC than SPECT (0.89 versus 0.79;  $p < 0.0001$ ) independently of the threshold used to define the presence of obstructive CAD (50% or 70% coronary artery stenosis) and regardless of the extension of vessel disease [36].

In detail, a subsequent gender-based subanalysis of the CE-MARC trial showed greater sensitivity of S-CMR than SPECT in both genders, and differently from SPECT, there were no relevant gender differences in the diagnostic accuracy [37].

Different meta-analyses have also evaluated the diagnostic accuracy of S-CMR in identifying CAD by using invasive FFR as reference standard.

In a meta-analysis by Danad et al., S-CMR had the highest performance for the diagnosis of hemodynamically significant CAD on both a per-vessel (AUC 0.97) and per-patient (AUC 0.94) basis, due to excellent sensitivity and specificity. Anatomical evaluation with CCTA and ICA yielded lower specificity, with functional assessment of coronary atherosclerosis by stress echo, SPECT, and FFR-CT improving accuracy [38].

Other data from meta-analyses showed that S-CMR sensitivities and specificities ranged between 89% and 91% and 81% and 86%, respectively [39–41].

Pontone et al. in 2019 compared the diagnostic performance of noninvasive tests using invasive FFR as a reference standard for CAD, including 77 studies. S-CMR showed a higher sensitivity in detecting functionally significant CAD (81%) than stress perfusion CT combined with CCTA (79%), stress perfusion CT (77%), stress echo (72%), and SPECT (64%), despite being inferior to CCTA (88%), FFR-CT (85%), and PET (85%). However, S-CMR showed a higher test performance to identify patients that needed subsequent invasive coronary artery procedures (91%) [42].

Of note, the majority of scientific studies on the diagnostic performance of S-CMR have been performed on adenosine perfusion stress tests, which actually represent the mainstay of S-CMR.

Little scientific evidence exists on other vasodilator agents, such as dipyridamole and regadenoson.

Compared to adenosine, dipyridamole demonstrated reduced sensitivity (86% versus 90%;  $p = 0.022$ ) and similar specificity (77% versus 81%;  $p = 0.065$ ) for diagnosing coronary stenosis  $\geq 50\%$  on ICA, but provided additional information by evaluating both perfusion and wall motion abnormalities [43].

Regadenoson and adenosine achieved equivalent vasodilator stress and myocardial perfusion reserve (MPR), but the latter is cheaper and better tolerated [44, 45].

Regarding dobutamine as a stress agent, although it is the only technique that has offered a comparative performance

against dobutamine stress echocardiography [46], it is still less used than vasodilator stressors that allow a simpler and safer vasodilatory myocardial perfusion. In a meta-analysis of 37 studies involving 2191 patients, dobutamine-induced RWMA demonstrated a sensitivity of 0.83 and a specificity of 0.86 on the patient level for revealing angiographically significant CAD (luminal stenosis  $\geq 50\%$ ), with higher specificity when assessed on the vessel level (0.93) [32]. However, the diagnostic accuracy of wall motion abnormalities induced by dobutamine S-CMR is significantly influenced by LV geometry, with the lowest performance in patients with increased LV concentricity compared to those with normal geometry and eccentric hypertrophy (0.73 versus 0.87 versus 0.90, respectively) in detecting coronary stenosis  $\geq 70\%$  [47].

All these data have provided a defined role of S-CMR in the diagnosis of known or suspected CAD, with a high accuracy in relation to both coronary artery assessment and functional examinations, in particular SPECT.

#### 4. Prognostic Role of Stress CMR

To allow appropriate management of CAD patients, a reliable prognostic assessment with information on patient outcome should be provided.

**4.1. Myocardial Ischemia.** Functional evidence of ischemia remains the major criterion for prognostically relevant CAD [48–50]. In 2011, a study by Krittayaphong et al. assessed the prognostic value of combined myocardial perfusion CMR and LGE, thus identifying myocardial ischemia as the strongest predictor for hard cardiac events and major adverse cardiac events (MACE) among patients with known or suspected CAD [51]. Buckert et al. in a large, consecutive, and thereby unselected population of patients presenting with stable angina pectoris reported how patients with reversible perfusion defects significantly showed more cardiac deaths ( $p < 0.0001$ ) and nonfatal myocardial infarction ( $p = 0.001$ ) than in the control group. Again, myocardial ischemia resulted as the strongest independent predictor for adverse events, with a high negative predictive value in the absence of a perfusion deficit [52]. Recently, Heitner et al., in a multicentre study involving 9151 patients followed up for up to 10 years, demonstrated that patients with positive perfusion S-CMR tests had significantly higher annual mortality rates, compared to those with normal tests. Additionally, there was a relevant improvement in predicting adverse events ( $p < 0.001$ ) when positive perfusion S-CMR was included as a variable in Cox regression models [53].

Currently, the exact definition of ischemic burden and thresholds for initiating revascularization remains a subject of considerable interest, since the extent of ischemia was proved to be directly related to the number of subsequent CAD events [54]. Observational data indicated that medical therapy alone may be associated with a reduced risk of death compared with revascularization in patients with less extensive ischemia ( $<10\%$  of the myocardium), while a more severe ischemia extent ( $\geq 10\%$  of the myocardium) demonstrated a reduced risk of CAD and all-cause death with



coronary revascularization compared with medical therapy [55]. A threshold of  $\geq 10\%$  ischemic myocardium was identified to define treatment effectiveness [56]. In 2017, Vincenti et al. performed a prospective study in 1024 patients with known or suspected CAD who were referred for perfusion CMR to detect myocardial ischemia. Data evidenced how an ischemia burden involving  $\geq 1.5$  ischemic segments was the strongest predictor of hard clinical events, and the authors concluded that patients with zero or 1 ischemic segment could be safely deferred to revascularization [57]. Concerning the ischemia extent, a technical advantage of S-CMR over SPECT relies on its higher spatial resolution ( $3\text{ mm} \times 3\text{ mm}$  vs.  $10\text{ mm} \times 10\text{ mm}$  in-plane spatial resolution), which allows recording of smaller myocardial areas of hypoperfusion resulting in an even better diagnostic performance [58].

Recently, the MR-INFORM study has suggested S-CMR as a selection criterion for patients to be initiated to revascularization. This is a large, multicentre, randomized controlled clinical effectiveness trial that randomized 918 patients with suspected CAD to a myocardial perfusion CMR-based strategy or an FFR-based strategy. In the results, S-CMR was associated with a significantly higher reduction of invasive revascularization procedures than FFR (35.7% vs. 45.0%,  $p = 0.005$ ), while the percentage of patients free from angina at 12 months did not differ significantly between the two groups (49.2% for S-CMR versus 43.8% for FFR,  $p = 0.21$ ), thus representing noninferiority of S-CMR versus FFR in predicting MACE [59].

**4.2. LGE and EF%.** Another advantage of S-CMR is based on its ability to give complementary information on cardiac function and myocardial viability, eventually supported by advanced deep learning-based analysis methods [60], which could additionally provide prognostic information [61].

Low left ventricular ejection fraction (LVEF) has traditionally represented a marker of poor outcome in post-MI patients, with LVEF  $\leq 35\%$  denoting high-risk patients who require more aggressive management [62]. Moreover, the prognostic role of LGE in the field of CAD has also been extensively assessed [63]. In a retrospective, multicentre study by Kwong et al. in 2019, among 2349 patients with stable chest pain, the absence of LGE, as well as of myocardial ischemia, was related to a low incidence of cardiac events ( $< 1\%$ ), reduced need for coronary revascularization (1-3%), and low spending on subsequent ischemia follow-up [64]. Among STEMI patients, early or deferred CMR provided equivalent and powerful stratification strategies for outcome prediction [65].

If large data support consistent and robust prognostic CAD stratification by adenosine S-CMR, fewer studies have investigated the usefulness of dipyridamole S-CMR for predicting adverse clinical events. In 2016, Pontone et al. demonstrated how dipyridamole stress CMR could predict adverse outcomes in 793 consecutive patients symptomatic for chest pain irrespectively of the amount of LGE, thus suggesting a relevant prognostic value of dipyridamole S-CMR by allowing the assessment of both key phases (perfusion and wall motion) of the ischemic cascade. Patients with nor-

mal dipyridamole S-CMR had a low annual hard event rate (1.8%) in comparison with patients with an abnormal perfusion defect alone (3.6%) or patients with perfusion defect plus WMA (9.4%) [66].

Strong evidence, therefore, is available demonstrating the value of S-CMR in excluding prognostically relevant ischemia, although it is an ideal test to exclude relevant disease in patients with known or suspected CAD.

## 5. Advanced Diagnostic and Prognostic Goals for Stress CMR

Since symptoms among patients with CAD are often not uniform and atypical, objective, thus reproducible, diagnostic tests are advisable to both confirm the diagnosis and assess the event risk.

**5.1. Quantitative Perfusion.** Commonly, the analysis of S-CMR image data is performed visually, and semiquantitative and quantitative perfusion techniques are mainly restricted to the research field [67], despite their potential clinical utility. Although quantitative approaches are more time-consuming, they provide very high accuracy in detecting segmental and global impaired myocardial perfusion and may help discriminate diagnosis in particular cases such as multivessel coronary disease, microvascular dysfunction, or suspicion of inadequate vasodilator response [68, 69].

Newer techniques allow direct quantification of the signal from the myocardium during first-pass perfusion and reflect the absolute value of myocardial blood flow in each pixel of the image data. Different approaches such as the Fermi model, uptake model, 1-compartment model, model-independent deconvolution method, and 2 model-independent methods have been proposed and have been shown to have similar diagnostic performance [70]. They would advantageously permit fully automated workflow, pixel-wise flow calculation, single-bolus contrast injection, and rapid processing, allowing an easier performable quantitative analysis [71, 72].

Only few studies provide comparative data among commonly used vasodilator agents regarding their hyperaemic effect. Vasu et al. determined the vasodilator power of each stress agent through both rest and stress myocardial blood flow (MBF) quantification [44]. In this analysis, regadenoson showed a higher stress MBF than adenosine and dipyridamole (3.58 vs. 2.81 vs. 2.78 ml/min/g, respectively,  $p < 0.001$ ), with equivalent vasodilator effect to adenosine (37.8 vs. 36.6  $\mu\text{l}/\text{sec}/\text{g}$ ,  $p = \text{NS}$ ) but with a persistent higher effect than dipyridamole (37.8 vs. 32.6  $\mu\text{l}/\text{sec}/\text{g}$ ,  $p = 0.03$ ) when corrected for heart rate. Therefore, based on quantitative data, a comparable hyperaemic effect of all stress agents could not be fairly assumed. Indeed, most recently Kotecha et al. demonstrated how direct quantification of MBF itself in adenosine stress studies provides a more accurate evaluation of hyperaemia than traditional splenic switch-off and blood pressure response [73], thus encouraging further comparison among stress agents in larger and randomized studies through MBF and coronary flow quantification.

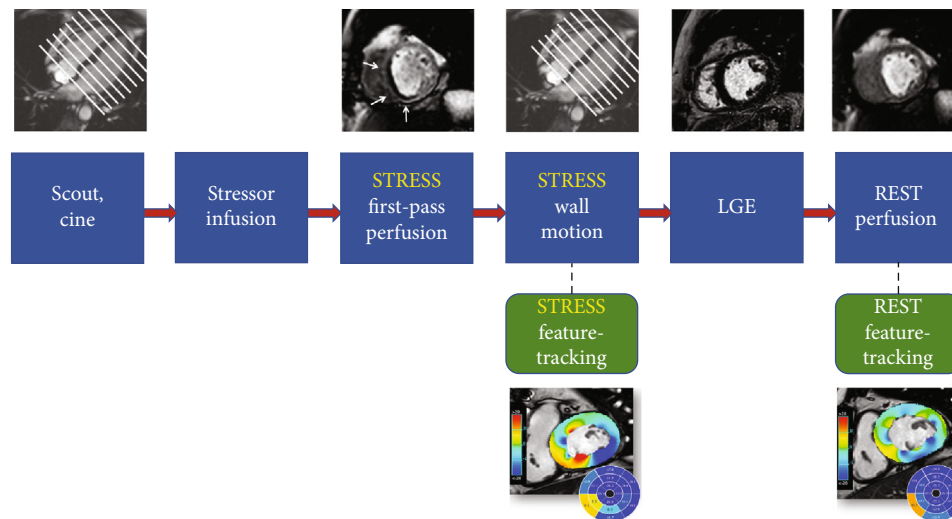


FIGURE 2: A potential protocol for stress cardiovascular magnetic resonance integrated with feature tracking analysis in both rest and stress phases.

**5.2. Mapping Sequences.** Multiple studies have enhanced the increasing role of additional mapping sequences in CMR protocols, and potentially, the application of mapping sequences may help detect myocardial ischemia [74]. Stress native T1-mapping T2-mapping could potentially target changes in native myocardial T1 values under vasodilation stress (“T1 reactivity”), which reflect alterations in myocardial blood volume consequent to inducible ischemia [75, 76]. However, currently little evidence exists to allow an affordable use of these sequences in S-CMR protocols, which is still under research.

**5.3. Feature-Tracking Analysis.** Strain analysis has been lastly demonstrated to provide useful information on the presence of ischemia and on patient outcome in S-CMR studies. As widely evidenced, myocardial strain imaging allows quantification of subtle changes of LV function that typically precede a reduction in LVEF [77]. Garg et al. in 2018 provided the first evidence that a reduction in global longitudinal strain (GLS) at peak myocardial hyperaemic stress could be related to the presence of a perfusion defect in patients with suspected CAD [78]. Eventually a protocol of S-CMR may be integrated with strain analysis, without even significantly prolonging overall time acquisition, as shown in Figure 2.

Interestingly, Palmisano et al. evaluated both adenosine S-CMR mapping and strain data in 28 patients with refractory angina who underwent a coronary sinus Reducer implantation. After implantation, myocardial perfusion along with longitudinal ( $-16$  to  $-19\%$ ;  $p = 0.0192$ ) and circumferential strain ( $-18$  to  $-21\%$ ;  $p = 0.0017$ ) improved, without significant changes in radial, circumferential, and longitudinal strain rate ( $p > 0.05$ ) and native T1 and extracellular volume (ECV) [79]. Advantages of both native mapping and feature tracking could relate to the possibility of achieving a sensitive, noninvasive, quantitative measure of myocardial ischemia and tissue alterations, even without the need for contrast agents, which is desirable due to increasing age and

frequent concomitant renal disease in CAD patients. Poli et al. have tested the feasibility and reliability of noncontrast adenosine S-CMR T1 mapping in 58 patients under haemodialysis treatment and proved excellent test-retest reliability of rest and stress native T1 [80].

More scientific evidence is needed to prove the diagnostic performance and risk stratification power of such quantitative approaches. If these become more feasible and robust, they will potentially impact routine CAD management.

## 6. Current Challenges of Stress CMR

**6.1. Main Limitations.** A major challenge of S-CMR in clinical practice relies on its limited spatial coverage (only three short-axis slices) in perfusion studies, which may miss the presence of disease, compared to PET [81]. Perfusion S-CMR also has reduced applicability in patients with cardiac devices, which are increasingly prevalent, often due to large susceptibility artefacts that significantly impact image quality, especially in perfusion studies [82]. Moreover, S-CMR provides limited direct coronary stenosis analysis with reduced spatial resolution in comparison to CCTA. Nonlinear relationship between blood flow and tracer as well as between tracer and image signal has been proved, with contrast agent nonlinearity further affecting myocardial ischemia quantification [83].

Although S-CMR is commonly known as a safe technique due to its nonionizing effect, recent discussion has been raised on the potential acute effect on leucocyte DNA in 1.5 T CMR studies. In a recent paper by Critchley et al., CMR was demonstrated in both *in vivo* and *in vitro* studies not to cause DNA double-strand breaks and not to cause loss of leucocyte activity *in vitro*. However, CMR caused a relevant reduction of leucocytes viability *in vivo* [84]. All these results might raise suspicion for new detrimental effects of CMR, but larger clinical studies should be provided to prove the clinical impact of the described phenomenon.

**6.2. Comparison with Other Imaging Modalities Assessing Myocardial Ischemia.** The greatest applicability of CCTA in relation to myocardial ischemia is based on its high spatial resolution with precise evaluation of coronary stenosis and plaque characterization, as outlined in a recent Consensus Statement [85]. However, disadvantages of CCTA regard the use of ionizing radiation, limited temporal resolution, and low contrast-to-noise ratio, which may affect image quality together with beam and scatter artefacts [86].

PET represents the current technical standard for quantitative perfusion imaging, and recently introduced tracers and  $^{13}\text{N}$ -ammonia cyclotrons have improved its clinical applicability and cost-effectiveness [87]. Despite its technical appropriateness for assessment of myocardial ischemia, PET is currently limited by reduced availability and lower spatial resolution in comparison to S-CMR [88]. A hybrid PET-CT approach may allow a more comprehensive study of complex diseases, such as multivessel CAD [85]. In opposition, SPECT is widely available in clinical practice and represents the most frequently used modality for perfusion imaging. Due to recent technological evolution, such as the introduction of new dedicated cameras and compartment modelling, absolute values of MBF may be provided by SPECT with improved sensitivity, even in patients with high BMI, previously considered challenging [89]. However, SPECT is also an ionizing technique, with lower spatial resolution and lower image quality with need for attenuation and motion correction [90]. Stress echocardiography provides a rapid, widely available, nonionizing evaluation of myocardial ischemia, with potential for bedside applications. But despite its clinical usefulness, stress echocardiography is not applicable for coronary stenosis severity analysis and actually lacks in automated quantification of perfusion studies [91].

In conclusion, all these imaging modalities present different advantages and disadvantages for myocardial perfusion assessment, and the best clinical practice should be based on the choice of the most appropriate test for each clinical presentation, disease stage, and centre expertise and availability.

**6.3. Future Perspectives.** Current challenges and limitations of S-CMR will potentially be overcome in the next future thanks to technical evolutions involving both study acquisition and postprocessing phases, eventually leading to less time-consuming and more cost-effective studies.

For example, multitasking CMR has been defined in a study by Christodoulou et al. as a motion-resolved imaging modality with multitime dimensions that can adequately perform quantitative studies based on T1 and T2 relaxation constants without need for cardiac and/or breathing synchronization [92]. This may represent a future direction for CMR and possibly also for stress studies, by providing complete dataset of first-pass time-resolved native T1 mapping perfusion together with quantitative information on oedema and fibrosis within a single sequence.

Another appraisal should be outlined on the evolving role of deep-learning algorithms for fully automated quantification of CMR data [93], possibly supported by supervision with a rapid and high-quality confirmation of clinical images [94].

## 7. Conclusions

Accurate and informative diagnostic capability and prognostic relevance are essential requirements for patient management in the context of CAD, as underlined by the recent 2019 ESC guidelines on CCS. Among the available diagnostic modalities, S-CMR showed an overall high sensitivity and specificity for the detection of anatomically significant CAD (90% and 80%, respectively) and functionally significant CAD (89% and 87%, respectively). Appropriate selection of patients who undergo S-CMR potentially provides further strength to its diagnostic accuracy, which has been widely validated in a large body of evidence and more recently demonstrated clinical effectiveness in direct guiding revascularization in the presence of myocardial ischemia. Moreover, S-CMR achieves valuable prognostic information that ranges from the extent of myocardial ischemia itself and presence and transmural of myocardial scarring to the entity of left ventricular remodelling and the impact on systolic function. Finally, future data on quantitative, objective, and sensitive parameters are expected to yield additional strength to S-CMR in a real-world setting, thus delivering measurements that are accurate and highly reproducible. Given its safety and multiparametric assessment both in terms of diagnosis and prognosis among CAD patients, S-CMR represents an invaluable modality for validating the efficacy of treatment as well as monitoring disease progress. However, despite being a powerful tool, more evidence is needed, especially for quantitative data, to directly translate S-CMR results into routine clinical practice and to provide greater feasibility of a customized patient-tailored approach.

## Data Availability

The scientific data supporting this review article are from previously reported studies and datasets, which have been cited. The processed data are available from the corresponding author upon request.

## Conflicts of Interest

The authors declare no conflict of interest.

## References

- [1] M. R. Patel, E. D. Peterson, D. Dai et al., "Low diagnostic yield of elective coronary angiography," *New England Journal of Medicine*, vol. 362, no. 10, pp. 886–895, 2010.
- [2] SCOT-HEART Investigators, "CT coronary angiography in patients with suspected angina due to coronary heart disease (SCOT-HEART): an open-label parallel-group, multicentre trial," *The Lancet*, vol. 385, no. 9985, pp. 2383–2391, 2015.
- [3] A. I. Guaricci, G. Pontone, L. Fusini et al., "Additional value of inflammatory biomarkers and carotid artery disease in prediction of significant coronary artery disease as assessed by coronary computed tomography angiography," *European Heart Journal-Cardiovascular Imaging*, vol. 18, no. 9, pp. 1049–1056, 2017.
- [4] A. I. Guaricci, T. Arcadi, N. D. Brunetti et al., "Carotid intima media thickness and coronary atherosclerosis linkage in



- symptomatic intermediate risk patients evaluated by coronary computed tomography angiography,” *International Journal of Cardiology*, vol. 176, no. 3, pp. 988–993, 2014.
- [5] G. D. Aquaro, G. di Bella, S. Castelletti et al., “Clinical recommendations of cardiac magnetic resonance, part I: ischemic and valvular heart disease: a position paper of the working group ‘Applicazioni della Risonanza Magnetica’ of the Italian Society of Cardiology,” *Journal of Cardiovascular Medicine*, vol. 18, no. 4, pp. 197–208, 2017.
  - [6] A. I. Guaricci, N. D. Brunetti, M. P. Marra, G. Tarantini, M. di Biase, and G. Pontone, “Diagnosis and prognosis of ischemic heart disease: the framework of cardiac magnetic resonance,” *Journal of Cardiovascular Medicine*, vol. 16, no. 10, pp. 653–662, 2015.
  - [7] A. Kiaos, I. Tziatzios, S. Hadjimiltiades, C. Karvounis, and T. D. Karamitsos, “Diagnostic performance of stress perfusion cardiac magnetic resonance for the detection of coronary artery disease: a systematic review and meta-analysis,” *International Journal of Cardiology*, vol. 252, pp. 229–233, 2018.
  - [8] J. Knuuti, H. Ballo, L. E. Juarez-Orozco et al., “The performance of non-invasive tests to rule-in and rule-out significant coronary artery stenosis in patients with stable angina: a meta-analysis focused on post-test disease probability,” *European Heart Journal*, vol. 39, no. 35, pp. 3322–3330, 2018.
  - [9] J. Knuuti, W. Wijns, A. Saraste et al., “2019 ESC guidelines for the diagnosis and management of chronic coronary syndromes,” *European Heart Journal*, vol. 41, no. 3, pp. 407–477, 2020.
  - [10] D. Neglia, D. Rovai, C. Caselli et al., “Detection of significant coronary artery disease by noninvasive anatomical and functional imaging,” *Circulation: Cardiovascular Imaging*, vol. 8, no. 3, 2015.
  - [11] C. M. Kramer, J. Barkhausen, C. Bucciarelli-Ducci, S. D. Flamm, R. J. Kim, and E. Nagel, “Standardized cardiovascular magnetic resonance imaging (CMR) protocols: 2020 update,” *Journal of Cardiovascular Magnetic Resonance*, vol. 22, no. 1, p. 17, 2020.
  - [12] L. Belardinelli, J. C. Shryock, S. Snowdy et al., “The A2A adenosine receptor mediates coronary vasodilation,” *Journal of Pharmacology and Experimental Therapeutics*, vol. 284, no. 3, pp. 1066–1073, 1998.
  - [13] J. R. Arnold and G. P. McCann, “Cardiovascular magnetic resonance: applications and practical considerations for the general cardiologist,” *Heart*, vol. 106, no. 3, pp. 174–181, 2020.
  - [14] G. Pontone, D. Andreini, A. I. Guaricci et al., “The STRATEGY study (stress cardiac magnetic resonance versus computed tomography coronary angiography for the management of symptomatic revascularized patients): resources and outcomes impact,” *Circulation: Cardiovascular Imaging*, vol. 9, no. 10, 2016.
  - [15] Task Force Members, G. Montalescot, U. Sechtem et al., “2013 ESC guidelines on the management of stable coronary artery disease: the task force on the management of stable coronary artery disease of the European Society of Cardiology,” *European Heart Journal*, vol. 34, no. 38, pp. 2949–3003, 2013.
  - [16] P. S. Douglas, U. Hoffmann, M. R. Patel et al., “Outcomes of anatomical versus functional testing for coronary artery disease,” *New England Journal of Medicine*, vol. 372, no. 14, pp. 1291–1300, 2015.
  - [17] G. Pontone, A. Baggiano, D. Andreini et al., “Stress computed tomography perfusion versus fractional flow reserve CT derived in suspected coronary artery disease: the PERFECTION study,” *JACC: Cardiovascular Imaging*, vol. 12, 8 Part 1, pp. 1487–1497, 2019.
  - [18] N. Carrabba, A. Migliorini, S. Pradella et al., “Old and new NICE guidelines for the evaluation of new onset stable chest pain: a real world perspective,” *BioMed Research International*, vol. 2018, Article ID 3762305, 7 pages, 2018.
  - [19] W. J. Stuijzand, A. R. van Rosendael, F. Y. Lin et al., “Stress myocardial perfusion imaging vs coronary computed tomographic angiography for diagnosis of invasive vessel-specific coronary physiology: predictive modeling results from the computed tomographic evaluation of atherosclerotic determinants of myocardial ischemia (CREDENCE) trial,” *JAMA Cardiology*, vol. 5, no. 12, pp. 1338–1348, 2020.
  - [20] G. Pontone, P. Carità, M. G. Rabbat et al., “Role of cardiac magnetic resonance imaging in myocardial infarction,” *Current Cardiology Reports*, vol. 19, no. 10, p. 101, 2017.
  - [21] M. van Assen, D. J. Kuijpers, and J. Schwitter, “MRI perfusion in patients with stable chest-pain,” *The British Journal of Radiology*, vol. 93, no. 1113, p. 20190881, 2020.
  - [22] B. de Bruyne, N. H. Pijls, B. Kalesan et al., “Fractional flow reserve-guided PCI versus medical therapy in stable coronary disease,” *New England Journal of Medicine*, vol. 367, no. 11, pp. 991–1001, 2012.
  - [23] E. Maffei, C. Martini, C. Tedeschi et al., “Diagnostic accuracy of 64-slice computed tomography coronary angiography in a large population of patients without revascularisation: registry data on the comparison between male and female population,” *La Radiologia Medica*, vol. 117, no. 1, pp. 6–18, 2012.
  - [24] G. Pontone, D. Andreini, E. Bertella et al., “Impact of an intracycle motion correction algorithm on overall evaluability and diagnostic accuracy of computed tomography coronary angiography,” *European Radiology*, vol. 26, no. 1, pp. 147–156, 2016.
  - [25] A. Baggiano, L. Fusini, A. Del Torto et al., “Sequential strategy including FFR<sub>CT</sub> plus stress-CTP impacts on management of patients with stable chest pain: the Stress-CTP RIPCORDER study,” *Journal of Clinical Medicine*, vol. 9, no. 7, p. 2147, 2020.
  - [26] N. Gaibazzi, C. Reverberi, A. Squeri, G. De Iaco, D. Ardissino, and T. Gherli, “Contrast stress echocardiography for the diagnosis of coronary artery disease in patients with chest pain but without acute coronary syndrome: incremental value of myocardial perfusion,” *Journal of the American Society of Echocardiography*, vol. 22, no. 4, pp. 404–410, 2009.
  - [27] A. I. Guaricci, N. Carrabba, G. D. Aquaro et al., “Advanced imaging techniques (CT and MR): gender-based diagnostic work-up in ischemic heart disease?,” *International Journal of Cardiology*, vol. 286, pp. 234–238, 2019.
  - [28] G. Muscogiuri, M. Chiesa, M. Trotta et al., “Performance of a deep learning algorithm for the evaluation of CAD-RADS classification with CCTA,” *Atherosclerosis*, vol. 294, no. p, pp. 25–32, 2020.
  - [29] G. Pontone, D. Andreini, A. Baggiano et al., “Functional relevance of coronary artery disease by cardiac magnetic resonance and cardiac computed tomography: myocardial perfusion and fractional flow reserve,” *BioMed Research International*, vol. 2015, Article ID 297696, 2015.
  - [30] A. Baggiano, M. Guglielmo, G. Muscogiuri, A. I. Guaricci, A. Del Torto, and G. Pontone, “(Epicardial and microvascular) angina or atypical chest pain: differential diagnoses with cardiovascular magnetic resonance,” *European Heart Journal Supplements*, vol. 22, Supplement\_E, pp. E116–E120, 2020.



- [31] J. Schwitter, D. Nanz, S. Kneifel et al., "Assessment of myocardial perfusion in coronary artery disease by magnetic resonance: a comparison with positron emission tomography and coronary angiography," *Circulation*, vol. 103, no. 18, pp. 2230–2235, 2001.
- [32] K. R. Nandalur, B. A. Dwamena, A. F. Choudhri, M. R. Nandalur, and R. C. Carlos, "Diagnostic performance of stress cardiac magnetic resonance imaging in the detection of coronary artery disease: a meta-analysis," *Journal of the American College of Cardiology*, vol. 50, no. 14, pp. 1343–1353, 2007.
- [33] J. Schwitter, C. M. Wacker, A. C. van Rossum et al., "MR-IMPACT: comparison of perfusion-cardiac magnetic resonance with single-photon emission computed tomography for the detection of coronary artery disease in a multicentre, multivendor, randomized trial," *European Heart Journal*, vol. 29, no. 4, pp. 480–489, 2008.
- [34] for the MR-IMPACT investigators, J. Schwitter, C. M. Wacker et al., "Superior diagnostic performance of perfusion-cardiovascular magnetic resonance versus SPECT to detect coronary artery disease: the secondary endpoints of the multicenter multivendor MR-IMPACT II (magnetic resonance imaging for myocardial perfusion assessment in coronary artery disease trial)," *Journal of Cardiovascular Magnetic Resonance*, vol. 14, no. 1, 2012.
- [35] J. Schwitter, C. M. Wacker, N. Wilke et al., "MR-IMPACT II: magnetic resonance imaging for myocardial perfusion assessment in coronary artery disease trial: perfusion-cardiac magnetic resonance vs. single-photon emission computed tomography for the detection of coronary artery disease: a comparative multicentre, multivendor trial," *European Heart Journal*, vol. 34, no. 10, pp. 775–781, 2013.
- [36] J. P. Greenwood, N. Maredia, J. F. Younger et al., "Cardiovascular magnetic resonance and single-photon emission computed tomography for diagnosis of coronary heart disease (CE-MARC): a prospective trial," *Lancet*, vol. 379, no. 9814, pp. 453–460, 2012.
- [37] J. P. Greenwood, M. Motwani, N. Maredia et al., "Comparison of cardiovascular magnetic resonance and single-photon emission computed tomography in women with suspected coronary artery disease from the clinical evaluation of magnetic resonance imaging in coronary heart disease (CE-MARC) trial," *Circulation*, vol. 129, no. 10, pp. 1129–1138, 2014.
- [38] I. Danad, J. Szymonifka, J. W. Twisk et al., "Diagnostic performance of cardiac imaging methods to diagnose ischaemia-causing coronary artery disease when directly compared with fractional flow reserve as a reference standard: a meta-analysis," *European Heart Journal*, vol. 38, no. 13, pp. 991–998, 2017.
- [39] R. R. Desai and S. Jha, "Diagnostic performance of cardiac stress perfusion MRI in the detection of coronary artery disease using fractional flow reserve as the reference standard: a meta-analysis," *American Journal of Roentgenology*, vol. 201, no. 2, pp. W245–W252, 2013.
- [40] M. Li, T. Zhou, L. F. Yang, Z. H. Peng, J. Ding, and G. Sun, "Diagnostic accuracy of myocardial magnetic resonance perfusion to diagnose ischemic stenosis with fractional flow reserve as reference: systematic review and meta-analysis," *JACC: Cardiovascular Imaging*, vol. 7, no. 11, pp. 1098–1105, 2014.
- [41] R. A. P. Takx, B. A. Blomberg, H. El Aidi et al., "Diagnostic accuracy of stress myocardial perfusion imaging compared to invasive coronary angiography with fractional flow reserve meta-analysis," *Circulation: Cardiovascular Imaging*, vol. 8, no. 1, 2015.
- [42] G. Pontone, A. I. Guaricci, S. C. Palmer et al., "Diagnostic performance of non-invasive imaging for stable coronary artery disease: a meta-analysis," *International Journal of Cardiology*, vol. 300, pp. 276–281, 2020.
- [43] M. Hamon, G. Fau, G. Née, J. Ehtisham, and R. Morello, "Meta-analysis of the diagnostic performance of stress perfusion cardiovascular magnetic resonance for detection of coronary artery disease," *Journal of Cardiovascular Magnetic Resonance*, vol. 12, no. 29, 2010.
- [44] S. Vasu, W. P. Bandettini, L.-Y. Hsu et al., "Regadenoson and adenosine are equivalent vasodilators and are superior than dipyridamole- a study of first pass quantitative perfusion cardiovascular magnetic resonance," *Journal of Cardiovascular Magnetic Resonance*, vol. 15, no. 1, p. 85, 2013.
- [45] H. L. Brink, J. A. Dickerson, J. A. Stephens, and K. K. Pickworth, "Comparison of the safety of adenosine and regadenoson in patients undergoing outpatient cardiac stress testing," *Pharmacotherapy: The Journal of Human Pharmacology and Drug Therapy*, vol. 35, no. 12, pp. 1117–1123, 2015.
- [46] E. Nagel, H. B. Lehmkuhl, W. Bocksch et al., "Noninvasive diagnosis of ischemia-induced wall motion abnormalities with the use of high-dose dobutamine stress MRI: comparison with dobutamine stress echocardiography," *Circulation*, vol. 99, no. 6, pp. 763–770, 1999.
- [47] R. Gebker, J. G. Mirelis, C. Jahnke et al., "Influence of left ventricular hypertrophy and geometry on diagnostic accuracy of wall motion and perfusion magnetic resonance during dobutamine stress," *Circulation: Cardiovascular Imaging*, vol. 3, no. 5, pp. 507–514, 2010.
- [48] E. Maffei, S. Seitun, C. Martini et al., "Prognostic value of computed tomography coronary angiography in patients with chest pain of suspected cardiac origin," *La Radiologia Medica*, vol. 116, no. 5, pp. 690–705, 2011.
- [49] A. I. Guaricci, V. Lorenzoni, M. Guglielmo et al., "Prognostic relevance of subclinical coronary and carotid atherosclerosis in a diabetic and nondiabetic asymptomatic population," *Clinical Cardiology*, vol. 41, no. 6, pp. 769–777, 2018.
- [50] N. Gaibazzi, T. Porter, V. Lorenzoni et al., "Effect of coronary revascularization on the prognostic value of stress myocardial contrast wall motion and perfusion imaging," *Journal of the American Heart Association*, vol. 6, no. 6, article e006202, 2017.
- [51] R. Krittayaphong, V. Chaithiraphan, A. Maneesai, and S. Udompanturak, "Prognostic value of combined magnetic resonance myocardial perfusion imaging and late gadolinium enhancement," *The International Journal of Cardiovascular Imaging*, vol. 27, no. 5, pp. 705–714, 2011.
- [52] D. Buckert, P. Dewes, T. Walcher, W. Rottbauer, and P. Bernhardt, "Intermediate-term prognostic value of reversible perfusion deficit diagnosed by adenosine CMR: a prospective follow-up study in a consecutive patient population," *JACC: Cardiovascular Imaging*, vol. 6, no. 1, pp. 56–63, 2013.
- [53] J. F. Heitner, R. J. Kim, H. W. Kim et al., "Prognostic value of vasodilator stress cardiac magnetic resonance imaging: a multicenter study with 48 000 patient-years of follow-up," *JAMA Cardiology*, vol. 4, no. 3, pp. 256–264, 2019.
- [54] M. Kolentinis, M. Le, E. Nagel, and V. O. Puntmann, "Contemporary cardiac MRI in chronic coronary artery disease," *European Cardiology Review*, vol. 15, article e50, 2020.

- [55] R. Hachamovitch, A. Rozanski, L. J. Shaw et al., "Impact of ischaemia and scar on the therapeutic benefit derived from myocardial revascularization vs. medical therapy among patients undergoing stress-rest myocardial perfusion scintigraphy," *European Heart Journal*, vol. 32, no. 8, pp. 1012–1024, 2011.
- [56] R. Hachamovitch, S. W. Hayes, J. D. Friedman, I. Cohen, and D. S. Berman, "Comparison of the short-term survival benefit associated with revascularization compared with medical therapy in patients with no prior coronary artery disease undergoing stress myocardial perfusion single photon emission computed tomography," *Circulation*, vol. 107, no. 23, pp. 2900–2907, 2003.
- [57] G. Vincenti, P. G. Masci, P. Monney et al., "Stress perfusion CMR in patients with known and suspected CAD: prognostic value and optimal ischemic threshold for revascularization," *JACC: Cardiovascular Imaging*, vol. 10, no. 5, pp. 526–537, 2017.
- [58] M. T. P. le, N. Zarinabad, T. D'Angelo et al., "Sub-segmental quantification of single (stress)-pass perfusion CMR improves the diagnostic accuracy for detection of obstructive coronary artery disease," *Journal of Cardiovascular Magnetic Resonance*, vol. 22, no. 1, p. 14, 2020.
- [59] E. Nagel, J. P. Greenwood, G. P. McCann et al., "Magnetic resonance perfusion or fractional flow reserve in coronary disease," *New England Journal of Medicine*, vol. 380, no. 25, pp. 2418–2428, 2019.
- [60] S. Moccia, R. Banali, C. Martini et al., "Development and testing of a deep learning-based strategy for scar segmentation on CMR-LGE images," *Magnetic Resonance Materials in Physics, Biology and Medicine*, vol. 32, no. 2, pp. 187–195, 2019.
- [61] G. Pontone, A. I. Guaricci, D. Andreini et al., "Prognostic stratification of patients with ST-segment-elevation myocardial infarction (PROSPECT): a cardiac magnetic resonance study," *Circulation: Cardiovascular Imaging*, vol. 10, no. 11, 2017.
- [62] P. Ponikowski, A. A. Voors, S. D. Anker et al., "2016 ESC guidelines for the diagnosis and treatment of acute and chronic heart failure: the task force for the diagnosis and treatment of acute and chronic heart failure of the European Society of Cardiology (ESC). Developed with the special contribution of the Heart Failure Association (HFA) of the ESC," *European Heart Journal*, vol. 18, no. 8, pp. 891–975, 2016.
- [63] S. Pica, G. Di Giovine, M. Bollati et al., "Cardiac magnetic resonance for ischaemia and viability detection. Guiding patient selection to revascularization in coronary chronic total occlusions: the CARISMA\_CTO study design," *International Journal of Cardiology*, vol. 272, pp. 356–362, 2018.
- [64] R. Y. Kwong, Y. Ge, K. Steel et al., "Cardiac magnetic resonance stress perfusion imaging for evaluation of patients with chest pain," *Journal of the American College of Cardiology*, vol. 74, no. 14, pp. 1741–1755, 2019.
- [65] P. G. Masci, A. G. Pavon, G. Pontone et al., "Early or deferred cardiovascular magnetic resonance after ST-segment-elevation myocardial infarction for effective risk stratification," *European Heart Journal - Cardiovascular Imaging*, vol. 21, no. 6, pp. 632–639, 2020.
- [66] G. Pontone, D. Andreini, E. Bertella et al., "Prognostic value of dipyridamole stress cardiac magnetic resonance in patients with known or suspected coronary artery disease: a mid-term follow-up study," *European Radiology*, vol. 26, no. 7, pp. 2155–2165, 2016.
- [67] J. Schulz-Menger, D. A. Bluemke, J. Bremerich et al., "Standardized image interpretation and post-processing in cardiovascular magnetic resonance - 2020 update : Society for Cardiovascular Magnetic Resonance (SCMR): Board of Trustees Task Force on Standardized Post-Processing," *Journal of Cardiovascular Magnetic Resonance*, vol. 22, no. 1, p. 19, 2020.
- [68] G. Morton, A. Chiribiri, M. Ishida et al., "Quantification of absolute myocardial perfusion in patients with coronary artery disease: comparison between cardiovascular magnetic resonance and positron emission tomography," *Journal of the American College of Cardiology*, vol. 60, no. 16, pp. 1546–1555, 2012.
- [69] T. Quinaglia, M. Jerosch-Herold, and O. R. Coelho-Filho, "State-of-the-art quantitative assessment of myocardial ischemia by stress perfusion cardiac magnetic resonance," *Magnetic Resonance Imaging Clinics of North America*, vol. 27, no. 3, pp. 491–505, 2019.
- [70] J. D. Biglands, D. R. Magee, S. P. Sourbron, S. Plein, J. P. Greenwood, and A. Radjenovic, "Comparison of the diagnostic performance of four quantitative myocardial perfusion estimation methods used in cardiac MR imaging: CE-MARC substudy," *Radiology*, vol. 275, no. 2, pp. 393–402, 2015.
- [71] P. Kellman, M. S. Hansen, S. Nielles-Vallespin et al., "Myocardial perfusion cardiovascular magnetic resonance: optimized dual sequence and reconstruction for quantification," *Journal of Cardiovascular Magnetic Resonance*, vol. 19, no. 1, p. 43, 2017.
- [72] K. D. Knott, J. L. Fernandes, and J. C. Moon, "Automated quantitative stress perfusion in a clinical routine," *Magnetic Resonance Imaging Clinics of North America*, vol. 27, no. 3, pp. 507–520, 2019.
- [73] T. Kotecha, J. M. Monteagudo, A. Martinez-Naharro et al., "Quantitative cardiovascular magnetic resonance myocardial perfusion mapping to assess hyperaemic response to adenosine stress," *European Heart Journal - Cardiovascular Imaging*, pp. 1–9, 2020.
- [74] S. Yimcharoen, S. Zhang, Y. Kaolawanich, P. Tanapibunpon, and R. Krittayaphong, "Clinical assessment of adenosine stress and rest cardiac magnetic resonance T1 mapping for detecting ischemic and infarcted myocardium," *Scientific Reports*, vol. 10, no. 1, p. 14727, 2020.
- [75] S. Piechnik, S. K. S. Neubauer, and V. M. Ferreira, "State-of-the-art review: stress T1 mapping-technical considerations, pitfalls and emerging clinical applications," *Magnetic Resonance Materials in Physics, Biology and Medicine*, vol. 31, no. 1, pp. 131–141, 2018.
- [76] J. Nickander, R. Themudo, S. Thalén et al., "The relative contributions of myocardial perfusion, blood volume and extracellular volume to native T1 and native T2 at rest and during adenosine stress in normal physiology," *Journal of Cardiovascular Magnetic Resonance*, vol. 21, no. 1, p. 73, 2019.
- [77] P. Gunasekaran, S. Panaich, A. Briasoulis, S. Cardozo, and L. Afonso, "Incremental value of two dimensional speckle tracking echocardiography in the functional assessment and characterization of subclinical left ventricular dysfunction," *Current Cardiology Reviews*, vol. 13, no. 1, pp. 32–40, 2017.
- [78] P. Garg, R. Aziz, T. Al Musa et al., "Effects of hyperaemia on left ventricular longitudinal strain in patients with suspected coronary artery disease : a first-pass stress perfusion cardiovascular magnetic resonance imaging study," *Netherlands Heart Journal*, vol. 26, no. 2, pp. 85–93, 2018.

- [79] A. Palmisano, F. Giannini, P. Rancoita et al., "Feature tracking and mapping analysis of myocardial response to improved perfusion reserve in patients with refractory angina treated by coronary sinus Reducer implantation: a CMR study," *The International Journal of Cardiovascular Imaging*, vol. 36, 2020.
- [80] F. E. Poli, G. S. Gulsin, D. S. March et al., "The reliability and feasibility of non-contrast adenosine stress cardiovascular magnetic resonance T1 mapping in patients on haemodialysis," *Journal of Cardiovascular Magnetic Resonance*, vol. 22, no. 1, p. 43, 2020.
- [81] R. Manka, L. Wissmann, R. Gebker et al., "Multicenter evaluation of dynamic three-dimensional magnetic resonance myocardial perfusion imaging for the detection of coronary artery disease defined by fractional flow reserve," *Circulation: Cardiovascular Imaging*, vol. 8, no. 5, 2015.
- [82] P. Lupo, R. Cappato, G. di Leo et al., "An eight-year prospective controlled study about the safety and diagnostic value of cardiac and non-cardiac 1.5-T MRI in patients with a conventional pacemaker or a conventional implantable cardioverter defibrillator," *European Radiology*, vol. 28, no. 6, pp. 2406–2416, 2018.
- [83] X. Li, C. S. Springer, and M. Jerosch-Herold, "First-pass dynamic contrast-enhanced MRI with extravasating contrast reagent: evidence for human myocardial capillary recruitment in adenosine-induced hyperemia," *NMR in Biomedicine*, vol. 22, no. 2, pp. 148–157, 2009.
- [84] W. R. Critchley, A. Reid, J. Morris et al., "The effect of 1.5 T cardiac magnetic resonance on human circulating leucocytes," *European Heart Journal*, vol. 39, no. 4, pp. 305–312, 2018.
- [85] on behalf of the Quantitative Cardiac Imaging Study Group, M. Dewey, M. Siebes et al., "Clinical quantitative cardiac imaging for the assessment of myocardial ischaemia," *Nature Reviews Cardiology*, vol. 17, no. 7, pp. 427–450, 2020.
- [86] K. Kitagawa, R. T. George, A. Arbab-Zadeh, J. A. Lima, and A. C. Lardo, "Characterization and correction of beam-hardening artifacts during dynamic volume CT assessment of myocardial perfusion," *Radiology*, vol. 256, no. 1, pp. 111–118, 2010.
- [87] Y. Petibon, Y. Rakvongthai, G. El Fakhri, and J. Ouyang, "Direct parametric reconstruction in dynamic PET myocardial perfusion imaging: in vivo studies," *Physics in Medicine and Biology*, vol. 62, no. 9, pp. 3539–3565, 2017.
- [88] R. S. Driessen, J. E. van Timmeren, W. J. Stuijzfand et al., "Measurement of LV volumes and function using oxygen-15 water-gated PET and comparison with CMR imaging," *JACC: Cardiovascular Imaging*, vol. 9, no. 12, pp. 1472–1474, 2016.
- [89] M. Bocher, I. M. Blevis, L. Tsukerman, Y. Shrem, G. Kovalski, and L. Volokh, "A fast cardiac gamma camera with dynamic SPECT capabilities: design, system validation and future potential," *European journal of nuclear medicine and molecular imaging*, vol. 37, no. 10, pp. 1887–1902, 2010.
- [90] on behalf of the Cardiovascular Committee of the European Association of Nuclear Medicine (EANM), D. Agostini, P. Y. Marie et al., "Performance of cardiac cadmium-zinc-telluride gamma camera imaging in coronary artery disease: a review from the cardiovascular committee of the European Association of Nuclear Medicine (EANM)," *European Journal of Nuclear Medicine and Molecular Imaging*, vol. 43, no. 13, pp. 2423–2432, 2016.
- [91] Y. Li, C. P. Ho, M. Toulemonde, N. Chahal, R. Senior, and M. X. Tang, "Fully automatic myocardial segmentation of contrast echocardiography sequence using random forests guided by shape model," *European Journal of Nuclear Medicine and Molecular Imaging*, vol. 37, no. 5, pp. 1081–1091, 2018.
- [92] A. G. Christodoulou, J. L. Shaw, C. Nguyen et al., "Magnetic resonance multitasking for motion-resolved quantitative cardiovascular imaging," *Nature Biomedical Engineering*, vol. 2, no. 4, pp. 215–226, 2018.
- [93] B. Böttcher, E. Beller, A. Busse et al., "Fully automated quantification of left ventricular volumes and function in cardiac MRI: clinical evaluation of a deep learning-based algorithm," *The International Journal of Cardiovascular Imaging*, vol. 36, no. 11, pp. 2239–2247, 2020.
- [94] Q. Zhang, E. Hann, K. Werys et al., "Deep learning with attention supervision for automated motion artefact detection in quality control of cardiac T1-mapping," *Artificial Intelligence in Medicine*, vol. 110, p. 101955, 2020.

## Review Article

# Artificial Intelligence in Coronary Computed Tomography Angiography: From Anatomy to Prognosis

**Giuseppe Muscogiuri,<sup>1</sup> Marly Van Assen,<sup>2</sup> Christian Tesche,<sup>3,4</sup> Carlo N. De Cecco,<sup>2</sup> Mattia Chiesa,<sup>1</sup> Stefano Scafuri,<sup>5</sup> Marco Guglielmo,<sup>1</sup> Andrea Baggiano,<sup>1</sup> Laura Fusini,<sup>1</sup> Andrea I. Guaricci,<sup>6</sup> Mark G. Rabbat,<sup>7,8</sup> and Gianluca Pontone<sup>1</sup>**

<sup>1</sup>Centro Cardiologico Monzino, IRCCS, Milan, Italy

<sup>2</sup>Division of Cardiothoracic Imaging, Nuclear Medicine and Molecular Imaging, Department of Radiology and Imaging Sciences, Emory University, Atlanta, GA, USA

<sup>3</sup>Department of Cardiology, Munich University Clinic, Ludwig-Maximilians-University, Munich, Germany

<sup>4</sup>Department of Internal Medicine, St. Johannes-Hospital, Dortmund, Germany

<sup>5</sup>Division of Interventional Structural Cardiology, Cardiothoracovascular Department, Careggi University Hospital, Florence, Italy

<sup>6</sup>Institute of Cardiovascular Disease, Department of Emergency and Organ Transplantation, University Hospital "Policlinico Consorziale" of Bari, Bari, Italy

<sup>7</sup>Loyola University of Chicago, Chicago, IL, USA

<sup>8</sup>Edward Hines Jr. VA Hospital, Hines, IL, USA

Correspondence should be addressed to Gianluca Pontone; [gianluca.pontone@ccfm.it](mailto:gianluca.pontone@ccfm.it)

Received 29 October 2020; Revised 30 November 2020; Accepted 9 December 2020; Published 18 December 2020

Academic Editor: Luca Liberale

Copyright © 2020 Giuseppe Muscogiuri et al. This is an open access article distributed under the Creative Commons Attribution License, which permits unrestricted use, distribution, and reproduction in any medium, provided the original work is properly cited.

Cardiac computed tomography angiography (CCTA) is widely used as a diagnostic tool for evaluation of coronary artery disease (CAD). Despite the excellent capability to rule-out CAD, CCTA may overestimate the degree of stenosis; furthermore, CCTA analysis can be time consuming, often requiring advanced postprocessing techniques. In consideration of the most recent ESC guidelines on CAD management, which will likely increase CCTA volume over the next years, new tools are necessary to shorten reporting time and improve the accuracy for the detection of ischemia-inducing coronary lesions. The application of artificial intelligence (AI) may provide a helpful tool in CCTA, improving the evaluation and quantification of coronary stenosis, plaque characterization, and assessment of myocardial ischemia. Furthermore, in comparison with existing risk scores, machine-learning algorithms can better predict the outcome utilizing both imaging findings and clinical parameters. Medical AI is moving from the research field to daily clinical practice, and with the increasing number of CCTA examinations, AI will be extensively utilized in cardiac imaging. This review is aimed at illustrating the state of the art in AI-based CCTA applications and future clinical scenarios.

## 1. Introduction

Coronary computed tomography angiography (CCTA) represents an excellent tool for the evaluation of patients with suspected stable coronary artery disease (CAD) [1–6]. There is strong evidence in the literature that CCTA can accurately rule out the presence of CAD, having a positive impact in terms of prognosis and cost [7–11].

CCTA represents an important step in clinical management of patients with suspected CAD; however, it is important to keep in mind that the majority of CCTA results in no evidence of significant CAD [12, 13]. Furthermore, the presence of obstructive CAD on CCTA is not always associated with the development of myocardial ischemia [14].

The application of artificial intelligence (AI) in cardiac radiology is aimed at facilitating the management of patients



with suspected CAD ranging from diagnosis to prognostic stratification [15]. In particular, the application of AI can be helpful in reducing the time of image analysis and rule out patients without evidence of significant disease that may benefit from medical therapy [16]. Furthermore, it can be helpful for detection of myocardial ischemia [17]. In terms of prognostic stratification, AI may play a promising role, identifying algorithms that can stratify the risk of major adverse cardiovascular events (MACE) with high accuracy [18].

## 2. Basic Concept of AI in Clinical Medicine

The AI industry has seen massive growth in a variety of fields in the past decade, with the field of medicine not being an exception. The basis of AI is mathematics and computer science with the three main pillars being (1) big data, (2) high performance computing infrastructure, and (3) algorithm development. The exponential growth in digital storage capabilities, data collection systems, and computing power enabled AI applications in a wide variety of fields. The current digital era leads to an increased amount of information, which is beneficial to the development of AI algorithms. The technological developments make it possible to develop algorithms that are able to deal with the large amount of data and complexity typical of the digital era we live in.

With AI currently entering the medical field, early stage applications have mainly focused on automatization of medical tasks; more recently, the focus has shifted towards prognostication and risk prediction. Many studies investigate the potential role of AI in supporting clinicians in their day-to-day tasks, assisting in workflow optimization, quantification, diagnosis and prognostication, and reporting. However, many clinical AI applications are currently only used in a research setting and are far from being implemented into clinical practice. There are examples of successful AI implementation [19]. The Data Science Institute of the American College of Radiology has published a list of all FDA cleared AI algorithms for radiology purposes [20] with their state of validation and clinical use. However, there are also examples of applications that are not ready for clinical utilization [21, 22]. For example, Zech et al. assessed how well convolutional neural networks (CNN) generalized across three hospital systems for a simulated pneumonia screening task. They found that their evaluated CNN performed systematically worse on unseen data from different hospitals compared to the training set. In addition, they reported that the CNN identified disease burden within hospital system and department, which may confound predictions [21]. A thorough clinical validation is essential for the acceptance and implementation of AI into clinical practice [22]. A study by Kim et al. evaluated the validation of AI algorithms reported in AI research papers from all medical fields, including radiology, dermatology, and pathology. They reported that only 6% of all studies used external validation to assess AI algorithm performance [22]. Since then, several guidelines have been published to improve the validation process of medical AI applications [23, 24]. Recently, we have seen an increase in publications that externally validate industry developed AI algorithms [25, 26]. In addition, regulations and guide-

lines regarding protection of patient privacy and cybersecurity are also needed. Creating awareness and increasing basic AI knowledge for clinicians are an essential step to promote wide AI acceptance among physicians and patients.

The European commission released a white paper on AI in February 2020, including statements on the use of AI for medical purposes [27, 28]. They state that current EU regulations already provide a high level of protection through medical device laws and data protection laws; however, they proposed to add specific regulations including requirements of training data, record-keeping of used datasets, transparency, robustness and accuracy, and human oversight. The US counterpart, the U.S. Food and Drug Administration, also released statements regarding the use of medical AI. While application for medical assistance, such as quantification applications, only requires a proof of equivalence to other software (510(k)) [20, 29], application for clinical interpretation of medical data is a more elaborate FDA approval (PMA).

Besides the legal framework for medical AI, there are some ethical considerations that will play a key role [30]. With the use of medical data, issues such as gender, race, or economical discrimination due to underrepresentation in the training populations should be discussed and evaluated. In addition, AI-based risk prediction and prognostication can be used to limit the choice and coverage of healthcare insurance in certain groups of patients or can affect important life choices. Like every new technology in the medical field, it is imperative to learn how to balance the benefits and risks associated with a broad AI implementation and how to democratize AI and make sure that everybody can benefit equally from its use. The Joint European and North American Multisociety task force discusses these issues in detail, emphasizing that more research is needed on the implementation of AI into clinical practice [31]. Figure 1 shows the process of DICOM images elaboration for development of DL algorithm.

## 3. AI Application for the Evaluation of Coronary Artery Stenosis

The grading and coronary segments involved with obstructive of CAD have been associated with a worse prognosis [32].

Often assessment of CAD stenosis is time consuming, requiring multiplanar reconstruction selection of the best phase in the cardiac cycle for a correct assessment of coronary arteries and depends on the experience of the reader [15]. After the CTA analysis, results may be reported extensively in the report following the guidelines of SCCT [33] or in a structured patient-based approach identifying a specific CAD-RADS grading [34].

Zreik et al. developed a 3D CNN that was able to characterize the plaque and evaluate the grading of stenosis [35]. The authors developed two models; the first one analyzed the performance of the algorithm to differentiate patients with/without obstructive CAD demonstrating a per-segment, vessel, and patient accuracy of 0.94, 0.93, and 0.85, respectively [35]. The second model was developed for identification of no stenosis, no significant stenosis, and significant

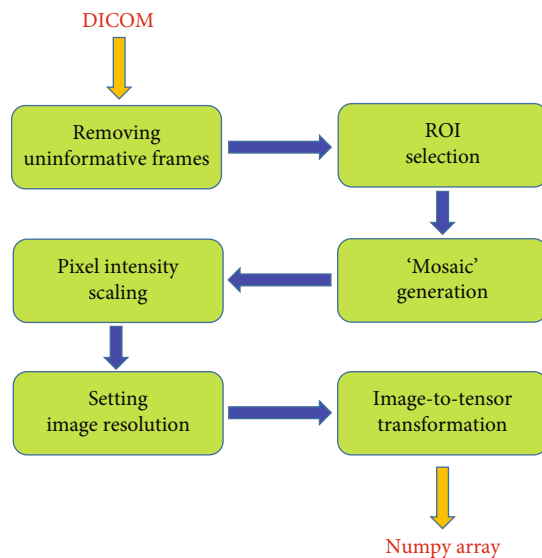


FIGURE 1: Streamline used for the development of images useful for DL algorithm starting from DICOM images.

stenosis; the second model showed a per-segment, vessel, and patient accuracy of 0.80, 0.76, and 0.75, respectively [35].

Kang et al. developed an AI technique based on a two-step algorithm with a vector machine that was useful for the evaluation of CAD stenosis [36]. On a population of 42 patients acquired with dual source CT, the algorithm was able to identify the grade of stenosis in one second with a sensitivity, specificity, and accuracy in the proximal and midsegments of 93%, 95%, and 94%, respectively [36].

Yoneyama et al. evaluated the possibility to identify the grading of coronary stenosis and its impact in terms of ischemia using a cohort of patients who underwent CCTA and perfusion single photon emission computed tomography (SPECT) [37]. The authors focused on the application of an artificial neural network (ANN) with hybrid imaging obtained by the combination of CCTA and myocardial perfusion SPECT [37]. Using this algorithm, the specificity, sensitivity, and accuracy to identify coronary artery stenosis >70% were 31%, 78%, and 67%, respectively [37].

Van Hamersvelt et al. developed an algorithm of AI that evaluated the presence of significant CAD using a combined approach of AI that analyzes the myocardium and compared it with invasive FFR [38]. They found that a combined approach was able to identify hemodynamically significant CAD with an AUC of 0.76.

Two studies developed an automated approach of CAD-RADS in clinical practice [16, 39].

Muscogiuri et al. evaluated the impact of a new deep learning algorithm based on CNN for the classification of CAD-RADS in a cohort of 288 patients who underwent CCTA for a clinical indication [16]. The time of analysis and accuracy for each of the following was extrapolated: Model A (CAD-RADS 0 vs. CAD-RADS 1-2 vs. CAD-RADS 3, 4, 5), Model 1 (CAD-RADS 0 vs. CAD-RADS > 0), and Model 2 (CAD-RADS 0-2 vs. CAD-RADS 3-5) [16]. The sensitivity, specificity, negative predictive value, positive predictive value, and accuracy of the models com-

pared to humans were the following: Model A, 47%, 74%, 77%, 46%, and 60%; Model 1, 66%, 91%, 92%, 63%, and 86%; and Model 2, 82%, 58%, 74%, 69%, and 71% [16]. The average time of analysis of CNN was significantly shorter compared to humans, with an average time of analysis around 104 seconds [16]. This study highlights the possibility to have an automatic discrimination between patients with CAD – RADS > 0 with a high diagnostic accuracy and short time. This is an important finding if we assume an increased number of CCTA scans in the future, many of which may not show CAD [12, 13]. A representative case showing the application of the CAD-RADS software for detection of AI is shown in Figure 2.

Another important application of automatic CAD-RADS classification was shown by Huang et al. [39]. The authors classified CAD-RADS using a deep learning algorithm and subsequently correlated the results with the presence of arterial breast calcification. The authors showed that the presence of high grade CAD-RADS was closely associated with increased presence of breast arterial calcification [39]. This finding is important because the assessment of breast arterial calcification in screening for breast cancer can be utilized for early identification of patients with CAD.

## 4. AI for Evaluation of Plaque Analysis

4.1. *Calcium Score.* Coronary Artery Calcium Score (CACS) is an independent predictor of adverse cardiovascular events [40–42].

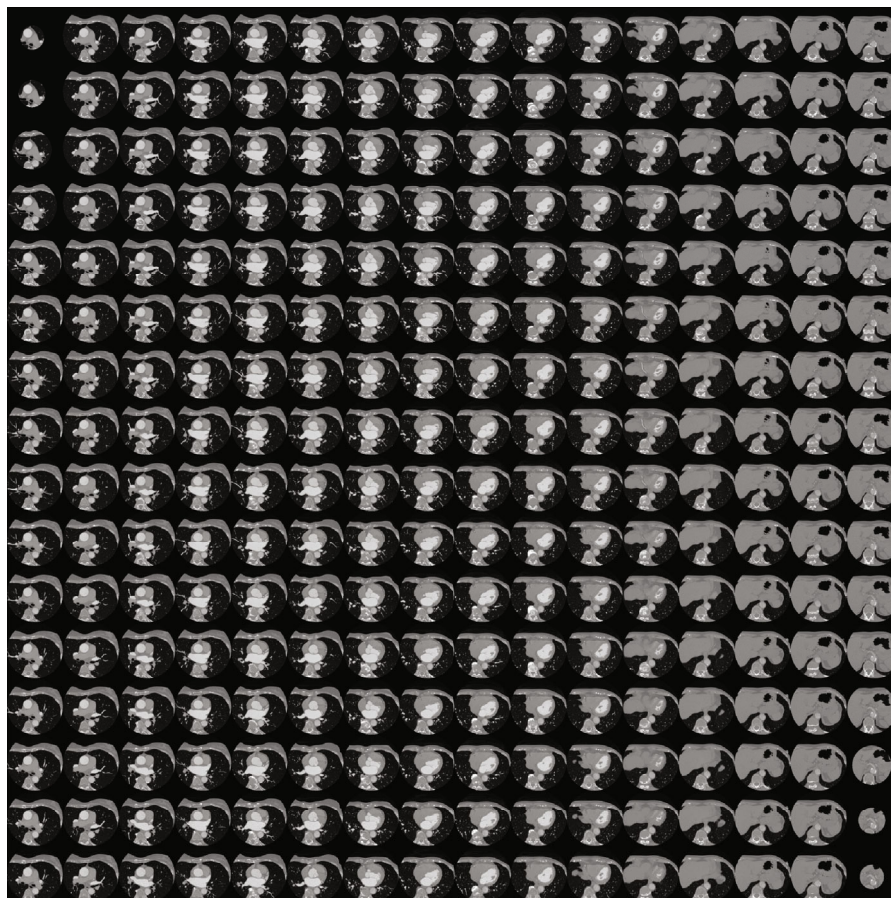
CT images for the evaluation of calcium score are often acquired using an ECG-gated, no contrast technique and segmented calculating a calcium volume, and mass obtaining a specific value of calcium score [43]. Currently, CACS is performed by semiautomatic segmentation and despite a time consuming approach is still the gold standard [44].

The evaluation of CACS using an AI algorithm can definitely speed up the time of reporting.

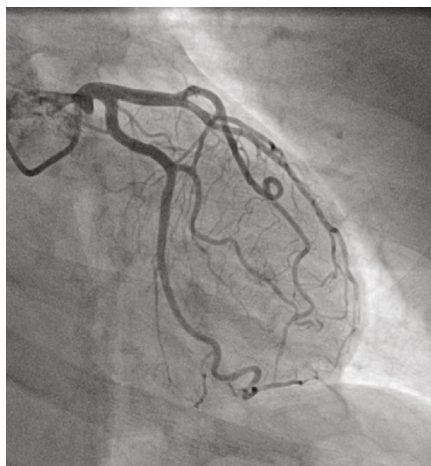
One of the first articles describing the evaluation of CACS using an algorithm of AI was developed by Isgum et al. [45]. The authors analyzed the impact of the automated algorithm on ECG-gated, noncontrast images, and identified coronary calcification in 73.8% of cases and 93.4% of cases was correctly classified in the respective risk group [45].

Sandsted et al. evaluated the performance of an AI algorithm for the evaluation of CACS compared to semiautomated CACS [46]. The authors found a Spearman's rank correlation coefficient for Agatston Score, Calcium Volume Score, and Calcium Mass Score between the AI algorithm and semiautomatic approach of 0.935, 0.932, and 0.934, respectively, while the intraclass correlations were 0.996, 0.996, and 0.991, respectively, [46].

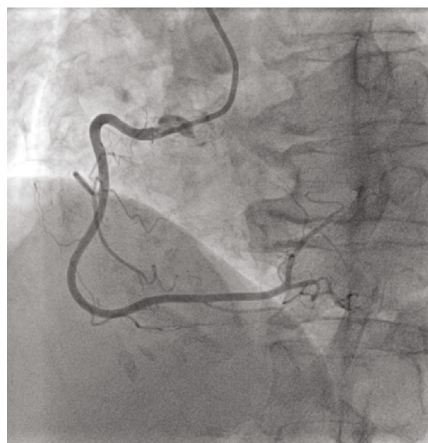
Despite CACS traditionally being evaluated using ECG-gated scans, recently, Takx et al. analyzed the impact of AI for evaluation of CACS in non-ECG-gated and noncontrast images acquired in a cohort of patients undergoing a CT for lung cancer screening [47]. In a cohort of 1793 patients, the authors analyzed the impact of an AI algorithm for detection of CACS. Despite a small percentage of the population (44 patients representing the 2.5%) being excluded from the



(a)



(b)



(c)

FIGURE 2: A 54-year-old female patient scheduled for invasive coronary angiography. Reconstruction for CAD-RADS algorithm is shown in (a). The algorithm provides a CAD – RADS = 0. This finding was confirmed on coronary angiography that shows no disease in the left coronary artery (b) and right coronary artery (c).

study due to image quality, the authors found good reliability with a weighted  $k$  of 0.85 for Agatston risk score between the automated and reference scores [47]; however, an underestimation in terms of volume of calcium was observed in the automatic segmentation compared to manual segmentation [47].

The combination of CACS analysis and lung cancer screening can be a powerful combination in clinical practice to identify patients that may benefit from therapy.

Wolterink et al. described the application of an automated algorithm for the evaluation of CAC in 250 patients who underwent CCTA [48]. The authors described a



supervised approach and developed a CNN algorithm that was able to identify CAC with a sensitivity of 0.72 and an interclass correlation of 0.94 between CAC derived from CCTA and standard evaluation of CAC [48]. This approach may lead to radiation dose reduction.

Finally, Van Velzen et al. evaluated calcium scores from different CT without contrast [49]. 7240 examinations were analyzed from PET attenuation CT images and CT of the chest demonstrating an intraclass correlation coefficient ranging from 0.79 to 0.97 when compared with manual segmentation [49]. An approach that is independent of ECG-gated acquisition, allowing for automated analysis, represents an important tool.

**4.2. Plaque Phenotype.** Assessment of plaque composition is extremely important in CCTA reporting; indeed, identification of fibrous or calcified plaques can be extremely important for patient management [50]. Presence of calcified plaques is associated with better outcome compared to fibrous plaques, especially in the presence of high-risk plaque characteristics [51].

The application of AI can facilitate and speed up the analysis of CCTA providing accurate information on plaque analysis in a relative short time.

Zreik et al. developed an algorithm that was able to identify the plaque morphology and severity of stenosis [35]. From a sample size of 95 patients, the authors developed an AI approach based on 3D CNN that extrapolated the characteristics of plaque along the coronary arteries. Subsequently, the images were tested on a smaller cohort composed of 65 patients showing an accuracy of 0.85 for differentiation between plaque and no plaque while the accuracy for differentiation between different types of plaque was 0.77 [35].

Another application of AI for identification of different plaque types was developed by Dey et al. The authors developed an algorithm that automatically differentiated calcified plaque ( $r$ : 0.88) and noncalcified plaque ( $r$ : 0.98) with a good correlation compared to manual segmentation [52].

A different, combined approach of radiomics and machine learning (ML) for the evaluation of plaque characteristics has been demonstrated to characterize plaque [53]. Using radiomics, from standard images, it is possible to obtain several parameters that can constitute the fingerprinting of a plaque.

Kolossvary et al. evaluated the radiomic features of plaques showing napkin ring sign (NRS) which has been associated with poor outcome [54]. The authors describe the parameter called “short-run low-gray-level emphasis”; this parameter was able to identify plaque with NRS with a better accuracy (AUC 0.89) compared to mean plaque attenuation (AUC 0.75), the latter used in standard clinical practice [54].

An ML approach can identify the presence of thin cap fibroatheroma (TCFA) overcoming the technical limitation of CCTA [53]. In particular, Masuda et al. analyzed the application of an ML histogram for the identification of fibrous and fatty or fibrous-fatty plaques compared to IVUS showing an accuracy of 0.92, while standard parameters showed an accuracy of 0.83 [55].

**4.3. AI for the Assessment of Ischemia: CT-Derived Fractional Flow Reserve and CT Perfusion.** Recent research and development in AI has been applied in multiple potential applications of cardiac CT-derived myocardial ischemia assessments. Most software applications hereby deal with CT-derived fractional flow reserve (FFR) for the detection of hemodynamically significant CAD. Only few studies of AI applications using CT perfusion have been published so far. In terms of CT-FFR, ML solutions have been provided by only one vendor [56, 57]. However, this approach is for research purposes only. More recently, a commercially available software application (DeepVessel FFR) has been introduced by Keya Medical (Beijing, China) [58].

ML-based CT-FFR employs a multilayer neural network framework that was trained and validated offline against the former CFD approach by using a virtual dataset of 12,000 synthetic 3D coronary models [56]. The clinical validation of the ML approach has been conducted in one multicenter trial and several single-center studies in relation to CCTA and invasive coronary angiography (ICA) assessing lesion-specific ischemia. The MACHINE registry (Diagnostic Accuracy of a Machine-Learning Approach to Coronary Computed Tomographic Angiography - Based Fractional Flow Reserve: Result from the MACHINE Consortium) investigated ML-based CT-FFR in 351 patients with 525 vessels from 5 sites in Europe, Asia, and the United States [57]. The diagnostic accuracy of ML-based CT-FFR was significantly better when compared to that of CCTA (ML CT-FFR 78% vs. cCTA 58%). Likewise, the AUC for identifying hemodynamically significant CAD was superior for ML-based CT-FFR (AUC: 0.84) in comparison to that of CCTA alone (AUC: 0.69,  $p < 0.05$ ). In accordance with the results of the MACHINE registry, several single-center studies have evaluated the diagnostic performance of ML-based CT-FFR, reporting sensitivities and specificities ranging from 79% to 82% and 91% to 94%, respectively [59, 60]. ML-based CT-FFR has also proven its feasibility in coronary calcification. A recent study by Tesche et al. [61] investigated the impact of coronary calcifications on the accuracy of ML-CT-FFR. The authors reported a good but statistically significant different diagnostic performance of ML CT-FFR in heavily calcified vessels in comparison to low-to intermediate ranges of calcifications (AUC: 0.71 vs. 0.85,  $p = 0.04$ ). Another sub-study of the MACHINE registry assessed the impact of gender on the diagnostic accuracy of ML CT-FFR with no significant difference in the AUCs in men when compared to that of women (AUC: 0.83 vs. 0.83,  $p = 0.89$ ) [62]. Overall, ML-based CT-FFR provides high diagnostic accuracy for the assessment of lesion-specific ischemia. A representative case is shown in Figure 3.

Only few studies have assessed the use of AI for CT perfusion. However, CT perfusion offers a field with great potential for the application of AI especially for automated identification of perfusion defects and myocardial segmentation. Preliminary results have demonstrated an AUC of 0.73 by using different ML approaches for automated segmentation and delineation of the left ventricle when compared to manual segmentation by an expert reader [63]. In another investigation, Han and colleagues [64] used a gradient



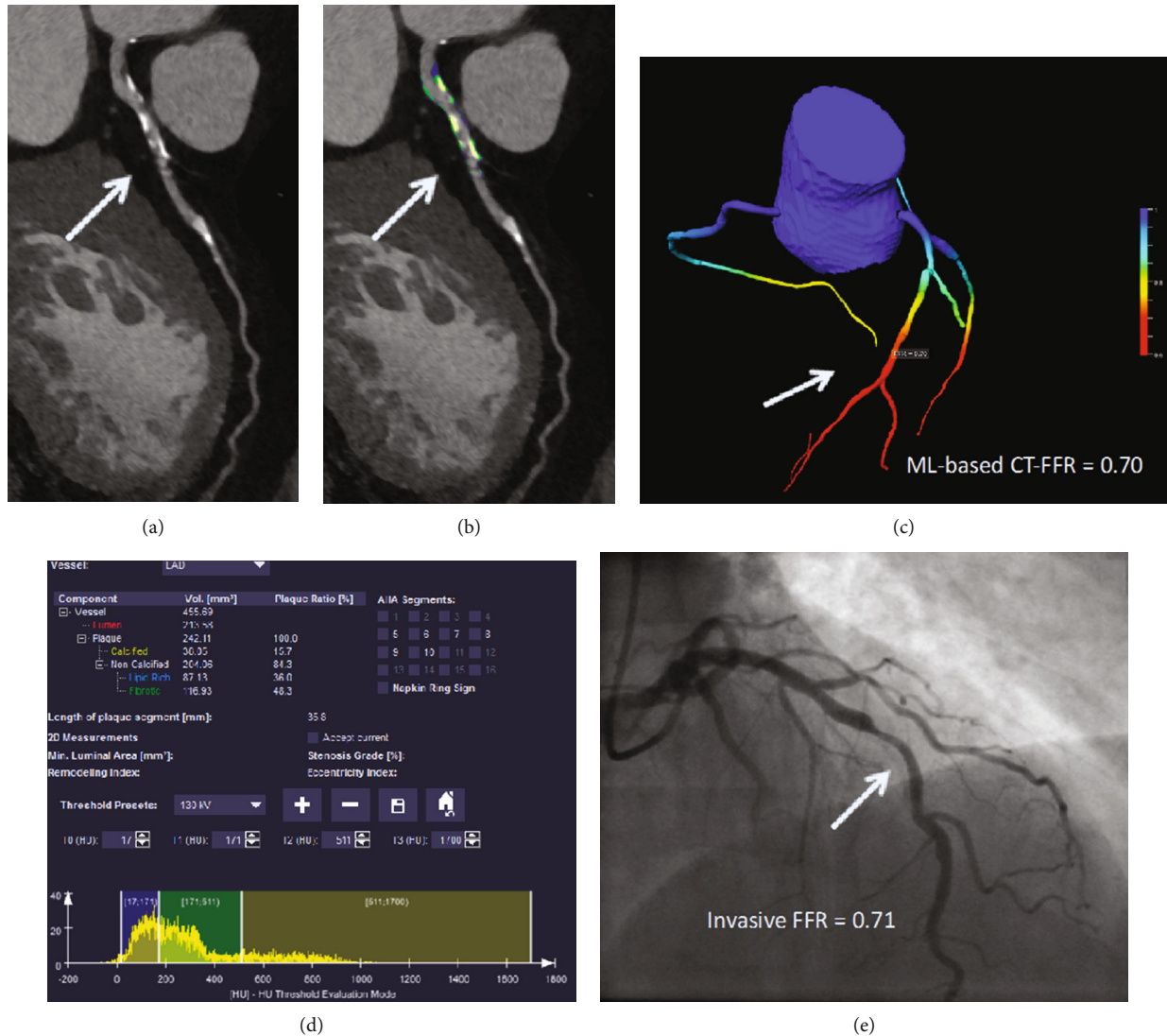


FIGURE 3: Coronary CT angiography in a 54-year-old man without known coronary artery disease. (a) Automatically generated curved multiplanar reformations showing  $>50\%$  stenosis of the proximal LAD (arrow). (c) 3-Dimensional color-coded mesh shows a CT-FFR value of 0.70, indicating ischemia of the underlying stenosis (arrow). (b, d) Color-coded automated plaque assessment of the lesion demonstrating the predominantly calcified composition of the atherosclerotic atheroma. (e) Invasive coronary angiography confirms obstructive stenosis of the LAD (arrow) with an FFR of 0.70.

boosting classifier for supervised ML in resting myocardial perfusion CT for the identification of lesion-specific ischemia. The authors showed a diagnostic accuracy, sensitivity, and specificity of 68%, 53%, and 85% of CTP added to cCTA stenosis  $>70\%$  for predicting hemodynamically significant CAD.

## 5. AI in CCTA Prognostication

Focusing on outcome, there are several manuscripts that show the impact of CAD depicted on CCTA and prognosis [8, 65]. An algorithm based on AI can improve risk stratification based on standard clinical parameters.

Motwani et al. evaluated the impact of an ML algorithm for prognostic stratification in a large cohort of 10030 patients with follow-up of 5 years and an endpoint of mortality [66]. A

TABLE 1: Impact of AI in CCTA.

Task	Accuracy
Coronary artery stenosis	++/+++
Coronary calcium	++
Plaque phenotype	++
Detection of ischemia	++/+++
Prognosis	++/+++

AI: artificial intelligence; CCTA: coronary computed tomography angiography.

total of 25 clinical parameters and 44 CCTA parameters were evaluated for a correct assessment of mortality that occurred in seven hundred and forty-five patients [66]. The ML algorithm was superior compared to Framingham Risk Score

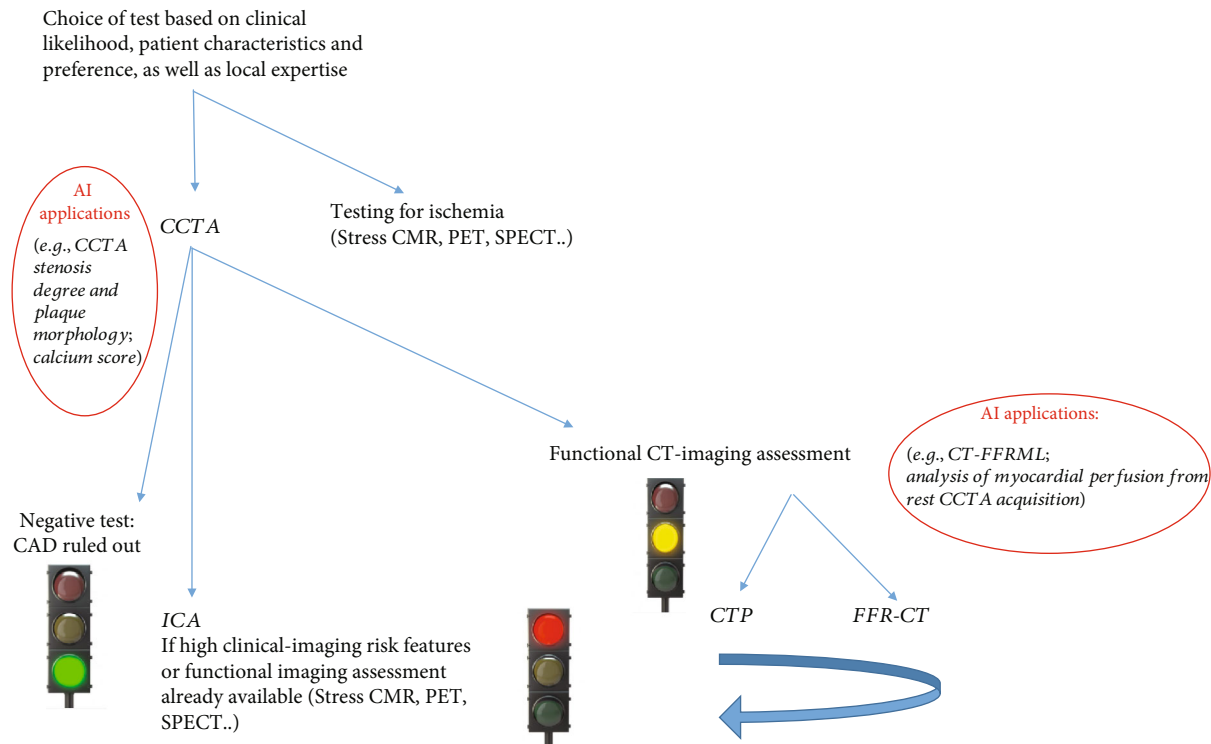


FIGURE 4: Application of AI on CCTA in the clinical setting. First, CCTA images are processed using an AI algorithm; subsequently, the patients can be further classified in three groups: patients without obstructive CAD, patients that need invasive coronary angiography, and patients with stenosis that could benefit from functional imaging. In the cohort of patients classified to functional imaging such as CT perfusion or CT-FFR, an algorithm of AI can be applied in order to speed up the process.

(FRS) or CCTA severity risk scores with an area under curve (AUC) of 0.79 while FRS showed an AUC of 0.61, segment stenosis score of 0.64, segment involved score of 0.64, and modified Duke index of 0.62 [66].

Van Rosendael et al. developed a model for risk stratification based on a population from the CONFIRM registry [67]. The primary endpoint was a composite of myocardial infarction and death, and the algorithm was able to predict the primary endpoint with an AUC of 0.77 versus the other scores that ranged from 0.65 to 0.70.

Tesche et al., in a small cohort of patients, developed an AI algorithm for risk stratification in patients who underwent CCTA with follow-up of 5.4 years [18]. The authors found that an ML approach showed an AUC of 0.96 for MACE, higher compared to Agatston calcium score (AUC: 0.84), segment involved score (AUC: 0.88), and segment stenosis score (AUC: 0.89).

## 6. Future Perspectives

In CCTA, the role of AI may be important for further radiation dose reduction [68] without impairment of image quality and help in CCTA reporting, evaluation of CAD burden, myocardial ischemia, and assessment of prognosis [15] (Table 1).

Human interpretation, despite their experience, is still prone to fatigue. Furthermore, the time of training of expert readers requires years of experience. The application of AI in

CCTA will not substitute the cardiac radiologist; rather, AI will represent a helpful tool for reporting and prognostic stratification. Indeed, following the ESC guidelines [7], over the next few years, the requests for CCTA will increase. Therefore, a helpful tool that can decrease the time of CCTA analysis should be embraced.

Furthermore, CCTA analysis is moving toward a model of precision medicine. The analysis of coronary stenosis grading is not sufficient alone. A comprehensive CCTA report needs to provide information regarding characterization of plaque and its hemodynamical effect; furthermore, the joint evaluation of clinical parameters can be helpful to stratify the patients in terms of worse outcome and can be helpful for individual treatment plans.

It is plausible that an algorithm will be composed for automatic analysis of CCTA images followed by detection of myocardial ischemia (Figure 4). Subsequently, the final results of CCTA will be evaluated according to the clinical parameters with an AI algorithm in order to obtain a patient-based risk profile.

Strict legislation focused on the application of AI in cardiac imaging will be necessary to clarify the medico-legal aspects of the AI algorithm application. Furthermore, the development of an AI algorithm implies the analysis of a large amount of data; this aspect is extremely important if we consider the legal aspects due to privacy.

All these aspects need to be clarified in the future before we consider the application of AI in routine clinical practice.

## 7. Conclusion

In the future, AI will be integrated in the CCTA workflow. AI applications will greatly benefit CCTA practice reducing the reporting time and providing a more accurate quantitative-based approach to CAD management, moving the entire field in the direction of precision-based medicine. However, before we can widely implement AI solutions in our clinical practice, we need to carefully validate the algorithms in the light of standards for good medical practice and new medical device utilization and carefully address possible issues on data protection, legal framework, and ethical principles.

## Data Availability

Data from our manuscript are obtained from the article cited in the manuscript.

## Conflicts of Interest

The authors declare that they have no conflicts of interest.

## References

- [1] G. Pontone, D. Andreini, A. L. Bartorelli et al., "A long-term prognostic value of CT angiography and exercise ECG in patients with suspected CAD," *JACC: Cardiovascular Imaging*, vol. 6, no. 6, pp. 641–650, 2013.
- [2] G. Pontone, D. Andreini, A. L. Bartorelli et al., "Diagnostic accuracy of coronary computed tomography angiography: a comparison between prospective and retrospective electrocardiogram triggering," *Journal of the American College of Cardiology*, vol. 54, no. 4, pp. 346–355, 2009.
- [3] A. Baggiano, L. Fusini, A. Del Torto et al., "Sequential strategy including FFRCT plus stress-CTP impacts on management of patients with stable chest pain: the Stress-CTP RIPCORD Study," *Journal of Clinical Medicine*, vol. 9, no. 7, p. 2147, 2020.
- [4] G. Pontone, A. I. Guaricci, S. C. Palmer et al., "Diagnostic performance of non-invasive imaging for stable coronary artery disease: a meta-analysis," *International Journal of Cardiology*, vol. 300, pp. 276–281, 2020.
- [5] A. I. Guaricci, G. Pontone, L. Fusini et al., "Additional value of inflammatory biomarkers and carotid artery disease in prediction of significant coronary artery disease as assessed by coronary computed tomography angiography," *European Heart Journal Cardiovascular Imaging*, vol. 18, no. 9, pp. 1049–1056, 2017.
- [6] G. Pontone, D. Andreini, E. Bertella et al., "Impact of an intracycle motion correction algorithm on overall evaluability and diagnostic accuracy of computed tomography coronary angiography," *European Radiology*, vol. 26, no. 1, pp. 147–156, 2016.
- [7] J. Knuuti, W. Wijns, A. Saraste et al., "2019 ESC Guidelines for the diagnosis and management of chronic coronary syndromes," *European Heart Journal*, vol. 41, no. 3, pp. 407–477, 2020.
- [8] M. C. Williams, A. Moss, E. Nicol, and D. E. Newby, "Cardiac CT improves outcomes in stable coronary heart disease: results of recent clinical trials," *Curr Cardiovasc Imaging Rep.*, vol. 10, no. 5, p. 14, 2017.
- [9] E. Hulten, A. Goehler, M. S. Bittencourt et al., "Cost and resource utilization associated with use of computed tomography to evaluate chest pain in the emergency department: the Rule Out Myocardial Infarction using Computer Assisted Tomography (ROMICAT) study," *Circulation. Cardiovascular Quality and Outcomes*, vol. 6, no. 5, pp. 514–524, 2013.
- [10] A. I. Guaricci, V. Lorenzoni, M. Guglielmo et al., "Prognostic relevance of subclinical coronary and carotid atherosclerosis in a diabetic and nondiabetic asymptomatic population," *Clinical Cardiology*, vol. 41, no. 6, pp. 769–777, 2018.
- [11] E. Maffei, S. Seitun, C. Martini et al., "Prognostic value of computed tomography coronary angiography in patients with chest pain of suspected cardiac origin," *La Radiologia Medica*, vol. 116, no. 5, pp. 690–705, 2011.
- [12] B. J. Chow, G. Small, Y. Yam et al., "Incremental prognostic value of cardiac computed tomography in coronary artery disease using CONFIRM," *Circulation: Cardiovascular Imaging*, vol. 4, no. 5, pp. 463–472, 2011.
- [13] B. Foldyna, J. E. Udelson, J. Karady et al., "Pretest probability for patients with suspected obstructive coronary artery disease: re-evaluating Diamond-Forrester for the contemporary era and clinical implications: insights from the PROMISE trial," *European Heart Journal Cardiovascular Imaging*, vol. 20, no. 5, pp. 574–581, 2019.
- [14] G. Pontone, G. Muscogiuri, D. Andreini et al., "The new frontier of cardiac computed tomography angiography: fractional flow reserve and stress myocardial perfusion," *Current Treatment Options in Cardiovascular Medicine*, vol. 18, no. 12, p. 74, 2016.
- [15] M. van Assen, G. Muscogiuri, D. Caruso, S. J. Lee, A. Laghi, and C. N. De Cecco, "Artificial intelligence in cardiac radiology," *La Radiologia Medica*, vol. 125, no. 11, pp. 1186–1199, 2020.
- [16] G. Muscogiuri, M. Chiesa, M. Trotta et al., "Performance of a deep learning algorithm for the evaluation of CAD-RADS classification with CCTA," *Atherosclerosis*, vol. 294, pp. 25–32, 2020.
- [17] C. Tesche and H. N. Gray, "Machine learning and deep neural networks applications in coronary flow assessment: the case of computed tomography fractional flow reserve," *Journal of Thoracic Imaging*, vol. 35, Suppl 1, pp. S66–S71, 2020.
- [18] C. Tesche, M. J. Bauer, M. Baquet et al., "Improved long-term prognostic value of coronary CT angiography-derived plaque measures and clinical parameters on adverse cardiac outcome using machine learning," *European Radiology*, 2020.
- [19] S. Greenstein and S. Gulick, *Zebra medical vision*, Harvard Business School, 2018.
- [20] ACR-DSI, *FDA cleared AI algorithms*, DSI-ACR, 2019, January 2020. <http://www.acrdsi.org/DSI-Services/FDA-Cleared-AI-Algorithms>.
- [21] J. R. Zech, M. A. Badgeley, M. Liu, A. B. Costa, J. J. Titano, and E. K. Oermann, "Variable generalization performance of a deep learning model to detect pneumonia in chest radiographs: a cross-sectional study," *PLoS Medicine*, vol. 15, no. 11, article e1002683, 2018.
- [22] D. W. Kim, H. Y. Jang, K. W. Kim, Y. Shin, and S. H. Park, "Design characteristics of studies reporting the performance of artificial intelligence algorithms for diagnostic analysis of medical images: results from recently published papers," *Korean Journal of Radiology*, vol. 20, no. 3, pp. 405–410, 2019.

- [23] S. H. Park and K. Han, "Methodologic guide for evaluating clinical performance and effect of artificial intelligence technology for medical diagnosis and prediction," *Radiology*, vol. 286, no. 3, pp. 800–809, 2018.
- [24] J. R. England and P. M. Cheng, "Artificial intelligence for medical image analysis: a guide for authors and reviewers," *AJR. American Journal of Roentgenology*, vol. 212, no. 3, pp. 513–519, 2019.
- [25] S. S. Martin, M. van Assen, S. Rapaka et al., "Evaluation of a deep learning-based automated CT coronary artery calcium scoring algorithm," *JACC: Cardiovascular Imaging*, vol. 13, no. 2, pp. 524–526, 2020.
- [26] A. M. Fischer, A. Varga-Szemes, M. van Assen et al., "Comparison of artificial intelligence-based fully automatic chest CT emphysema quantification to pulmonary function testing," *AJR. American Journal of Roentgenology*, vol. 214, no. 5, pp. 1065–1071, 2020.
- [27] European-Commission, *White paper on artificial intelligence*, 2020.
- [28] M. van Assen, S. J. Lee, and C. N. De Cecco, "Artificial intelligence from A to Z: from neural network to legal framework," *European Journal of Radiology*, vol. 129, p. 109083, 2020.
- [29] D. M. Zuckerman, P. Brown, and S. E. Nissen, "Medical device recalls and the FDA approval process," *Archives of Internal Medicine*, vol. 171, no. 11, pp. 1006–1011, 2011.
- [30] E. Tat, D. L. Bhatt, and M. G. Rabbat, "Addressing bias: artificial intelligence in cardiovascular medicine," *The Lancet Digital Health*, vol. 2, no. 12, pp. e635–e636, 2020.
- [31] J. R. Geis, A. P. Brady, C. C. Wu et al., "Ethics of artificial intelligence in radiology: summary of the joint European and North American multisociety statement," *Journal of the American College of Radiology*, vol. 16, no. 11, pp. 1516–1521, 2019.
- [32] J. K. Min, L. J. Shaw, R. B. Devereux et al., "Prognostic value of multidetector coronary computed tomographic angiography for prediction of all-cause mortality," *Journal of the American College of Cardiology*, vol. 50, no. 12, pp. 1161–1170, 2007.
- [33] J. Leipsic, S. Abbara, S. Achenbach et al., "SCCT guidelines for the interpretation and reporting of coronary CT angiography: a report of the Society of Cardiovascular Computed Tomography Guidelines Committee," *Journal of Cardiovascular Computed Tomography*, vol. 8, no. 5, pp. 342–358, 2014.
- [34] R. C. Cury, S. Abbara, S. Achenbach et al., "CAD-RADS™ Coronary Artery Disease - Reporting and Data System. An expert consensus document of the Society of Cardiovascular Computed Tomography (SCCT), the American College of Radiology (ACR) and the North American Society for Cardiovascular Imaging (NASCI). Endorsed by the American College of Cardiology," *Journal of Cardiovascular Computed Tomography*, vol. 10, no. 4, pp. 269–281, 2016.
- [35] M. Zreik, R. W. van Hamersvelt, J. M. Wolterink, T. Leiner, M. A. Viergever, and I. Isgum, "A recurrent CNN for automatic detection and classification of coronary artery plaque and stenosis in coronary CT angiography," *IEEE Transactions on Medical Imaging*, vol. 38, no. 7, pp. 1588–1598, 2019.
- [36] D. Kang, D. Dey, P. J. Slomka et al., "Structured learning algorithm for detection of nonobstructive and obstructive coronary plaque lesions from computed tomography angiography," *Journal of Medical Imaging*, vol. 2, no. 1, article 014003, 2015.
- [37] H. Yoneyama, K. Nakajima, J. Taki et al., "Ability of artificial intelligence to diagnose coronary artery stenosis using hybrid images of coronary computed tomography angiography and myocardial perfusion SPECT," *European Journal of Hybrid Imaging*, vol. 3, no. 1, p. 4, 2019.
- [38] R. W. van Hamersvelt, M. Zreik, M. Voskuil, M. A. Viergever, I. Isgum, and T. Leiner, "Deep learning analysis of left ventricular myocardium in CT angiographic intermediate-degree coronary stenosis improves the diagnostic accuracy for identification of functionally significant stenosis," *European Radiology*, vol. 29, no. 5, pp. 2350–2359, 2019.
- [39] Z. Huang, J. Xiao, Y. Xie et al., "The correlation of deep learning-based CAD-RADS evaluated by coronary computed tomography angiography with breast arterial calcification on mammography," *Scientific Reports*, vol. 10, no. 1, p. 11532, 2020.
- [40] P. Greenland, R. O. Bonow, B. H. Brundage et al., "ACCF/AHA 2007 Clinical Expert Consensus Document on Coronary Artery Calcium Scoring By Computed Tomography in Global Cardiovascular Risk Assessment and in Evaluation of Patients With Chest Pain: A Report of the American College of Cardiology Foundation Clinical Expert Consensus Task Force (ACCF/AHA Writing Committee to Update the 2000 Expert Consensus Document on Electron Beam Computed Tomography)," *Journal of the American College of Cardiology*, vol. 49, no. 3, pp. 378–402, 2007.
- [41] B. O. Hartaigh, V. Valenti, I. Cho et al., "15-Year prognostic utility of coronary artery calcium scoring for all-cause mortality in the elderly," *Atherosclerosis*, vol. 246, pp. 361–366, 2016.
- [42] C. Tesche, T. M. Duguay, U. J. Schoepf et al., "Current and future applications of CT coronary calcium assessment," *Expert Review of Cardiovascular Therapy*, vol. 16, no. 6, pp. 441–453, 2018.
- [43] A. S. Agatston, W. R. Janowitz, F. J. Hildner, N. R. Zusmer, M. Viamonte Jr., and R. Detrano, "Quantification of coronary artery calcium using ultrafast computed tomography," *Journal of the American College of Cardiology*, vol. 15, no. 4, pp. 827–832, 1990.
- [44] B. D. de Vos, J. M. Wolterink, T. Leiner, P. A. de Jong, N. Lessmann, and I. Isgum, "Direct automatic coronary calcium scoring in cardiac and chest CT," *IEEE Transactions on Medical Imaging*, vol. 38, no. 9, pp. 2127–2138, 2019.
- [45] I. Isgum, A. Rutten, M. Prokop, and B. van Ginneken, "Detection of coronary calcifications from computed tomography scans for automated risk assessment of coronary artery disease," *Medical Physics*, vol. 34, no. 4, pp. 1450–1461, 2007.
- [46] M. Sandstedt, L. Henriksson, M. Janzon et al., "Evaluation of an AI-based, automatic coronary artery calcium scoring software," *European Radiology*, vol. 30, no. 3, pp. 1671–1678, 2020.
- [47] R. A. Takx, P. A. de Jong, T. Leiner et al., "Automated coronary artery calcification scoring in non-gated chest CT: agreement and reliability," *PLoS One*, vol. 9, no. 3, article e91239, 2014.
- [48] J. M. Wolterink, T. Leiner, B. D. de Vos, R. W. van Hamersvelt, M. A. Viergever, and I. Isgum, "Automatic coronary artery calcium scoring in cardiac CT angiography using paired convolutional neural networks," *Medical Image Analysis*, vol. 34, pp. 123–136, 2016.
- [49] S. G. M. van Velzen, N. Lessmann, B. K. Velthuis et al., "Deep learning for automatic calcium scoring in CT: validation using multiple cardiac CT and chest CT protocols," *Radiology*, vol. 295, no. 1, pp. 66–79, 2020.
- [50] E. Conte, S. Mushtaq, G. Pontone et al., "Plaque quantification by coronary computed tomography angiography using intravascular ultrasound as a reference standard: a comparison



- between standard and last generation computed tomography scanners,” *European Heart Journal - Cardiovascular Imaging*, vol. 21, pp. 191–201, 2019.
- [51] D. Andreini, M. Magnoni, E. Conte et al., “Coronary plaque features on CTA can identify patients at increased risk of cardiovascular events,” *JACC: Cardiovascular Imaging*, vol. 13, no. 8, pp. 1704–1717, 2020.
- [52] D. Dey, V. Y. Cheng, P. J. Slomka et al., “Automated 3-dimensional quantification of noncalcified and calcified coronary plaque from coronary CT angiography,” *Journal of Cardiovascular Computed Tomography*, vol. 3, no. 6, pp. 372–382, 2009.
- [53] D. Opincariu, T. Benedek, M. Chitu, N. Rat, and I. Benedek, “From CT to artificial intelligence for complex assessment of plaque-associated risk,” *The International Journal of Cardiovascular Imaging*, vol. 36, no. 12, pp. 2403–2427, 2020.
- [54] M. Kolossvary, J. Karady, B. Szilveszter et al., “Radiomic features are superior to conventional quantitative computed tomographic metrics to identify coronary plaques with napkin-ring sign,” *Circulation. Cardiovascular Imaging*, vol. 10, no. 12, 2017.
- [55] T. Masuda, T. Nakaura, Y. Funama et al., “Machine-learning integration of CT histogram analysis to evaluate the composition of atherosclerotic plaques: validation with IB-IVUS,” *Journal of Cardiovascular Computed Tomography*, vol. 13, no. 2, pp. 163–169, 2019.
- [56] L. Itu, S. Rapaka, T. Passerini et al., “A machine-learning approach for computation of fractional flow reserve from coronary computed tomography,” *Journal of Applied Physiology*, vol. 121, no. 1, pp. 42–52, 2016.
- [57] A. Coenen, Y. H. Kim, M. Kruk et al., “Diagnostic accuracy of a machine-learning approach to coronary computed tomographic angiography-based fractional flow reserve: result from the MACHINE consortium,” *Circulation: Cardiovascular Imaging*, vol. 11, no. 6, article e007217, 2018.
- [58] C. X. Tang, C. Y. Liu, M. J. Lu et al., “CT FFR for ischemia-specific CAD with a new computational fluid dynamics algorithm: a Chinese multicenter study,” *JACC: Cardiovascular Imaging*, vol. 13, no. 4, pp. 980–990, 2020.
- [59] C. Tesche, C. N. de Cecco, S. Baumann et al., “Coronary CT angiography-derived fractional flow reserve: machine learning algorithm versus computational fluid dynamics modeling,” *Radiology*, vol. 288, no. 1, pp. 64–72, 2018.
- [60] P. L. von Knebel Doeberitz, C. N. De Cecco, U. J. Schoepf et al., “Coronary CT angiography-derived plaque quantification with artificial intelligence CT fractional flow reserve for the identification of lesion-specific ischemia,” *European Radiology*, vol. 29, no. 5, pp. 2378–2387, 2019.
- [61] C. Tesche, K. Otani, C. N. De Cecco et al., “Influence of coronary calcium on diagnostic performance of machine learning CT-FFR: results from MACHINE registry,” *JACC: Cardiovascular Imaging*, vol. 13, no. 3, pp. 760–770, 2020.
- [62] S. Baumann, M. Renker, U. J. Schoepf et al., “Gender differences in the diagnostic performance of machine learning coronary CT angiography-derived fractional flow reserve -results from the MACHINE registry,” *European Journal of Radiology*, vol. 119, p. 108657, 2019.
- [63] G. Xiong, D. Kola, R. Heo, K. Elmore, I. Cho, and J. K. Min, “Myocardial perfusion analysis in cardiac computed tomography angiographic images at rest,” *Medical Image Analysis*, vol. 24, no. 1, pp. 77–89, 2015.
- [64] D. Han, J. H. Lee, A. Rizvi et al., “Incremental role of resting myocardial computed tomography perfusion for predicting physiologically significant coronary artery disease: a machine learning approach,” *Journal of the American College of Cardiology*, vol. 25, no. 1, pp. 223–233, 2018.
- [65] M. C. Williams, J. Kwieciniski, M. Doris et al., “Low-attenuation noncalcified plaque on coronary computed tomography angiography predicts myocardial infarction: results from the multicenter SCOT-HEART trial (Scottish Computed Tomography of the HEART),” *Circulation*, vol. 141, no. 18, pp. 1452–1462, 2020.
- [66] M. Motwani, D. Dey, D. S. Berman et al., “Machine learning for prediction of all-cause mortality in patients with suspected coronary artery disease: a 5-year multicentre prospective registry analysis,” *European Heart Journal*, vol. 38, article ehv188, 2016.
- [67] A. R. van Rosendaal, G. Maliakal, K. K. Kolli et al., “Maximization of the usage of coronary CTA derived plaque information using a machine learning based algorithm to improve risk stratification; insights from the CONFIRM registry,” *Journal of Cardiovascular Computed Tomography*, vol. 12, no. 3, pp. 204–209, 2018.
- [68] D. C. Benz, G. Benetos, G. Rampidis et al., “Validation of deep-learning image reconstruction for coronary computed tomography angiography: impact on noise, image quality and diagnostic accuracy,” *Journal of Cardiovascular Computed Tomography*, vol. 14, no. 5, pp. 444–451, 2020.